

UNIVERSIDADE FEDERAL DO RIO GRANDE DO NORTE
PROGRAMA DE PÓS-GRADUAÇÃO EM NEUROCIÊNCIAS
INSTITUTO DO CÉREBRO
LABORATÓRIO DE NEUROFISIOLOGIA COMPUTACIONAL

FÁBIO VIEGAS CAIXETA

**EFEITOS DA ADMINISTRAÇÃO AGUDA DE QUETAMINA SOBRE AS
OSCILAÇÕES ELETROFISIOLÓGICAS DA REGIÃO CA1 HIPOCAMPAL**

*(Effects of the acute administration of ketamine on hippocampal CA1
electrophysiological oscillations)*

Natal, Brasil.

2014

FÁBIO VIEGAS CAIXETA

**EFEITOS DA ADMINISTRAÇÃO AGUDA DE QUETAMINA SOBRE AS
OSCILAÇÕES ELETROFISIOLÓGICAS DA REGIÃO CA1 HIPOCAMPAL**

*(Effects of the acute administration of ketamine on hippocampal CA1
electrophysiological oscillations)*

Tese apresentada à Pós-Graduação em Neurociências
da Universidade Federal do Rio Grande do Norte
como requisito parcial para a obtenção do título de
Doutor em Neurociências.

Orientador: Prof. Dr. Adriano Bretanha Lopes Tort
Co-orientador: Prof. Dr. Sidarta Tollendal Gomes Ribeiro
Área de concentração: Neurofisiologia computacional

Natal, Brasil.

2014

Apoio ao Usuário
Catalogação de Publicação na Fonte. UFRN - Biblioteca Setorial do Instituto do Cérebro

C133e Caixeta, Fábio Viegas.

Efeitos da administração aguda de quetamina sobre as oscilações eletrofisiológicas da região ca1 hipocampal / Fabio Viegas Caixeta. - Natal, 2014. 100f: il.

Tese (Doutorado em Ciências, Área de concentração: Neurociências). Universidade Federal do Rio Grande do Norte. Orientador: Profº. Drº. Adriano B. L. Tort.

1. Neurociências - Tese. 2. NMDAR. 3. Ritmos Cerebrais. I. Título

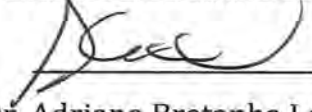
FÁBIO VIEGAS CAIXETA

**EFEITOS DA ADMINISTRAÇÃO AGUDA DE QUETAMINA SOBRE AS
OSCILAÇÕES ELETROFISIOLÓGICAS DA REGIÃO CA1 HIPOCAMPAL**

Tese apresentada à Pós-Graduação em Neurociências
da Universidade Federal do Rio Grande do Norte
como requisito parcial para a obtenção do título de
Doutor em Neurociências.

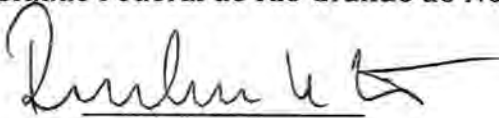
Tese apresentada em fevereiro de 2014

BANCA EXAMINADORA



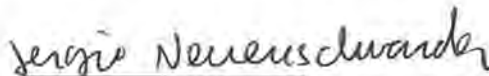
Prof. Dr. Adriano Bretanha Lopes Tort

Universidade Federal do Rio Grande do Norte



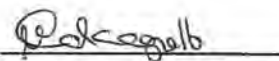
Prof. Dr. Richardson N. Leão

Universidade Federal do Rio Grande do Norte



Prof. Dr. Sergio Neuenschwander

Universidade Federal do Rio Grande do Norte



Prof. Dra. Maria Elisa Calcagnotto

Universidade Federal do Rio Grande do Sul



Prof. Dr. Olavo Bohrer Amaral

Universidade Federal do Rio de Janeiro

*"Serras que vão saindo, para destapar outras
serras. Tem de todas as coisas. Vivendo se aprende;
mas o que se aprende, mais, é só a fazer outras
maiores perguntas."*

(Guimarães Rosa, nas palavras de Riobaldo, em Grande Sertão: Veredas)

Para o meu pai.

Agradecimentos

Agradeço aos colegas Alianda Maira Cornélio e Robson Scheffer Teixeira pela colaboração com o trabalho principal desta tese;

A Cláudio Marcos Teixeira de Queiroz e Kelly Soares pelo auxílio com o registro dos potenciais evocados, e a Richardson Leão pelos registros com *U-probe*.

Aos professores Rodrigo Romcy-Pereira e Cláudio Marcos Teixeira de Queiroz pelos conselhos e sugestões oferecidos no Comitê de Acompanhamento;

Aos professores Olavo Bohrer Amaral, Maria Elisa Calcagnotto, Richardson Leão e Sergio Neuenschwander por se disporem a participar da minha Banca de Defesa;

A Hindiael Belchior, Arthur França, Anderson Brito da Silva, Rodrigo Pavão, Diego Laplagne, Annie da Costa Souza, Bryan da Costa Souza, Kelly Soares, Sérgio Conde, Flávio Barbosa, Gilvan Barbosa, José Henrique Targino, Helton Maia, Markus Hilscher, Juliana Alves Brandão, Ana Maria Soares, Cristiano Kohler, Larissa Muratori, Daniel de Almeida Filho, Carolina Corado, Daniela Moura, Laila Asth, Fábio Freitag, Natália Bezerra Mota e todos outros colegas e amigos do IINN-ELS e do Instituto do Cérebro pelas horas de convivência e pelo auxílio prestado em diversas etapas dos meus estudos nos últimos anos;

À toda equipe de funcionários do Instituto do Cérebro e do IINN-ELS por manterem os Instituto funcionando e bem cuidados;

À minha família, que me ofereceu as melhores condições possíveis para que eu perseguisse meus estudos longe de casa, e que esteve presente me incentivando a fazer o meu melhor.

À minha esposa Patrícia Cordeiro pelo auxílio prestado como assessora de imprensa VIP, e por ter aturado os meus horários de trabalho malucos e o meu constante mau humor;

Ao Guilherme, que apareceu de repente e me fez o pai mais feliz do mundo;

À CAPES, pela concessão da bolsa de mestrado e de doutorado;

Ao professor Sidarta Ribeiro que me abriu as portas de seu laboratório, e me educou durante o mestrado e o doutorado, sempre apontando o melhor caminho a ser seguido, e principalmente por ter sido um exemplo inspirador de como fazer ciência;

E, finalmente, agradeço ao professor Adriano Tort, que pacientemente me guiou através do doutorado. Além de desempenhar o papel de orientador impecavelmente, ele também se tornou um grande amigo que esteve presente em todos momentos importantes nos últimos quatro anos, me auxiliando nas horas difíceis, e celebrando nas horas felizes. Os méritos deste trabalho são dele, e as falhas são provavelmente minhas.

Summary

Preface	1
List of abbreviations	2
Resumo (in Brazilian portuguese)	3
Abstract	4
1. Introduction	
1.1 Brain oscillations in cognition and in schizophrenia	5
1.2 Schizophrenia and the glutamate hypothesis	11
1.3 Brief history of phencyclidine and ketamine	15
1.4 NMDAR blockade pharmacology	18
1.5 Evidence for NMDAR dysfunction in schizophrenia	25
2. Thesis aim	28
3. Methods	
3.1 Ethical aspects	29
3.2 Surgical implantation of electrodes	29
3.3 Experimental procedures	33
3.4 Electrophysiological recordings	34
3.5 Behavioural analysis	34
3.6 Data analysis	34
3.7 Filter settings and extraction of the instantaneous phase and amplitude	34
3.8 Spectral analyses	35
3.9 Estimation of phase-amplitude coupling and comodulation maps	35
3.10 Triggered LFP averages and current source density (CSD)	39
3.11 Statistics	40

4. Results	
4.1 Ketamine induces dose-dependent transient immobility and hyperlocomotion	41
4.2 Ketamine-induced immobility is associated with increased delta power	43
4.3 Ketamine modulates hippocampal theta oscillations in a layer-dependent manner	46
4.4 Ketamine increases the power of gamma and high frequency oscillations	49
4.5 Ketamine leads to increased phase synchrony in multiple high-frequency bands	53
4.6 Ketamine alters cross-frequency coupling	55
4.7 Ketamine does not alter the distribution of electrical dipoles in the hippocampus	61
5. Discussion	62
6. Concluding remarks	68
7. References	70
8. List of publications (2010-2013)	
8.1 Publication related to the thesis	96
8.2 Other publications	96
8.3 Media coverage of our work	96
Annexes	
Annex A – Letter of approval from the AASDAP Committee of Ethics in the Use of laboratory Animals for research (CEUA)	98
Annex B – Letter of approval from the CEUA-UFRN	99
Annex C – Histological sections from animals used in the study	100
Annex D – Published article in Scientific Reports, 2013	101

Preface

The history of electrophysiology is entwined with the study of brain oscillations. In 1929 Hans Berger was the first to find that different rhythms could be measured on the human scalp, using his innovative electroencephalogram, depending on whether the subject had his/her eyes opened or closed. Berger was also the first to point out that brain waves are disrupted in brain diseases such as epilepsy. Nowadays, although many studies suggest how oscillations might be related to virtually every mental process known, no experiment has conclusively shown that oscillations are actually necessary for proper brain functioning.

Rather than treating this lack of evidence as a stop sign, the scientific community has dedicated tremendous effort in order to solve this 100 years old charade: the functional role of brain oscillations. In order to solve this mystery, new recording techniques and analytical tools are constantly being developed. Of particular importance for this work, a new metric that measures the coupling of brain oscillations of different frequencies has recently been described by Tort and collaborators (Tort et al., 2008; Tort et al., 2010a), paving the way for the study for a novel high-frequency oscillation, referred to as HFO (Scheffer-Teixeira et al., 2012), and consequently creating new tools for the study of brain oscillations in health and in altered brain states.

The present thesis recapitulates the major points of the research developed at the Brain Institute – UFRN, Natal, during the last four years, where we applied electrophysiological recordings in rats and recently developed signal processing techniques to better characterize the alterations of hippocampal oscillations in a well accepted model of psychosis and schizophrenia. Most of the findings and substantial portions of text presented here have been published previously (Caixeta et al., 2013), which makes this thesis more of an extended version of the article, with an in-depth review of the field and some unpublished results and observations that did not fit in the scope of the original article.

List of abbreviations

- 5-HT** – 5-hydroxytryptamine (serotonin)
ANOVA – Analysis of variance
AP – anteroposterior
CA1 – *Cornu Ammonis* hippocampal area number 1
CFC – cross-frequency coupling
CSD – current source density
DSM – Diagnostic and statistical manual of mental disorders
DV – dorsoventral
EEG – electroencephalogram
GABA – γ -Aminobutyric acid
HFO – high frequency oscillations
HG – high gamma
IP – intraperitoneal
ITC – inter-trial phase coherence
IV – intravenous
LFP – local field potential
LSD – d-lysergic acid diethylamide
MAP – multi-channel acquisition processor
MI – modulation index
ML – mediolateral
NMDA – N-methyl-D-aspartate
NMDAR – N-methyl-D-aspartate receptor
OLM – *oriens lacunosum-moleculare*
PCP – phencyclidine
PV – parvalbumin
REM – rapid eye movement
SC – subcutaneous
SEM – standard error of the mean

Resumo

Em humanos, a administração de quetamina - um antagonista não-competitivo do receptor glutamatérgico do tipo NMDA - causa um amplo espectro de sintomas associados à esquizofrenia. Dado o papel dos ritmos cerebrais na realização de tarefas cognitivas, tem sido sugerido que a patofisiologia da esquizofrenia estaria relacionada a desordens de oscilações corticais. Neste estudo utilizamos o registro *in vivo* do potencial de campo elétrico em múltiplos eletrodos implantados no hipocampo de ratos sob o efeito de injeções sistêmicas de doses sub-anestésicas de quetamina (25, 50 e 75 mg/kg IP) para investigarmos as alterações comportamentais e eletrofisiológicas neste modelo animal de psicose. A quetamina alterou o padrão de locomoção e causou diversas mudanças na dinâmica de oscilações neurais. A potência nas bandas de frequência gama e oscilações de alta frequência (OAF) aumentou em todas as profundidades do eixo CA1-giro denteado, enquanto a potência de teta variou dependendo da camada registrada. A coerência de fase de gama e de OAF aumentou entre as camadas de CA1. A quetamina aumentou o acoplamento entre frequências (AEF) de fase-amplitude entre teta e OAF em todas as doses, mas teve efeitos opostos no AEF entre teta e gama de acordo com a dose. Nossos resultados demonstram que o modelo de esquizofrenia induzido por hipofunção dos receptores NMDA está associado com alterações de interações de alta ordem entre oscilações neurais.

Palavras-chave: NMDAR, modelo animal, potencial de campo elétrico, ritmos cerebrais, eletrofisiologia *in vivo*.

Abstract

In humans, acute administration of ketamine – a noncompetitive antagonist of glutamatergic NMDA receptors – causes a wide spectrum of symptoms associated with schizophrenia. Given the role of cerebral rhythms in cognitive processing, it has been suggested that the pathophysiology of schizophrenia might be related to cortical oscillations disorders. In the present study we employed *in vivo* multi-site hippocampal local field potential recordings of freely moving rats treated with systemic injections of sub-anaesthetic doses of ketamine (25, 50 and 75 mg/kg IP) in order to investigate the behavioural and electrophysiological alterations in this animal model of acute psychosis. We found that ketamine induced abnormal locomotor activity and changes in multiple parameters of oscillatory dynamics. Oscillations in the gamma and high-frequency oscillations (HFO) bands showed increased power across the CA1-dentate axis, while changes in theta power varied in a layer-dependent manner. Gamma and HFO showed increased phase coherence across CA1 layers. Ketamine increased phase-amplitude cross-frequency coupling (CFC) between theta and HFO at all doses, but had opposite effects on theta-gamma CFC depending on the dose. Our results demonstrate that NMDA receptor hypofunction model for schizophrenia is associated with alterations of higher-order oscillatory interactions.

Keywords: NMDAR, animal model, LFP, brain rhythms, *in vivo* electrophysiology.

1. Introduction

1.1 Brain oscillations in cognition and in schizophrenia

Oscillations are a hallmark of central nervous system activity (Buzsaki and Draguhn, 2004; Buzsáki, 2006). Since the first recordings of the electrical activity in humans (Berger, 1929; Bremer, 1958) it became apparent that different cognitive states are associated with various dominant frequencies of neuronal oscillations. Electroencephalogram (EEG) recordings during wakefulness are generally dominated by low amplitude high-frequency oscillations -above 10Hz-, while high amplitude slow frequencies are predominant during sleep, and are paramount in discriminating among sleep stages (Buzsáki, 2006).

Mammalian neurons form neuronal ensembles and oscillating networks of multiple sizes, spanning five orders of magnitude in frequency, from 0.05Hz up to 500Hz that are associated with different behavioural states (Buzsaki and Draguhn, 2004). These oscillations are relatively stable across different taxa, suggesting a functional role in neural processing (Buzsáki, 2006). According to Buzsaki and Draguhn (2004), *“this emerging new field, ‘neuronal oscillations’, has created an interdisciplinary platform that cuts across psychophysics, cognitive psychology, neuroscience, biophysics, computational modelling, physics, mathematics, and philosophy.”*

Brain oscillations are frequently separated according to their frequency ranges [although recent studies advise against defining brain rhythms solely based on

frequency ranges (Kopell et al., 2010; Tort et al., 2010b; Tort et al., 2013)], most of which have been associated with characteristic cognitive processing. Following Berger's tradition, the name of different oscillations has little correspondence to their frequencies, and refers to the order in which they were described. Alpha rhythm is about 8-13Hz and is associated with quiet, waking states, and was first observed in the occipital cortex of subjects with their eyes closed. Beta encompasses 14-30Hz, and has long been associated with motor control in the motor cortex (Conway et al., 1995), and correlates inversely with voluntary movement in the basal ganglia (Brown and Williams, 2005). Gamma oscillations span from 30-100Hz, and are associated with alert wakefulness and cognition. A prominent hypothesis in neurosciences proposes gamma synchrony as a correlate of perceptual binding (Singer and Gray, 1995), while others relate gamma to selective attention (Fries et al., 2001), transient neuronal assembly formation (Harris et al., 2003), and information routing (Colgin et al., 2009). Delta waves (1-4Hz) are mostly present during anaesthesia and sleep, when cortical neurons are not actively processing sensorial inputs, and are majorly synchronized by phasic thalamic activity (Steriade et al., 1993; Billard et al., 1997). Theta rhythms (5-10Hz) are a distinctive feature of REM sleep, and also occur during wakefulness in the rodent hippocampus, being involved in various roles such as spatial navigation, plasticity and memory (Buzsaki, 2002). With a somewhat distinctive name, ripple oscillations are one of the fastest oscillations known (100-250Hz), originate in the hippocampal CA1 pyramidal layer, and have been proposed to gate memory transfer between the hippocampus and the cortex during sleep (Ylinen et al., 1995). Finally, a recently described rhythm (Tort et al., 2008; Scheffer-Teixeira et al., 2012) referred to as high-frequency

oscillation (HFO) spans from 110-160Hz is strongly associated with theta rhythms and may be related to memory processing (Tort et al., 2013).

A representative model of interacting oscillatory units and networks is the mammalian hippocampus. As explained by Jones (2010), theta oscillations entrain the firing rate of hippocampal cells, with most spikes occurring during specific phase windows in a theta cycle, a phenomenon usually referred to as phase-locking, which is thought to be enabled by oscillating levels of inhibition imposed on pyramidal cells. Theta oscillations seem to play a role in temporal organization in a variety of functions, such as sensorimotor integration (Caplan et al., 2003) and coordination of cell assemblies by means of phase modulating gamma oscillations (Sirota et al., 2008). The relation between the precise moment when a neuron is active (spike) and the relative phase of on-going oscillation has functional implications and has been associated, for example, to the animal's location relative to a hippocampal place-field (O'Keefe and Recce, 1993); to either encoding or retrieving of a memory (Manns et al., 2007); and to the mutual influence between dispersed neuronal groups (Womelsdorf et al., 2007). The functional relations between spike times and subjacent oscillations are becoming increasingly well established, and are currently deemed to represent the mechanism by which the brain dynamically routes information during cognitive processing (Engel et al., 2001; Buzsaki, 2010).

Probably the most well studied network-generated oscillation that is thought to influence spike timing is the gamma oscillation. Gamma oscillations are found in many regions of the mammalian brain and, as noted previously, are thought to

take part in organizing neural assembly formation. Interneuron activity is essential for synchronizing neurons in the gamma frequency, and two simplified models may explain the origin of this rhythm: the I-I model (Inhibitory-Inhibitory model, also known as ING: Interneuronal Network Gamma) and the E-I model (Excitatory-Inhibitory model, also known as PING: Pyramidal-Interneuronal Network Gamma), as reviewed in Buzsaki and Wang (2012). According to the I-I model, a network composed of mutually interconnected spiking interneurons that reciprocally activate GABA_A receptors is sufficient to generate the gamma rhythm; while the E-I model describes how a network of excitatory and inhibitory interneurons behave with volleys of fast excitation and delayed inhibition, leading to a cyclic interaction among these cells generating a rhythmic interplay in the gamma range (Buzsaki and Wang, 2012).

Other than influencing the functional significance of spiking activity, brain rhythms of different frequencies are not independent, but can rather interact in many different ways (Jensen and Colgin, 2007). There seems to be a functional role for the cross-frequency coupling (CFC) exerted by the phase of low frequency oscillations (usually delta or theta) over the amplitude of higher frequency oscillations (usually gamma or HFO), which has attracted much interest to this phenomena recently (Tort et al., 2010a). Phase-amplitude CFC correlates with brain functions such as detection of sensory signals (Handel and Haarmeier, 2009), reward signalling (Cohen et al., 2009b), decision-making (Tort et al., 2008; Cohen et al., 2009a), working memory (Axmacher et al., 2010), attention (Lakatos et al., 2008; Schroeder and Lakatos, 2009) and learning (Tort et al., 2009). Further, CFC patterns differ across brain areas (Tort et al., 2010a;

Voytek et al., 2010; Scheffer-Teixeira et al., 2012), and change dynamically in response to motor, sensory, and cognitive events (Tort et al., 2008; Canolty and Knight, 2010; Voytek et al., 2010). Theta-gamma coupling has been hypothesised to form a neural coding system that allows the representation of multiple items in a sequential order (Lisman and Buzsaki, 2008). Abnormalities in theta-gamma coupling have been thus suggested as a possible electrophysiological substrate of disordered thoughts and impaired working memory (Lisman and Buzsaki, 2008; Moran and Hong, 2011). Also, it should be noted that recent CFC studies have demonstrated that theta modulates multiple higher frequency bands, which occur within (30-100 Hz) and beyond (>100 Hz) the traditional gamma band (Tort et al., 2008; Tort et al., 2010a; Scheffer-Teixeira et al., 2012; Tort et al., 2013). For instance, theta preferentially modulates high-gamma (60-100 Hz) in CA1 and low-gamma (30-60 Hz) in CA3 (Tort et al., 2008; Tort et al., 2009; Tort et al., 2010a). Additionally, theta phase also modulates higher frequency activity circumscribed into the HFO band in *stratum oriens-alveus* (Scheffer-Teixeira et al., 2012; Tort et al., 2013). For an extended review on the functional role of CFC, see Canolty and Knight (2010).

Due to the association between neuronal oscillations and many cognitive tasks, it has been suggested that altered oscillatory activity is associated with dysfunctional cognition and behaviour (Uhlhaas and Singer, 2010). Disturbance in cortical oscillations has been suggested as a possible neural basis for symptoms found in schizophrenia (Uhlhaas and Singer, 2006; Ford et al., 2007; Uhlhaas et al., 2008; Haenschel et al., 2009; Uhlhaas and Singer, 2010; Moran and Hong, 2011; Whittington et al., 2011; Gandal et al., 2012). Aberrant oscillatory

activity in schizophrenic patients has been found in various frequency bands, including the delta-band (Sponheim et al., 1994; Keshavan et al., 1998; Boutros et al., 2008; Siekmeier and Stufflebeam, 2010); theta-band (Sponheim et al., 1994; Jansen et al., 2004; Boutros et al., 2008; Brockhaus-Dumke et al., 2008; Hong et al., 2008; Siekmeier and Stufflebeam, 2010; Kirihaara et al., 2012); alpha-band (Sponheim et al., 1994; Jin et al., 2006; Boutros et al., 2008); beta-band (Sperling et al., 1999; Tekell et al., 2005; Lee et al., 2006; Ford et al., 2008b; Uhlhaas and Singer, 2010); and more recently in the HFO band (Grutzner et al., 2013; Sun et al., 2013). In particular, aberrant gamma-frequency oscillations have been reported in schizophrenic patients (Kwon et al., 1999; Lee et al., 2003; Spencer et al., 2003; Spencer et al., 2004; Krishnan et al., 2005; Cho et al., 2006; Light et al., 2006; Uhlhaas et al., 2006; Ferrarelli et al., 2008; Flynn et al., 2008; Ford et al., 2008a; Spencer et al., 2008; Rutter et al., 2009; Spencer, 2009; Leicht et al., 2010; Mulert et al., 2010; Woo et al., 2010; Barr et al., 2011; Kirihaara et al., 2012). However, although a tantalizing amount of correlates link disrupted oscillatory activity to schizophrenia, comparison between studies is hindered by many subtle (and sometimes not so subtle) aspects that are hard to control for such as variations in recording techniques employed, electrode placement, subject's heterogeneous symptomatology, medication, and experimental setting (Jones, 2010). Finally, although CFC has been implied in several brain functions, few studies have attempted to characterize CFC in schizophrenia (Allen et al., 2011; Kirihaara et al., 2012), and have found divergent results.

1.2 Schizophrenia and the glutamate hypothesis

According to the Diagnostic and Statistical Manual of Mental Disorders (DSM-IV-TR, American Psychiatric Association, 2000): Schizophrenia is a chronic debilitating mental disease of unknown aetiology that is characterized by positive symptoms (excess or distortion of normal functions) such as irrational beliefs (delusions) and perceptions (hallucinations), and grossly disorganized or catatonic behaviour; negative symptoms (diminished or loss of normal functioning) such as lack of goal-oriented behaviour (avolia), distorted speech and thought (alogia) and lack of emotional empathy (blunted affect) and social withdrawal; and general cognitive impairment (American Psychiatric Association, 2000). A recent meta-analysis by McGrath and collaborators (2008) indicated that schizophrenia has an incidence of approximately 0.7% worldwide with a considerable geographical variation on its incidence, and also some novel associations such as males being 40% more affected than females, and schizophrenia being associated with urban settings, high latitude and migration (McGrath et al., 2008).

We acknowledge that a new version of the DSM has recently been released (DSM-5, American Psychiatric Association, 2013), but since it has received much criticism by both the psychiatric and the scientific community (more on the topic on <http://en.wikipedia.org/wiki/DSM-5#Criticism>), we opted to use the definitions found in the DSM-IV-TR. Moreover, the latter has been the reference standard for schizophrenia research over the past 13 years and therefore is more faithful to most of the literature reviewed here.

To date, all psychiatric drugs that effectively alleviate psychotic symptoms block the D₂ dopamine receptor to some degree (Tort, 2005; Coyle, 2006; Kapur et al., 2006). This observation led to the proposition that dopaminergic mechanisms are central to schizophrenia, particularly psychosis, which became known as the dopamine hypothesis of schizophrenia, and has been presented in at least three different increasingly sophisticated formats since it first appeared in the 70's (see Howes and Kapur, 2009 for an up-to-date review and the most recent format of this hypothesis). Although enduring and influential, the dopamine hypothesis is an acknowledged poor model of negative symptoms and patterns of cognitive deficit associated with schizophrenia (Javitt et al., 2012). Further, both typical and atypical antipsychotics are ineffective against most negative symptoms and cognitive impairments, leaving a substantial burden even on medicated patients (Coyle, 2006). The fact that noncompetitive and nonselective antagonists of the NMDAR, such as phencyclidine (Javitt and Zukin, 1991) and ketamine (Krystal et al., 1994), when administered to healthy subjects consistently induce most symptoms of schizophrenia, caused the main focus of pharmacological models of schizophrenia to change from dopaminergic to glutamatergic dysfunction (Coyle, 2006; Frohlich and Van Horn, 2013). Moreover, the glutamate hypothesis encompasses negative and cognitive symptoms of schizophrenia, and potentially explains dopamine dysfunction itself (Moghaddam et al., 1997; Javitt et al., 2012).

In its simplest form, the glutamate hypothesis proposes that NMDAR hypofunction might *"be viewed as a model for a disease mechanism that could explain the symptoms and natural course of schizophrenia"* (Olney et al., 1999). It

does not suggest that glutamate is the main nor the only neurotransmitter responsible for the complex and heterogeneous subset of alterations found in schizophrenia, but rather that the NMDAR hypofunction might lead to downstream neurochemical dysfunction in multiple neurotransmitter systems (including glutamate, GABA, acetylcholine, serotonin and dopamine), and that schizophrenia symptoms result from these multiple neural malfunctions (Jentsch and Roth, 1999). In other words, the aetiology of schizophrenia may involve dysfunction of the NMDAR, or it may alternatively involve downstream effects that can be modelled by NMDAR blockade (Olney et al., 1999). Alternatively, it has been suggested that schizophrenia may not exist as a unitary disease per se, but rather is a syndrome composed of overlapping phenotypical alterations with various aetiologies, suggesting a need for a reconceptualization of what schizophrenia means (Keshavan et al., 2011).

Two of the major arguments in favour of the glutamate hypothesis are that NMDAR blockade induces most core symptoms of schizophrenia, including negative, positive, and cognitive symptoms (Javitt and Zukin, 1991; Krystal et al., 1994; Newcomer et al., 1999); and that there is a remarkable resemblance between genuine and drug-induced psychotic symptoms. Lahti et al. (2001) administered sub-anaesthetic doses of ketamine to healthy and schizophrenic volunteers and found that all subjects had an acute increase of psychotic symptoms that was dose-dependent and that 70% of the schizophrenic subjects reported an increase of previously experienced symptoms. Also, the prolonged use of phencyclidine (PCP) is more similar to the schizophrenia symptomatology both quantitatively (duration of symptoms) and qualitatively (e.g. auditory

hallucinations become more frequent than visual hallucinations) compared to the acute use of this substance [see Jentsch and Roth (1999) for a review on this topic].

Other psychotomimetic drugs have been proposed as models of schizophrenia (Javitt et al., 2012). Dopamine agonists such as amphetamines and methylphenidates, for example, induce only positive symptoms (Javitt et al., 2012) and cause heterogeneous responses in schizophrenic patients (van Kammen et al., 1982 apud Lahti et al., 2001). Serotonin agonists such as d-lysergic acid diethylamide (LSD) and psilocybin induce psychedelic experience *“with vivid hallucinatory experience, fusion of visual and other sensory experiences, and emotional alterations”* (Aghajanian and Marek, 2000), but with less correspondence to schizophrenia symptomatology when compared to NMDAR blockade (Lahti et al., 2001). Finally, based on recent reports that postnatal NMDA ablation exclusively in interneurons recapitulates most behavioural abnormalities induced by NMDAR blockade (Belforte et al., 2010; Korotkova et al., 2010; Carlen et al., 2011), a novel theory has been put forward suggesting that the NMDAR hypofunction model acts mainly through the GABAergic system (Nakazawa et al., 2012). We would like to add that, in our view, none of these models is necessarily completely right, nor completely useless, and that due to the widespread presence of NMDAR in the brain, it is reasonable to suggest that NMDAR dysfunction may affect all of these neurotransmitter systems, and that what actually remains to be explained is the precise correspondence between each of these neurochemical malfunctions and the unique symptoms of schizophrenia.

1.3 Brief history of phencyclidine and ketamine

PCP is a synthetic cyclohexylamine developed in 1956 by the Parke Davis Company (Maddox et al., 1965 apud Domino, 2010). Early preclinical testing on animals had indicated that PCP *“caused an excited drunken state in rodents, but a cataleptoid immobilized state in pigeons (...) produced canine delirium. In monkeys, it was a remarkable anaesthetic”* and clinical tests indicated that *“As in monkeys, phencyclidine was a safe anaesthetic in humans”* (Domino, 2010). The first record of psychotic symptoms associated with PCP appeared soon, when Luby and collaborators tested it on healthy and schizophrenic subjects and found that the drug had *“an impressive similarity to the schizophrenic syndrome”* (Luby et al., 1959 apud Domino, 2010). With more clinical studies, it became clear that PCP was not suitable for human anaesthesia. At this point new PCP-derived drugs were synthesized and screened in preclinical studies at Parke Davis, and one of these new substances produced excellent anaesthesia and was short acting, suggesting it would serve as an adequate replacement to PCP. Initially called ‘CI-581’, this new drug was first synthesized in 1962 (Dorandeu, 2013) and studied in humans in 1964, yielding safe general anaesthesia with minimal emergence delirium (Domino, 2010). In order to facilitate the approval from the American Food and Drug Administration for human use, Parke Davis Company decided not to contact Dr. Luby to carry out human trials, believing he would conclude that ketamine mimicked schizophrenia similarly to PCP (Domino, 2010). As an alternative, Parke Davis’ own psychiatrists tested the drug in humans and officially concluded it led to altered states such as *“dreaming”*, and came up with the euphemistic coinage of *“dissociative anaesthesia”*, a term that is still used

today, in order to describe the feeling of being disconnected from the body and from the environment when emerging from the drug effects (Domino, 2010). In spite of the transient psychotomimetic effects such as delusions, severe anxiety and agitation (referred to in the clinical literature as emergence phenomena), the large margin of safety of ketamine assured its widespread usage in veterinary (Green et al., 1981) and medical practice, ranging from paediatric settings to battlefield anaesthesia (Reich and Silvey, 1989).

Another common use of PCP and ketamine is as a recreational drug or as a drug of abuse. Although PCP use in humans was discontinued in 1965, and rarely used in veterinary practice, many clandestine laboratories have manufactured PCP since the mid 60's (Petersen and Stillman, 1978). At first it was referred to as the PeaCe Pill (notice the acronym) and later became more known as Angel Dust. PCP users have reported that the desired effect induced by the drug relates to feeling of dissociation, mood elevation, inebriation and relaxation, but are acknowledged as being far less frequent than the induced negative effects (Petersen and Stillman, 1978). Due to the ease to synthesize it, PCP is often found mixed to other illicit drugs with the intent of generating a "more intense high". PCP can be administered in many ways, such ingestion, smoking, inhaling or injection, and is associated with violent crimes (Siegel, 1978).

Ketamine, on the other hand, has a somewhat less tragic history as a drug of abuse and more widespread use as a recreational drug. Initially employed by many new-age spiritualists as an entheogen ("generating the divine within") during the 70's (Jansen, 2004; Domino, 2010), and has been referred to as "the

latest futile attempt to cleanse Blake's 'doors of perception' by chemical means" (Pai and Heining, 2007). The vast availability of ketamine vials in veterinary and hospital supplies granted its place as one of the safest and easiest to acquire hallucinogens of modern society (Jansen, 2004). Ketamine is usually diverted or stolen from legitimate supplies, and became a regular "club drug" used mainly in dance settings like *rave parties*, particularly in Europe, being often mixed with ecstasy (Wolff and Winstock, 2006), and known by various slang names such as Special K, vitamin K, K, Super K, Ketaset, Ket, Kit Kat, Kizzo, CatValium, Bump, Jet, Super Acid, Mean Green, Monkey Mix, and Monkey Business. With a good physical safety profile when used in sub-anaesthetic doses, and fast acting effects (lasting for one hour or less), the main concerns about the non-medical use of ketamine regard the lack of self-preservation and confusion users experience after drug use, the increased susceptibility to aggression and problems with compulsive use and addiction (Jansen, 2000; Wolff and Winstock, 2006). Also, prolonged abuse of ketamine has been associated with urinary tract problems (Chu et al., 2008).

A third NMDAR noncompetitive blocker often used in animal studies as a model of psychosis and schizophrenia is dizocilpine, also known as MK-801. Developed by Merck at 1982, MK-801 has a similar effect on NMDARs (in spite of being structurally unrelated to PCP), but is much more potent and has longer lasting effects (Ogden and Traynelis, 2011). Because of its low safety profile, dizocilpine is less used in veterinary and clinical settings, making it difficult to perform translational studies.

1.4 NMDAR blockade pharmacology

NMDA receptors are glutamatergic ionotropic channels located throughout the brain and spinal cord better known for their role as cationic postsynaptic channels. In order to be activated, NMDARs require the binding of glutamate and two additional elements: a co-agonist, either glycine or D-serine, which are mainly derived from astrocytes; and the depolarization of the postsynaptic terminal at roughly the same time that glutamate is released from the presynaptic terminal. The postsynaptic depolarization causes the displacement of the Mg^{++} ion that blocks the NMDAR pore at the resting membrane potential. The fact that NMDAR activation requires voltage-dependent events at both the pre and postsynaptic terminal confers these receptors the unique role of molecular coincidence detectors, a key element in spike-time-dependent synaptic plasticity (Sanz-Clemente et al., 2013). NMDARs are also expressed at extra, peri and presynaptic sites, where they participate in functions such as neuronal survival, nitric oxide release and regulating spontaneous and evoked excitatory postsynaptic currents (Paoletti et al., 2013).

NMDARs' structure is heterogeneous across brain regions, and present an overwhelming functional diversity depending on its composition (see Paoletti et al., 2013 for a recent review). NMDARs are commonly composed of four different subunits, and typically are di-heteromers composed of two GluN1 and either two GluN2 or GluN3 subunits, which are assembled as a dimer of dimers, although tri-heteromers also exist (Sanz-Clemente et al., 2013). There is only one gene that encodes the GluN1 subunit, but due to alternative splicing there are eight

known isoforms, each with unique gating and pharmacological properties. There are four different GluN2 subtypes, which are responsible for most of the NMDAR's functional variability, and are differentially expressed at various development stages. There are three kinds of GluN3 subunits, all of which have different gating properties and do not bind to glutamate, creating the curious scenario in which NMDARs formed exclusively by GluN1 and GluN3 subunits function as glycine receptors, without the participation of glutamate and with distinct pharmacological characteristics (Sanz-Clemente et al., 2013). Furthermore, NMDAR composition is plastic both during development and in adults, and can occur within minutes (Paoletti et al., 2013). Also, NMDARs are mobile and can move laterally between synaptic and nonsynaptic regions, permitting subtle regulations in receptor numbers and subunit composition. Finally, the complexity of NMDAR functioning is increased by the existence of atypical non-neuronal NMDARs in astrocytes and oligodendrocytes (Paoletti et al., 2013).

Typical NMDAR blockers such as PCP, ketamine and MK-801 are noncompetitive antagonists that target the most highly conserved part of the NMDA receptor, sometimes referred to as the phencyclidine receptor, and present little selectivity (<10-fold) for NMDA receptor subunits (Ogden and Traynelis, 2011). Additionally, ketamine is known to decrease the frequency of channel opening by an allosteric mechanism (Orser et al., 1997), although the functional significance of this modulation is currently unknown. Given that NMDARs blockers have been known for 50 years, until recently there was a surprisingly limited amount of pharmacological tools available for discriminating between NMDAR receptor

subtypes (Paoletti and Neyton, 2007). Until then, Ifenprodil and associated compounds were the only synthetic tools known to selectively block NMDAR subunits, having a >400 fold selectivity for the GluN2B subunit (Williams, 1993 apud Paoletti and Neyton, 2007); while zinc was found to selectively antagonize GluN2A-containing receptors at low (nanomolar) concentrations (Paoletti et al., 1997 apud Paoletti and Neyton, 2007). Recent years have witnessed a spur of interest in NMDAR pharmacology with the discovery of new allosteric modulatory binding sites, as well the advent of novel selective antagonists for NMDAR subunits (see Ogden and Traynelis, 2011 for a review). Future studies with these selective blockers will surely increase our current knowledge regarding the involvement of different types of NMDARs in the various schizophrenia symptoms modelled by NMDAR blockade.

Chen and collaborators were the first to document the effects of NMDAR blockade in animals, in preclinical screening tests at Parke Davis Company, with phencyclidine being tested in 1959 and ketamine (at the time known as CI-581) in 1965 (Domino, 2010). From these early experiments it became clear that both drugs caused excitation at low doses and had a cataleptic effect at higher doses (Chen et al., 1966), while it also became clear that both drugs differed in some aspects, with high doses of phencyclidine inducing convulsion, whereas ketamine induced deep anaesthesia even at the highest doses (Chen et al., 1966). However, since an influential review by Javitt and Zukin concluded that the PCP psychotomimetic effects in humans are induced by very low concentrations of the drug, in which PCP binds the NMDA receptor selectively (Javitt and Zukin, 1991), it is generally accepted that the behavioural effects induced by sub-

anaesthetic doses of PCP and ketamine are mediated exclusively by NMDAR blockade. For this reason, it is usual to see studies using PCP, ketamine, MK-801 interchangeably in order to induce NMDAR blockade, regardless of the pharmacological differences between these compounds (but see Gilmour et al., 2009; Gilmour et al., 2012).

Although PCP and ketamine are mainly regarded as noncompetitive and nonselective NMDA channel blockers, they also bind to other receptors presenting unique pharmacological profiles. Philip Seeman's group (Kapur and Seeman, 2002; Seeman et al., 2005) found in *in vitro* assays that both PCP and ketamine at concentrations similar to those required to induce psychotomimetic effects also bind to D₂ dopamine and 5-HT₂ serotonin receptors. These results, however, are not corroborated by findings from other laboratories (Nishimura and Sato, 1999; Rabin et al., 2000; Aalto et al., 2002; Liu et al., 2006), and have been contested on more than one occasion (Svenningsson et al., 2003; Svenningsson et al., 2004; Jordan et al., 2006) generating some heated argumentation (Seeman, 2004; Seeman et al., 2009). If proved true, this lack of specificity raises serious problems concerning the use of these drugs as evidence in favour of the glutamate hypothesis of schizophrenia. However, as suggested in the section above, this limitation would not be fatal for the current study, nor for the enterprise of modelling schizophrenia in general. In the words of Seeman et al. (2005): *"even if ketamine and PCP are non-specific in vivo, it does not invalidate the ketamine/PCP as models for studying schizophrenia. It could well be that schizophrenia itself is a multi-transmitter dysfunction and ketamine and PCP, by virtue of their relatively broad-based neurotransmitter perturbation, provide a*

better model of the complexity of this illness than a primary dopaminergic or a primary hypoglutamate model."

Ketamine is widely used in translational studies, and is often reviewed in the literature to account for updates in research both in clinical and veterinary settings as an anaesthetic, as well as its uses as a research tool, particularly as a model of schizophrenia (Frohlich and Van Horn, 2013; Kocsis et al., 2013). The ketamine molecule (RS)-2-(2-Chlorophenyl)-2-(methyldamino)cyclohexanone has a molecular weight of 238. Ketamine is highly soluble in lipids and crosses the blood-brain barrier efficiently, reaching concentrations 3-5 times higher in the rat brain than in the serum (Pai and Heining, 2007; Palenicek et al., 2011). It is metabolized in the liver where it undergoes demethylation and hydroxylation, and its metabolites are conjugated and excreted in the urine. Norketamine is the main ketamine metabolite. It has approximately 25% of the activity of the original compound and reaches up to 2 times the ketamine concentration in the serum, but is less efficient in crossing the blood-brain barrier, reaching roughly the same concentration of ketamine in the brain. In both humans and rodents, ketamine and norketamine reach peak levels in the serum and in the brain within 10 minutes, and return to base levels within 60-240 minutes (although the total clearance time varies depending on the dosage) (Pai and Heining, 2007; Palenicek et al., 2011).

Ketamine is a chiral compound and is available in both racemic mixtures and in its enantiomer forms (S+ ketamine and R- ketamine), which exhibit pharmacological and clinical differences. S+ ketamine is approximately 4 times

more potent as a NMDAR blocker than the racemic mixture, is less psychotomimetic in humans (White et al., 1985) and rodents (Liu et al., 2006), and has a faster recovery time, making it a more adequate choice for use in human anaesthesia than the racemic mixture (Pai and Heining, 2007). Other pharmacological differences between the enantiomers are shown below (Table 1).

Table I. Affinity of ketamine enantiomers for various receptors

Receptor	K _i (μmol/l)	
	S+ ketamine	R- ketamine
NMDA receptor ¹	0.9	2.5
Opioid μ receptor ¹	28.6	83.8
Opioid κ receptor ¹	23.7	60.0
Opioid δ receptor ¹	205.0	286.0
σ receptor ¹	131.0	19.0
Acetylcholine (muscarinic) ¹	125.0	91.0
Dopamine transporter ¹	46.9	390.0
Noradrenaline transporter ¹	64.8	68.9
Serotonin transporter ¹	156.0	148.0
NMDA receptor ²	1.82	2.7
D ₂ receptor ²	–	–
5-HT ₂ receptor ²	–	–
HCN receptors ³	7.4	23.8 (inferred)

K_i = inhibition constant; ¹ from Nishimura and Sato (1999); ² from Liu et al. (2006); ³ from Chen et al. (2009). We note that the racemic mixture of ketamine is composed of equal amounts of its enantiomers.

Ketamine also induces mild tachycardia, increased blood pressure, and a minimal decrease in ventilation, with these being the main reasons for its high safety profile as an anaesthetic (Pai and Heining, 2007).

Ketamine increases cerebral metabolism, cerebral blood flow, and intracranial pressure, which might account for a hitherto little studied mechanism of action

(Jerabek et al., 2010), and probably induce alterations in brain temperature [as is the case for MK-801 (Colbourne et al., 1996)], that acknowledgedly affect neuronal functioning (Andersen and Moser, 1995; Kim and Connors, 2012).

Novel therapeutic approaches have been proposed for ketamine as a treatment for chronic pain and depression. Ketamine is effective in the treatment of opioid resistant chronic pain (Bell, 2009), and can be used to reduce opioid requirements and chronic postsurgical pain (Quibell et al., 2011). These effects are thought to be mediated by ketamine's action as an antagonist of nitric oxide release (Lin et al., 1996). Antidepressant effects of very low doses of ketamine were first documented in 2000 (Berman et al., 2000), and have been shown to occur within 2 hours of a single injection, and last for up to 1 week afterwards (Zarate et al., 2006). This hot topic of research is on going, and recent findings suggest that the antidepressant effect is mediated by the synthesis of brain-derived neurotrophic factor (Autry et al., 2011) and by an increased formation of spine synapses in the prefrontal cortex (Li et al., 2010).

1.5 Evidence for NMDAR dysfunction in schizophrenia

In addition to the observation that NMDAR blockade exacerbates symptoms in schizophrenics and produces behaviour in healthy subjects that mimics schizophrenia's psychotic, negative, and cognitive symptoms (Javitt and Zukin, 1991; Krystal et al., 1994; Lahti et al., 1995a; Lahti et al., 1995b; Malhotra et al., 1996; Lahti et al., 2001), a wealth of converging evidence implicates NMDAR dysfunction in the pathophysiology of schizophrenia (Kantrowitz and Javitt, 2010; Javitt et al., 2012). Post-mortem studies from various groups have found that schizophrenia is associated with disrupted NMDA signalling (Tsai and Coyle, 2002; Woo et al., 2004; Hahn et al., 2006; Kristiansen et al., 2007; Beneyto and Meador-Woodruff, 2008). Moreover, a recent study of ante-mortem and post-mortem cohorts of schizophrenics found lower expression of various NMDAR subunits in the prefrontal cortex, and genetic variations related to the expression of NMDAR subunits predicted significantly lower reasoning ability in schizophrenia (Weickert et al., 2013). Of note, many of the neuroanatomical abnormalities consistently found in schizophrenia are located in the hippocampus (Benes, 1999; Harrison, 2004), suggesting that the hippocampus may be central to the neuropathology and pathophysiology of schizophrenia.

In animals, acute, sub-chronic and chronic sub-anaesthetic NMDAR blockade induces behavioural (Ellison, 1995; Andine et al., 1999; Ma and Leung, 2000; Becker et al., 2003; Becker and Grecksch, 2004; Imre et al., 2006; Littlewood et al., 2006; Rujescu et al., 2006; Chen et al., 2009; Chatterjee et al., 2011; Sabbagh et al., 2012), biochemical (Moga et al., 2002; Keilhoff et al., 2004; Cunningham et

al., 2006; Rujescu et al., 2006; Harte et al., 2007; Romon et al., 2011) and electrophysiological alterations (Leung and Desborough, 1988; Ma and Leung, 2000; Cunningham et al., 2006; Pinault, 2008; Roopun et al., 2008; Ehrlichman et al., 2009; Hakami et al., 2009; Lazarewicz et al., 2010; Anver et al., 2011; Kittelberger et al., 2012; Kocsis, 2012) that resemble those found in schizophrenia (Bubenikova-Valesova et al., 2008; Gonzalez-Burgos and Lewis, 2012; Frohlich and Van Horn, 2013; Hunt and Kasicki, 2013; Kocsis et al., 2013).

Referring specifically to electrophysiological findings, Ma and Leung (2000) showed that phencyclidine induced hyperlocomotion and increased gamma oscillations. Other studies in rodents have shown that ketamine increases the power of gamma (Pinault, 2008), (Kittelberger et al., 2012) and delta (Zhang et al., 2012) oscillations, and may differentially affect theta power depending on recording region (Lazarewicz et al., 2010; Kittelberger et al., 2012; Hinman et al., 2013). Some of the effects induced by ketamine such as increased gamma oscillations have been dissociated from its motor effects, and are found even in deeply anesthetized animals (Hakami et al., 2009). Of note, humans treated with ketamine display abnormalities in the delta, theta, alpha and gamma bands mimicking those found in schizophrenia (Hong et al., 2010), giving further support to the pharmacological validity of studying the electrophysiological effects of ketamine in translational animal studies.

Recent studies with transgenic animals have generated some compelling evidence linking NMDAR dysfunction with behavioural and electrophysiological abnormalities found in schizophrenia. An animal model with postnatal ablation

of the GluN1 NMDAR subunit restricted to corticolimbic interneurons presented distinct schizophrenia-like symptoms that emerged after adolescence (Belforte et al., 2010). Further, postnatal ablation of NMDAR subunits in a specific subpopulation of PV+ interneurons resulted in aberrations in the gamma band that resemble those found in schizophrenia (Korotkova et al., 2010; Carlen et al., 2011).

In all, accumulating evidence from studies using different techniques suggest NMDAR dysfunction in schizophrenia, and NMDAR dysfunction in animals is sufficient to recapitulate many schizophrenia symptoms, giving support to the construct validity of the NMDAR hypofunction animal model for schizophrenia. Although this model has intrinsically little face validity (which in all honesty is a shared featured of all psychotomimetic animal models due to the inherent complexity of inferring mind states in non-human animals), NMDAR blockade is deemed to have a reasonable construct and predictive validity (Large, 2007), warranting further studies into the complex phenotypical aberrations induced by NMDAR disruption and its relations to schizophrenia symptoms (Adell et al., 2012).

2. Thesis aim

Although electrophysiological alterations have been described in schizophrenia and in its animal models, no study has provided a thorough analysis of the electrophysiological alterations in the hippocampus induced by acute NMDAR blockade, and particularly almost no attention has been given to alterations in CFC. The aim of the experiments presented in this thesis is to characterize the behavioural and electrophysiological alterations in the CA1 region of the hippocampus induced by acute administration of ketamine in adult rats. We focused on cognitively relevant LFP frequency bands such as delta (1-4Hz), theta (5-10Hz), gamma (30-100Hz) and high-frequency oscillations (HFO; 110-160Hz), as well as on theta-high gamma and theta-HFO cross-frequency coupling (CFC).

We hypothesized that theta-HG and theta-HFO CFC might be disrupted during the period associated with psychotomimetic effects of ketamine, which is marked by altered behaviour. Also, we wanted to inspect whether the alterations previously described in the delta, theta and gamma frequency bands were similar across hippocampal CA1 layers or varied in different cellular laminae.

A better understanding of the electrophysiological alterations induced in this animal model for schizophrenia, as well as its behavioural correlates, might suggest novel translational markers for further research, as well as give insights into the network alterations of hippocampal function associated with psychotic symptoms.

3. Methods

3.1 Ethical aspects

Animal care and surgery procedures were approved by the Edmond and Lily Safra International Institute of Neuroscience of Natal Committee for Ethics in Animal Experimentation (permit 02/2011- Annex A); and by the *Universidade Federal do Rio Grande do Norte* Committee for Ethics in Animal Experimentation (permit 60/2011 – Annex B).

3.2 Surgical implantation of electrodes

Eight male Wistar rats (2-3 months old, 280–380g), born and raised in our breeding colony, kept under a 12 h light-dark cycle (lights on at 07:00) with food and water ad libitum, were used in the experiments. Seven animals were anesthetized with intraperitoneal (IP) ketamine hydrochloride and xylazine hydrochloride (100 and 10 mg/kg, respectively; Agener União - Brazil) and chronically implanted in the left dorsal hippocampus with one electrode bundle (Figure 1) consisting of 8 vertically staggered polyimide insulated tungsten microwires (California Fine Wire, Grover City, CA) with a diameter of 50 μ m¹. Electrodes were vertically aligned and spaced by 250 μ m, spanning from CA1 *stratum oriens-alveus* to the hilus of the dentate gyrus (deepest electrode in AP: -3.6mm, ML: -2.5mm, DV: -3.5mm).

¹ Of note, the microelectrodes used in our study yield excellent recording quality of LFP signals, but not of spiking activity. In order to improve the neuron yield, (which was not the focus of the present study) we found that microelectrodes of smaller diameter (12-35 μ m) with low impedance (0.2-0.5M Ω) were far more consistent in recording spiking activity, and should be preferred in studies that address the activity of multi-unit and/or single neurons.

The placement of electrodes in CA1 was confirmed by inspecting coronal brain sections stained with cresyl violet (Figure 2 and Annex C). In two animals we also estimated the electrode's positioning during surgery by means of evoked response to perforant path stimulation with a single pulse of 500 μ A (Figure 2).

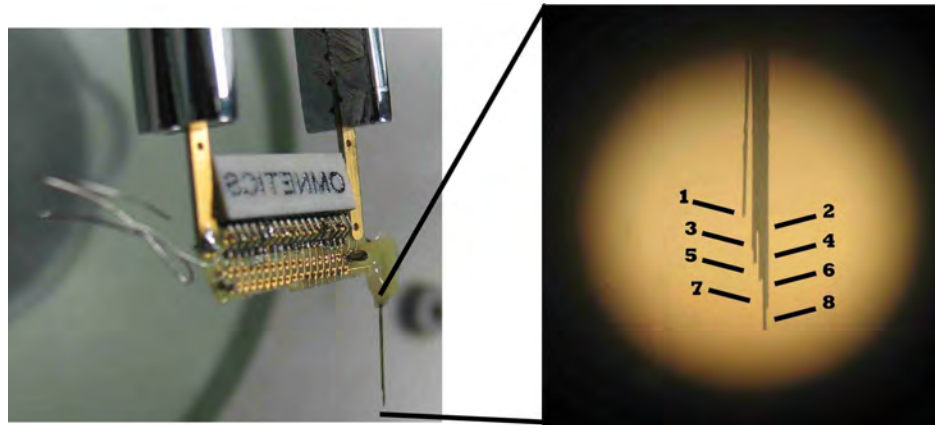


Figure 1. Typical electrode bundle used in the experiments. Left: electrode array during the fabrication process. Right: magnified view of the tips of the 50 μ m electrodes.

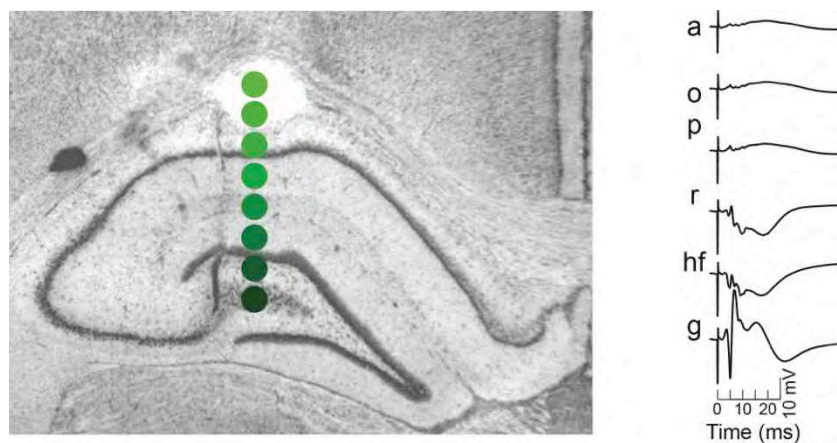


Figure 2. Left: Nissl stained histology evidencing electrode track lesion across the dorso-ventral depths of hippocampal CA1. Estimated electrode depths are indicated by green dots at the right of the lesion. Right: Typical responses evoked by perforant path stimulation during surgery and estimated positions for the first five electrodes, which are located across CA1 layers, and for the seventh electrode, in the dentate gyrus. a= *stratum alveus*; o = *stratum oriens*; p = *stratum pyramidale*; r = *stratum radiata*; hf = hippocampal fissure; g = granular layer.

However, we realized that this procedure was not reliable enough, as the signal recorded in the freely behaving animals was different from that anticipated during surgery, suggesting that the electrodes' tips had changed their depths after surgery (probably due to accommodation of the nervous tissue during the recovery period). Therefore, electrode position was inferred in all animals based on standard electrophysiological parameters recorded while the animals behaved freely after recovering from surgery. The parameters used were the presence of ripple oscillations and multi-unit activity at the pyramidal cell layer, theta phase reversal across *stratum radiatum* (Brankack et al., 1993), maximal theta power at the hippocampal fissure (Bragin et al., 1995), and depth profile of theta CFC comodulogram pattern (Figure 3, and see section 3.9 for methods used to calculate comodulograms).

One additional animal was implanted with a 16-site probe across the left hippocampus (NeuroNexus Technologies; site area: $703\mu\text{m}^2$; separation: $100\mu\text{m}$; impedance: $1\text{-}1.5\text{M}\Omega$; location: AP: -3.6mm , ML: -2.5mm). All recordings were referenced to an epidural screw electrode implanted in the right parietal bone.

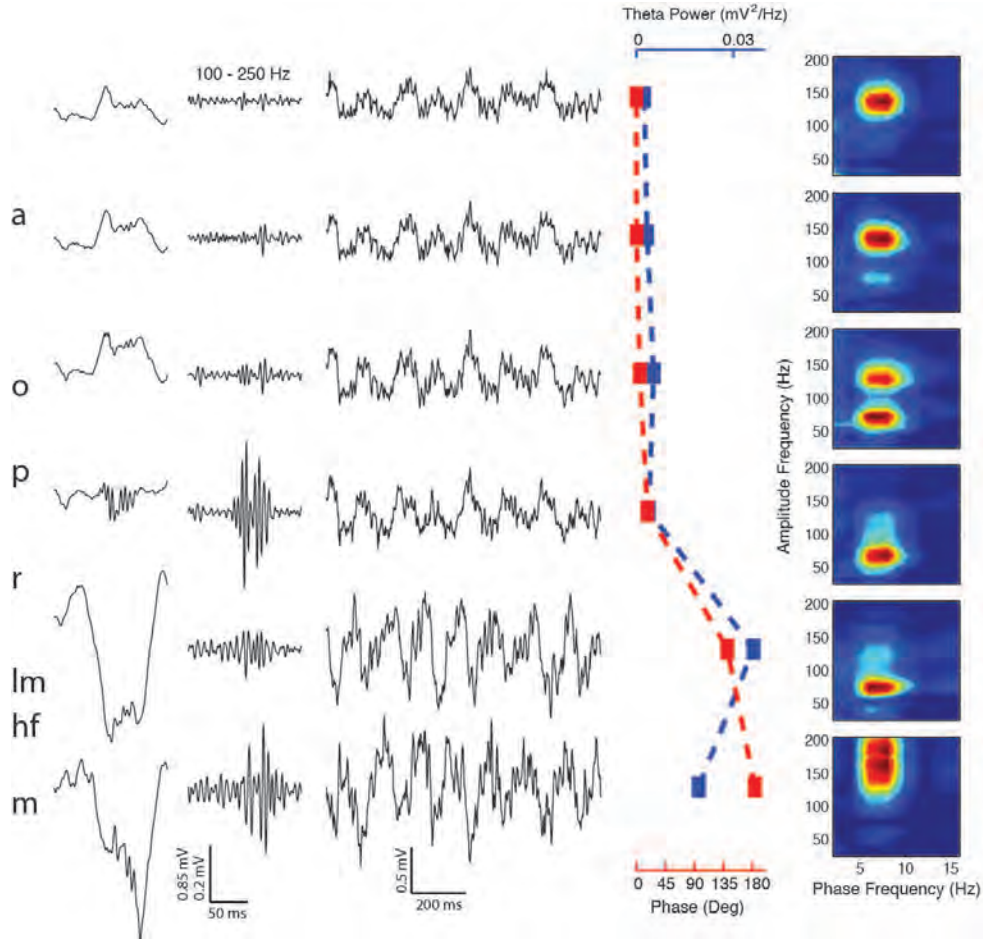


Figure 3. Electrophysiological markers across CA1 hippocampal layers used in order to verify electrode positioning. Six electrodes from a representative animal were used to depict ripple events in the raw LFP (first column) and in the filtered LFP in the 100-250Hz band (second column) recorded during awake period without overt locomotion; and one second of raw LFP presenting high theta activity (third column). Peak theta power (blue rectangles) and phase difference in relation to the most superficial electrode (red rectangle) are shown for a period of 300 seconds of high locomotor activity, as well as the CFC patterns of theta-HG and theta-HFO coupling found for each electrode in the same period (see section 3.9 for methods used to calculate comodulograms). Electrophysiological markers of hippocampal depth such as increased ripple activity near the pyramidal layer, theta phase reversal and increased theta power toward deeper electrodes, as well as different CFC patterns across hippocampal strata were used for all animals to ensure electrode positioning in the hippocampus during data analysis. Estimated CA1 strata are indicated in the leftmost column. a-stratum alveus; o-stratum oriens; p-stratum pyramidale; r-stratum radiatum; lm-stratum lacunosum-moleculare; hf-hippocampal fissure; m-molecular layer. Adapted with permission from Scheffer-Teixeira et al., 2012.

3.3 Experimental procedures

After recovering for 7-10 days, animals were individually habituated to the recording room and to the experimenter for 3 days. Experiments consisted of electrophysiological and video recordings of freely moving rats in a rectangular arena (50x40x40 cm) placed in a dimly lighted room. Recordings consisted of 3 stages: animals were first allowed to explore the arena for one hour (basal); then were injected with saline and recorded for another hour (saline); finally, animals received a single ketamine injection of either 25 (n=6 rats), 50 (n=7 rats) or 75mg/kg (n=5 rats) and were recorded for three additional hours (ketamine). All injections were intraperitoneal (IP). Depending on the stability of the recordings, each rat received up to 3 different doses separated by at least 3 days. All animals were first tested under the effect of 50mg/kg of ketamine, and then in randomized order under the effect of either 25 or 75mg/kg.

It should be noted that there is no current consensus on what would be an adequate dose of ketamine for rodents that would mimic the drug-induced psychotic episodes observed in humans. Although the original studies that associated acute ketamine with psychosis used intravenous injection and found that 0.5mg/kg, but not 0.1mg/kg, induced psychotomimetic effects that lasted for approximately one hour (Krystal et al., 1994), most animal studies employ SC and IP routes of administration, making it difficult to draw precise comparisons. Ketamine effects vary widely across species (Green et al., 1981): while 1-4mg/kg of intravenous (IV) ketamine induces deep anaesthesia in humans, 20mg/kg of IV ketamine induces only hypnosis in rats (Cohen et al., 1973). Complicating matters even further, subdermic injections of 10 mg/kg in rats induce similar

behavioral and electrophysiological effects as those observed after 20-40 mg/kg of IP injections (Kittelberger et al., 2012). Used in isolation, the reported anaesthetic dose of ketamine in rats is 200mg/kg IP (Moghaddam et al., 1997).

3.4 Electrophysiological recordings

Continuous recordings were performed using a multi-channel acquisition processor (MAP, Plexon Inc). Local field potentials (LFPs) were pre-amplified (1000x), filtered (0.7–300Hz), and digitised at 1000Hz.

3.5 Behavioural analysis

Animals were video-recorded at 30 frames/second. Tracking of the animals position was made using MouseLabTracker an open-source MATLAB version of a previously described software (Tort et al., 2006) that is freely available for download at (<http://www.neuro.ufrn.br/software/mouselabtracker>). In order to avoid measuring small movements such as head and tail movements, only displacements $\geq 2.0\text{mm/frame}$ were considered. Locomotor activity was binned into 5 minutes blocks.

3.6 Data analysis

We analysed behavioural and electrophysiological data by using proprietary toolboxes and custom-made routines in MATLAB (MathWorks, Natick, MA).

3.7 Filter settings and extraction of the instantaneous phase and amplitude

Filtering was obtained using a linear finite impulse response filter by means of the eegfilt function from the EEGLAB toolbox (<http://scn.ucsd.edu/eeglab/>),

which applies the filter forward and then again backwards to ensure that phase delays are nullified. The instantaneous amplitude and phase time series of a filtered signal were computed from the analytical representation of the signal based on the Hilbert transform (hilbert function, Signal Processing Toolbox).

3.8 Spectral analyses

Power spectra density (PSD) estimation was done by means of the Welch periodogram method using the pwelch function from the Signal Processing Toolbox (50% overlapping 4 seconds Hamming windows). The mean power over frequency ranges of interest [delta (1-4Hz), theta (5-10Hz), gamma (30-100Hz) and high-frequency oscillations (HFO; 110-160Hz)] was calculated for each electrode individually, then averaged across electrodes and animals. Phase coherence was calculated using the multitaper method by means of the coherencysegc function from the Chronux toolbox [as described in Mitra and Bokil (2007) and available for download at <http://chronux.org/>] with parameters TW = 3 and K = 5 tapers, and window length of 4 seconds. Phase coherence was averaged from all electrode pairs in all animals. Power and phase coherence time-courses were obtained by averaging their values in 5 minutes blocks.

3.9 Estimation of phase-amplitude coupling and comodulation maps

To assess phase-amplitude CFC, we used the Modulation Index (MI) recently described (Tort et al., 2008; Tort et al., 2010a). This index measures coupling strength between two frequency ranges of interest: a phase-modulating and an amplitude-modulated frequency. The comodulation map is obtained by

expressing the MI for several frequency band pairs (4Hz bin width with 2Hz steps for phase-modulating, and 10Hz bin width with 5Hz steps for phase-modulated frequencies) in a bi-dimensional pseudocolour plot. As illustrated in Figure 4, in order to compute each entry of the comodulation map (top left), the raw LFP (top right) signal is band-pass filtered into two frequencies: a phase-modulating frequency (i.e. theta) and an amplitude-modulated frequency (i.e. high-gamma). Next, the phase (third row) and amplitude (fourth row, thick line) time series are calculated from each of the filtered signals and used to compute phase-amplitude distribution-like plots (bottom left). In this example, “**a**” shows the mean 80Hz amplitude distribution over 20° phase bins of the 8Hz oscillation, and “**b**” shows the mean 80Hz distribution over 20° phase bins of the 16Hz oscillation.

The modulation index (MI) for each of these frequency pairs (8Hz & 80Hz and 16Hz & 80Hz) is a measure of divergence of the amplitude distribution from the uniform distribution (see Tort et al., 2010a for details). This procedure is repeated for several frequency pairs (2-20Hz x 20-200Hz), and the MI values for each pair are displayed in a pseudocolor comodulation map (top left). Notice that in this example “**a**” has stronger coupling (and, therefore, higher MI values) than “**b**”. The example shown in this figure was obtained from a CA1 recording during active exploration.

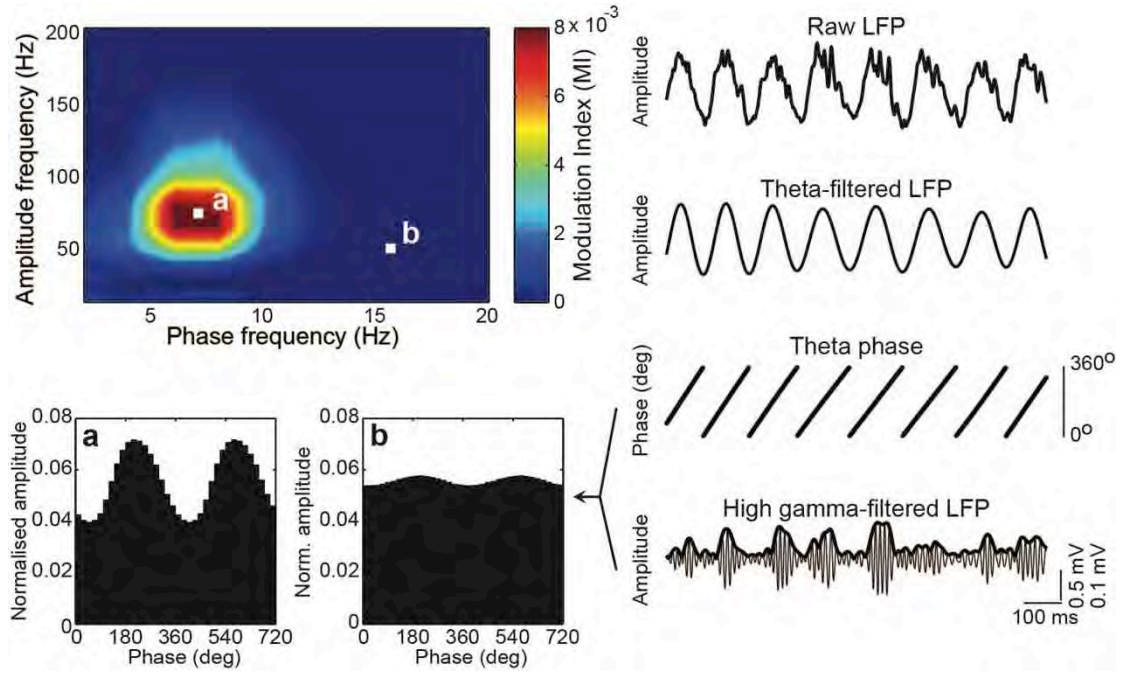


Figure 4. Example of a cross-frequency phase-amplitude comodulation map (adapted, with permission, from Scheffer-Teixeira et al., 2012).

Comodulation maps were computed using 5 minutes long LFPs recorded from single electrodes. The entire recording session (5 hours for each experiment) was binned into sixty 5 minutes epochs, and subjected to visual analysis by two experimenters. Only time windows associated with robust theta oscillations were used. Mean CFC strength between two frequency ranges was obtained by averaging the corresponding MI values; for example, mean theta-HG coupling corresponds to the average of MI values in the (4-10Hz) x (60-100Hz) region of the comodulation map, and similarly for theta-HFO coupling. Theta-HFO coupling strength was only considered for electrodes that exhibited theta-HFO or theta-HG (or both) coupling in the comodulation map during baseline recordings. Examples of electrodes included in the CFC analysis are presented in Figure 5 (theta-HFO coupling in left and middle panels and theta-HG coupling in middle and right panels).

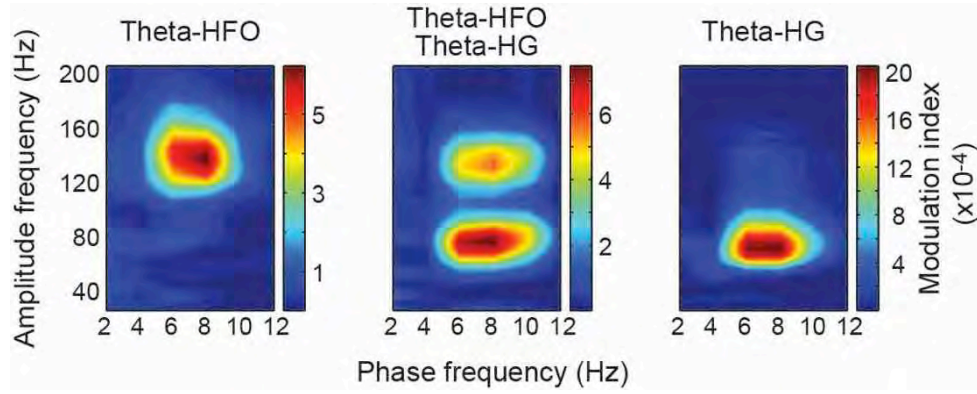


Figure 5. Typical examples of comodulation maps included in the CFC analysis presenting (from left to right, respectively) theta-HFO, simultaneous theta-HFO and theta-HG, and theta-HG CFC.

During visual inspection, electrodes that exhibited comodulation maps in which theta modulates a wide range of higher-frequency oscillations (Figure 6, left panel) were manually excluded from analysis.

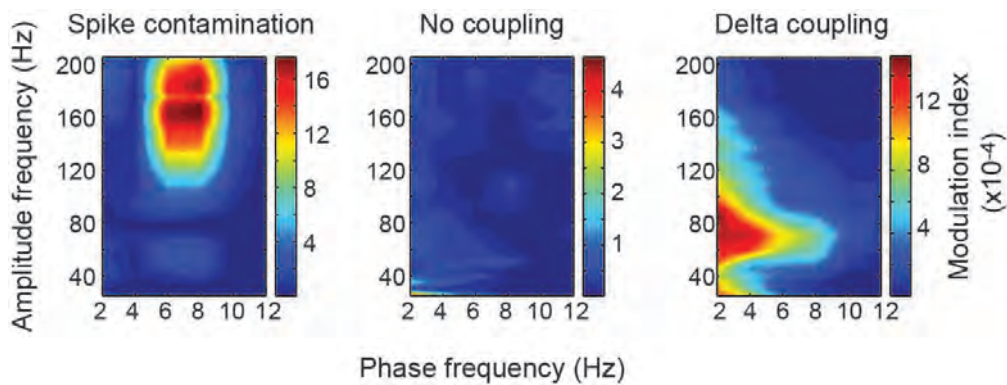


Figure 6. Typical examples of electrodes discarded from CFC analysis due to spike-leaked HFO (left), lack of visible comodulation (middle) or strong coupling between the delta band and higher frequency bands (right).

This type of coupling has recently been shown to correspond to contamination of the LFP signal by multiunit activity (Scheffer-Teixeira et al., 2013; Tort et al., 2013, Kramer et al., 2008) and is common in recordings from the CA1 pyramidal layer (Scheffer-Teixeira et al., 2013) and dentate gyrus (Scheffer-Teixeira et al., 2012). Electrodes that exhibited no coupling in the comodulation map during baseline (Figure 6, middle panel) or that presented strong delta band coupling to higher frequency bands (Figure 6, right panel) were also not considered. Consistent with recent reports (Scheffzuk et al., 2011; Scheffer-Teixeira et al., 2012), theta-HFO coupling was mainly present in electrodes in *stratum oriens-alveus*, and theta-HG coupling from the CA1 pyramidal layer to *stratum lacunosum-moleculare*/hippocampal fissure (see Figure 3).

3.10 Triggered LFP averages and current source density (CSD)

In order to analyse the data of the single animal implanted with a 16-site probe, signals were amplified (200x), filtered (1 Hz - 7.5kHz), and digitised at 25kHz (RHA2116, Intan Technologies). LFP averages were obtained by first filtering the LFP signal into the frequency ranges of interest; the amplitude peaks of each band were then identified and used for averaging 500ms epochs centred at these timestamps. CSD analysis was obtained by $-A+2B-C$ for adjacent sites. We used 60 seconds periods of prominent theta oscillations selected by visual inspection from periods of freely moving behaviour in these analyses. For each frequency colour scaling is the same before and after ketamine injection. Electrode 2 was used as the reference electrode in all analyses.

3.11 Statistics

Group means were compared by t-test for independent samples or by repeated measures ANOVA followed by Bonferroni post-hoc test. Multiple regression was performed to study changes in CFC level corrected for changes in locomotion and theta activity (as assessed by the theta/delta ratio; see Figure 15).

4. Results

4.1 Ketamine induces dose-dependent transient immobility and hyperlocomotion

Consistent with previous reports (Chen et al., 1966; Hunt et al., 2006), we found that systemic administration of ketamine caused a marked increase in locomotor activity at all doses studied. Typical post-saline and post-ketamine exploration trajectories are depicted in Figure 7.

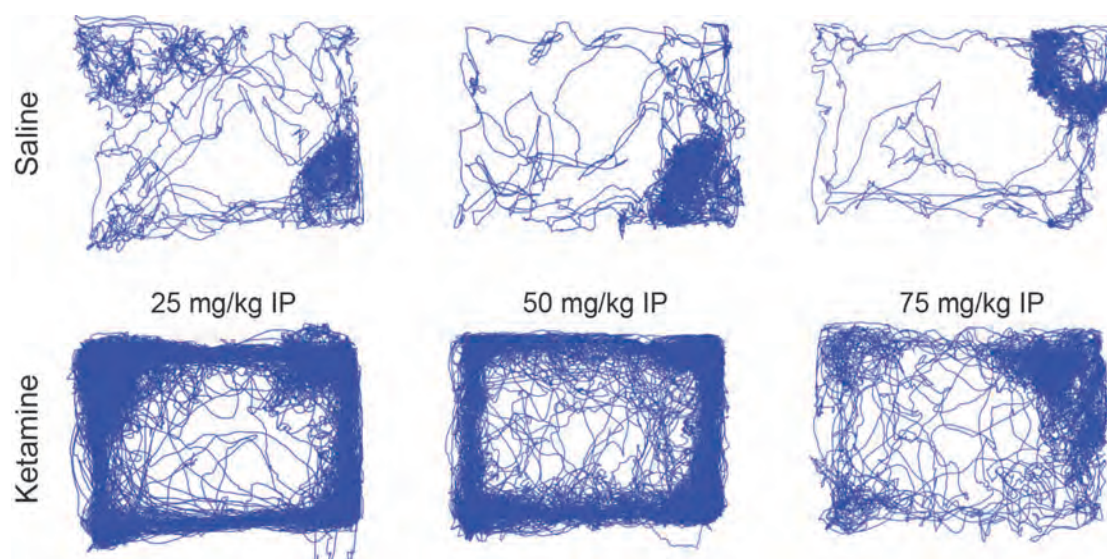


Figure 7. Examples of post-saline and post-ketamine locomotor activity patterns for all the doses used. Each plot indicates total horizontal activity in the first hour post-injection. Notice that exploratory behaviour is markedly intensified after ketamine injection. The increase in locomotor activity after 75mg/kg of ketamine is not so evident in the first hour due to transient immobility, as explained below.

The mean locomotor activity after animals were placed in the arena (0-60 minutes) and after saline injection (60-120 minutes) was quantitatively and qualitatively similar across doses (Figure 8a). Ketamine injections induced an

increase in locomotor activity (henceforth referred to as hyperlocomotion period) for all doses (Figure 8a). A clear dose-dependent effect was found for total locomotion in the 3 hours post ketamine injection (Figure 8b).

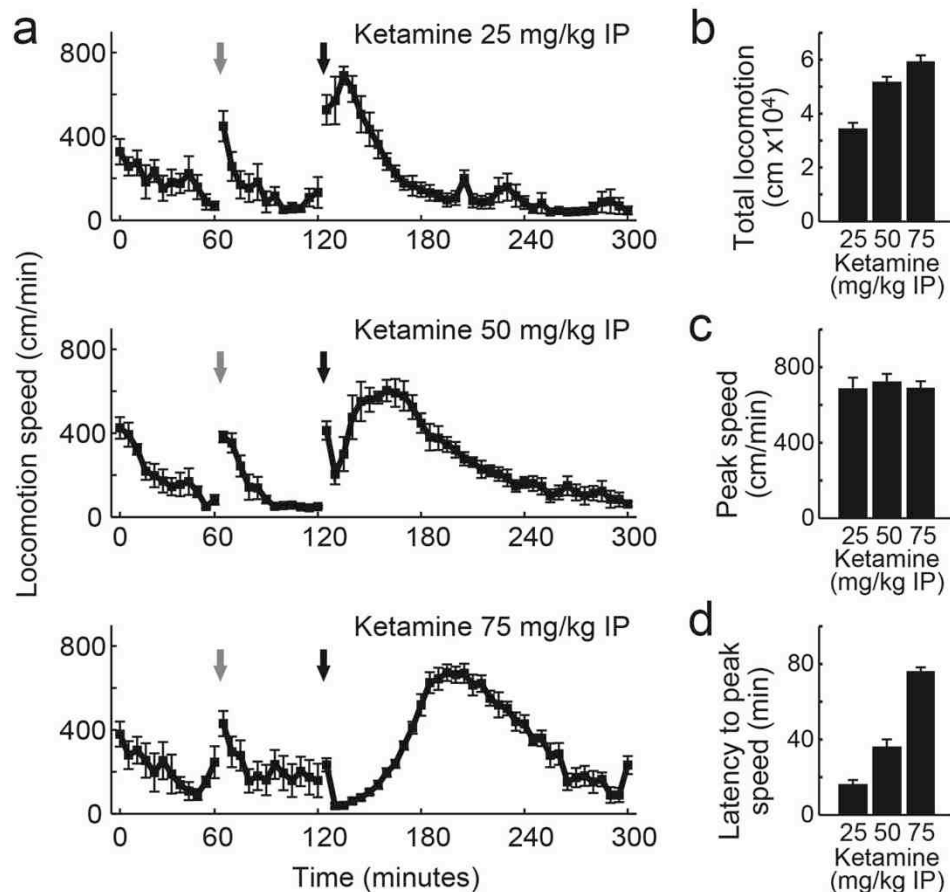


Figure 8. Acute injection of sub-anaesthetic doses of ketamine induces hyperlocomotion in rodents. In this and all other figures, grey and black arrows denote saline and ketamine injections, respectively. (a) Ketamine increases locomotion speed at all doses. (b) Total locomotion, (c) peak speed values, (d) and latency to peak locomotion speed after ketamine injection are shown for each dose. Data are shown as mean \pm SEM over animals.

Of note, during the hyperlocomotion period animals moved in a highly stereotypical fashion, with bouts of running the around the edges of the arena either clockwise or anti-clockwise, with brief stops, followed by more running, usually in the opposite direction. While peak locomotion speed was similar for all

doses (Figure 8c), higher ketamine doses were associated with greater latency to peak locomotor activity (16, 36 and 76 minutes, respectively; Figure 8d). The increased latency to peak activity found in the two highest doses of ketamine was caused by a transient immobility period, and lasted approximately 20 minutes after the injection of 50mg/kg and 60 minutes after the injection of 75mg/kg of ketamine.

4.2 Ketamine-induced immobility is associated with increased delta power

A recent study suggested that increased delta power after systemic treatment with a NMDAR blocker might be a translational biomarker for schizophrenia symptoms (Zhang et al., 2012), since elevation of delta power during the awake state has been observed in schizophrenia (Boutros et al., 2008). The increase in hippocampal delta power found by Zhang and collaborators peaked 5 minutes after the injection of 50mg/kg - but not 20mg/kg - of IP ketamine, presented high coherence with delta oscillations recorded in the *nucleus reuniens* of the thalamus, and returned to baseline within 15 minutes. This effect was inhibited by muscimol injection in the *nucleus reuniens*, and could be instated by direct injection of ketamine in the thalamus (Zhang et al., 2012). Of note, the increase in delta power induced by NMDAR had been documented previously (Leung and Desborough, 1988).

We found that 50 and 75mg/kg of IP ketamine induced an increase in delta power both for electrodes located in *stratum oriens-alveus* and in pyramidal layers (Figure 9, top row), and in *stratum lacunosum-moleculare*, hippocampal fissure and dentate gyrus (Figure 9, bottom row)

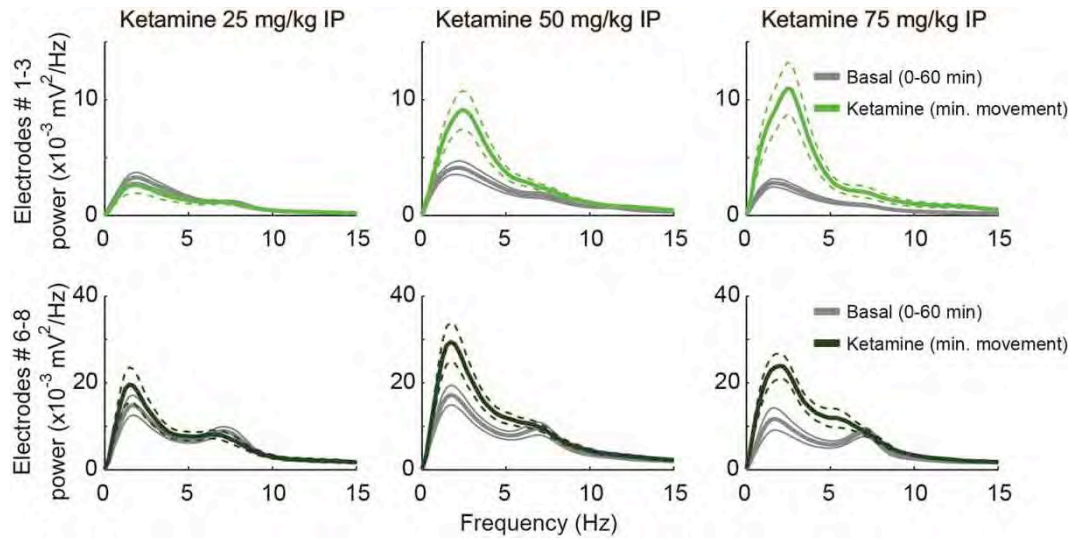


Figure 9. Group average power spectra during baseline and during minimum movement induced by ketamine in the first hour post-injection. Data are shown as mean \pm SEM over electrodes.

However, this effect was restricted to the immobility period, and faded once the hyperlocomotion peaked, giving place to an increase in theta power (Figure 10).

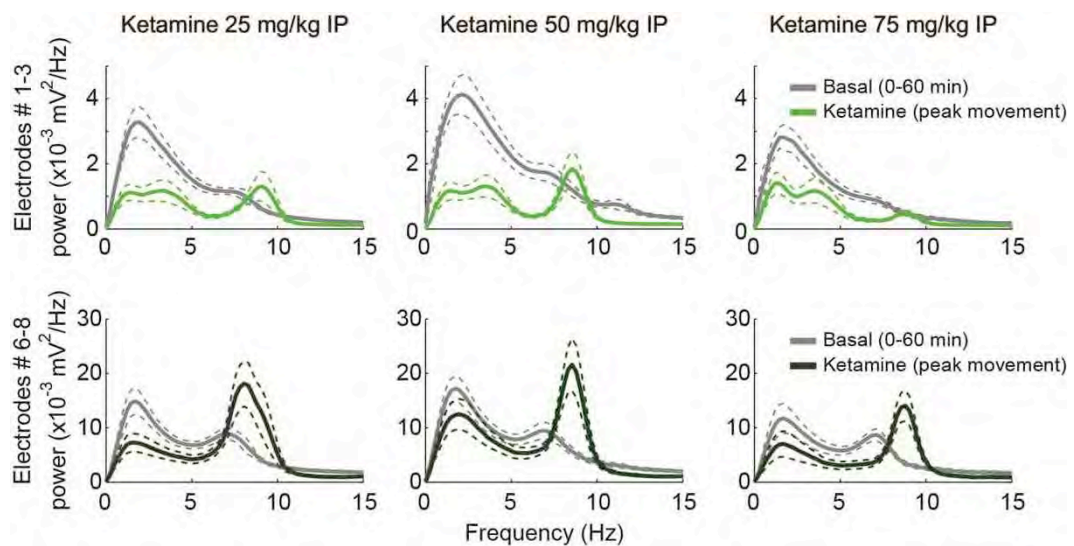


Figure 10. Group average power spectra during baseline and during peak hyperlocomotion induced by ketamine. Data are shown as mean \pm SEM over electrodes.

Indeed, the time course of increased delta power found by Zhang and collaborators matches with great precision the period of immobility found in our study after treatment with 50mg/kg of ketamine IP (see Figure 8a, middle row). Also, delta power levels for all doses studied were not quantitatively different from those measured before ketamine injection, provided that locomotor activity was approximately the same, nearing immobility (Figure 11).

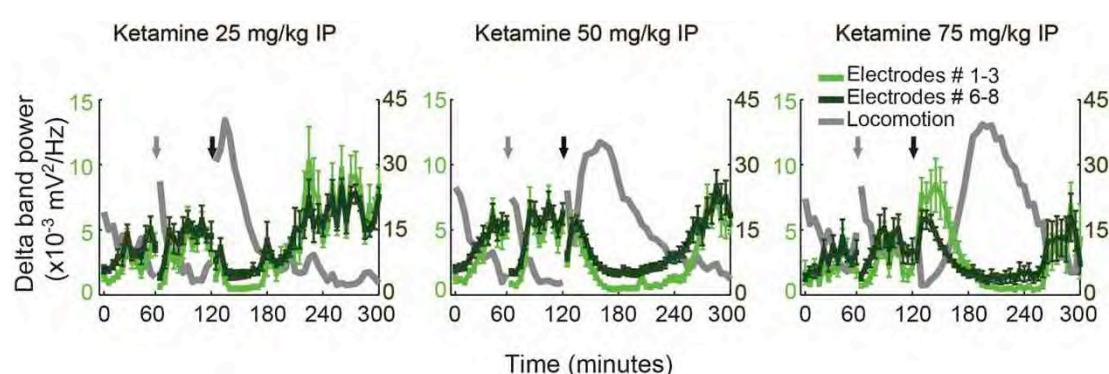


Figure 11. Group time-course of mean delta power in two subsets of electrodes located in different hippocampal layers (see Figure 13b for electrode positions). Grey and black arrows indicate saline and ketamine injections, respectively. Mean locomotor activity is shown in grey in arbitrary units (see Figure 8 for actual units). Notice that different y-axis scales are used for each subset of electrodes to facilitate comparison. Data are shown as mean \pm SEM over electrodes.

These results suggest that the induced increase in delta power is not a hallmark of NMDAR blockade, but rather represents a common electrophysiological feature associated with immobility (Hinman et al., 2013).

4.3 Ketamine modulates hippocampal theta oscillations in a layer-dependent manner

After investigating the effects of ketamine on delta power, we found theta power was also modulated by ketamine. In Figure 12 we show the power spectral density in the theta range of three electrodes recorded simultaneously from an animal during 25-min of baseline recordings (grey) and during 25-min after administration of 50mg/kg ketamine IP (black) in a representative animal.

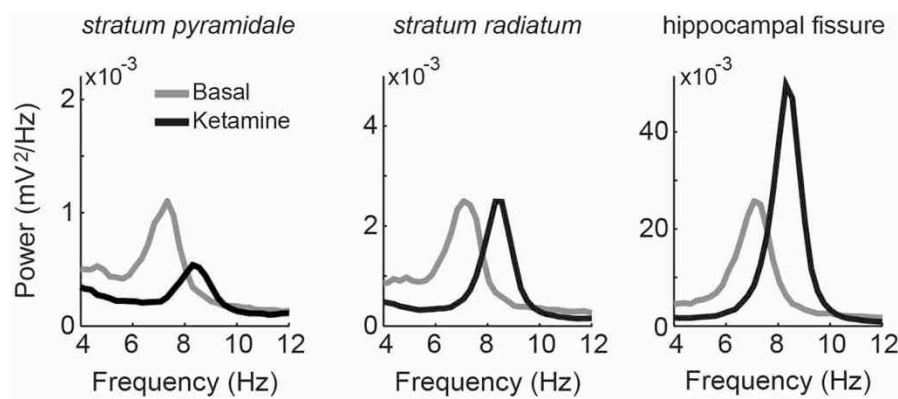


Figure 12. Power spectral densities pre- and post- administration of 50mg/kg ketamine IP (black) for three electrodes simultaneously recorded from a representative animal.

Notice in this example that while theta band power decreased after ketamine injection in *stratum pyramidale*, it did not change in *stratum radiatum*, and was markedly increased at the hippocampal fissure. Notice further that theta peak frequency was shifted in all recording sites from 6-8Hz during drug-free locomotion periods to 7-10Hz following ketamine injections, probably due to increases in locomotion speed (Hinman et al., 2013). Figure 13a shows group results for theta band power modulation during the 5 minutes epoch of peak hyperlocomotion induced by ketamine in a subset of electrodes (see electrode positions in Figure 13b) located in *stratum oriens-alveus* and *stratum pyramidale* (Electrodes #1-3) and another subset located in *stratum lacunosum-moleculare*,

hippocampal fissure and dentate gyrus (Electrodes #6-8). The mean power spectral density during peak hyperlocomotion is displayed in Figure 7.

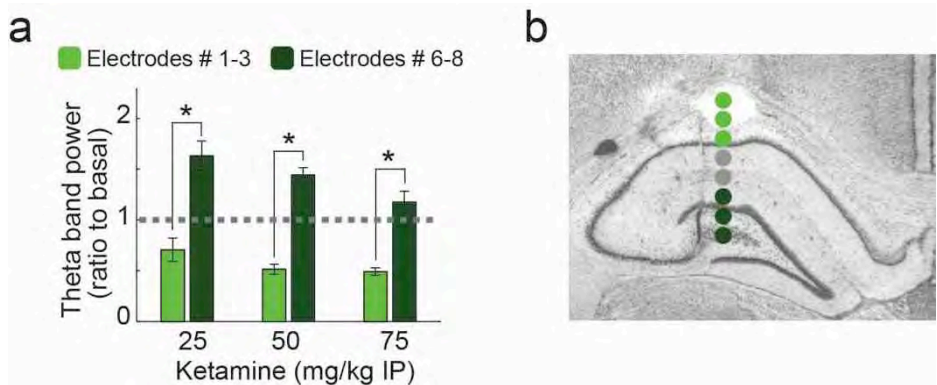
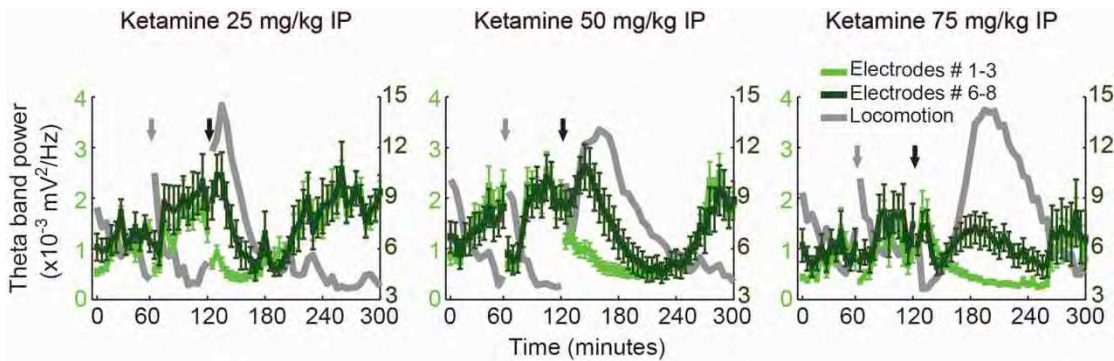


Figure 13. (a) Group results of mean theta band power recorded in two subsets of electrodes during peak hyperlocomotion induced by ketamine, normalised by the mean theta power during baseline (dashed line); * $p < 0.001$ (repeated measures ANOVA followed by Bonferroni post-hoc test). Data are shown as mean \pm SEM over electrodes. (b) Histology with estimated electrode depths indicated by green dots at the right of the lesion.

Ketamine differentially affected theta band power in the two subsets of electrodes at all doses studied (Figure 13a), but no dose effect was observed. Interestingly, this effect occurred specifically during hyperlocomotion (Figure



14).

Figure 14. Group time-course of mean theta power in two subsets of electrodes located in different hippocampal layers (see Figure 13b for electrode positions). Grey and black arrows indicate saline and ketamine injections, respectively. Mean locomotor activity is shown in grey in

arbitrary units (see Figure 8 for actual units). Notice that different y-axis scales are used for each subset of electrodes to facilitate comparison. Data are shown as mean \pm SEM over electrodes.

During our analyses we realized that high levels of delta power can potentially lead to a greater area under the curve of the power spectral density in the theta range [spectral leakage (Scheffer-Teixeira et al., 2013)] even in the absence of a theta peak. Therefore, we next investigated whether putative changes in delta power could account for the changes in theta power reported above. As shown in Figure 11, delta power was highly modulated by locomotion speed; in particular, delta power was high during periods of low locomotion preceding saline and ketamine injections, and also after the hyperlocomotion episode had ceased. Thus, the apparent high levels of theta band power in these periods (Figure 14) are actually due to spectral leakage from delta power and do not correspond to a genuine theta activity. Consistent with a previous report (Zhang et al., 2012), the doses of 50 and 75mg/kg transiently increased delta power, which returned to basal levels during the peak of ketamine-induced hyperlocomotion activity (Figure 11), i.e., when the layer-dependent variations in theta power were most striking (Figure 14). Moreover, contrary to theta, delta power time-course was qualitatively similar in all electrodes (Figure 11). Therefore, ketamine-induced changes in delta power cannot account for the dichotomy in theta modulation across the CA1-dentate gyrus axis observed during hyperlocomotion.

We note that due to the spectral leakage of delta power into the theta range that occurs during periods of low locomotor activity and immobility, the theta/delta ratio is a better measure of genuine theta activity in the LFP than the mean power in the theta range. Moreover, the theta/delta ratio is a spectral measure

highly correlated with locomotion speed (Figure 15). For these reasons, we used the theta/delta power ratio as a surrogate of theta power ratio in subsequent analysis when the power of theta might interfere with the interpretation of our results (see CFC section below).

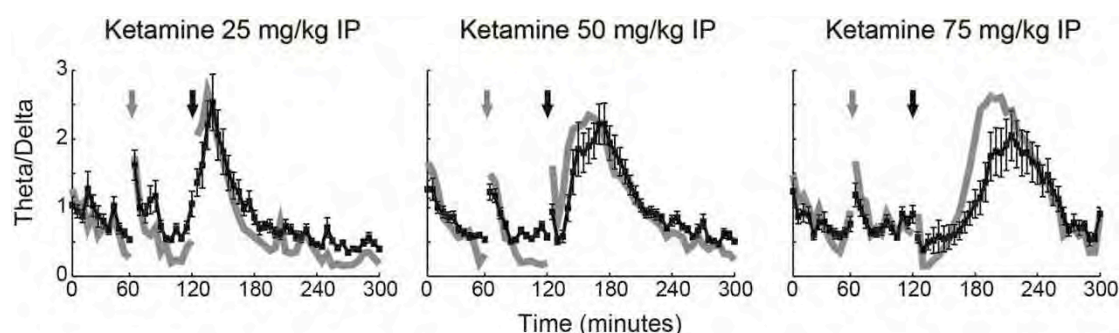


Figure 15. Theta/delta power ratio (black) is associated with locomotor activity (gray, in arbitrary units). Group time-course of theta/delta power ratio averaged for different ketamine doses, as labelled. Data are shown as mean \pm SEM over all electrodes.

4.4 Ketamine increases the power of gamma and high frequency oscillations

Along with low-frequency alterations, we found that high-frequency LFP signals were also modulated by ketamine. In Figure 16a we show the gamma band power averaged across all electrodes (mean over all 8 electrodes; 5Hz moving average smoothing) in a representative animal treated with ketamine. Peak gamma power occurred during the first hour post-ketamine injection, and approached baseline levels three hours afterwards. In Figure 16b we show time-courses of gamma power variations in each of the 8 electrodes in the same animal (Figure 16b inset); notice that total gamma power increases along the CA1-dentate gyrus axis, as previously reported (Bragin et al., 1995).

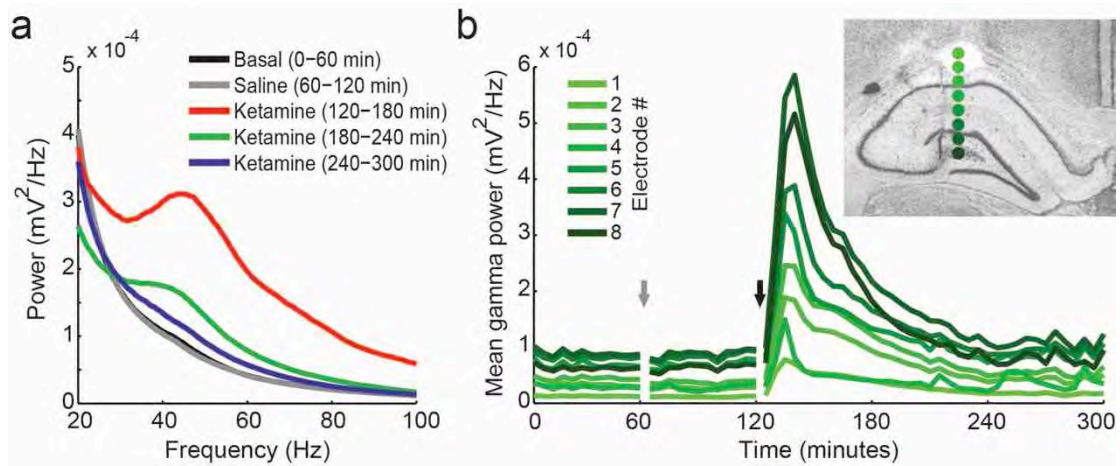


Figure 16. (a) Representative power spectra of an animal treated with 50mg/kg ketamine IP. (b) Time-course of mean gamma power for all electrodes in the same animal as in a. Inset shows histology with estimated electrode depths (indicated by green dots at the right of the lesion).

Grey and black arrows denote saline and ketamine injections, respectively.

The increase in gamma power induced by ketamine was apparent in all recording sites; in fact, baseline normalised gamma power provided similar time-courses for all electrodes in the bundle (data not shown). At the group level, in contrast to the time-course of locomotor activity (Figure 8a), gamma power peaked within 5-10 minutes after ketamine injection for all doses studied (Figure 17).

Our results show that the time-course of locomotor and gamma power increase caused by ketamine may be dissociated. To further stress this argument, in Figure 18 we show cross-correlations between gamma power and locomotor activity for different time lags. Notice that for increasing doses the dissociation becomes increasingly clearer. These results are in accordance to previously published work from Hakami et al. (2009).

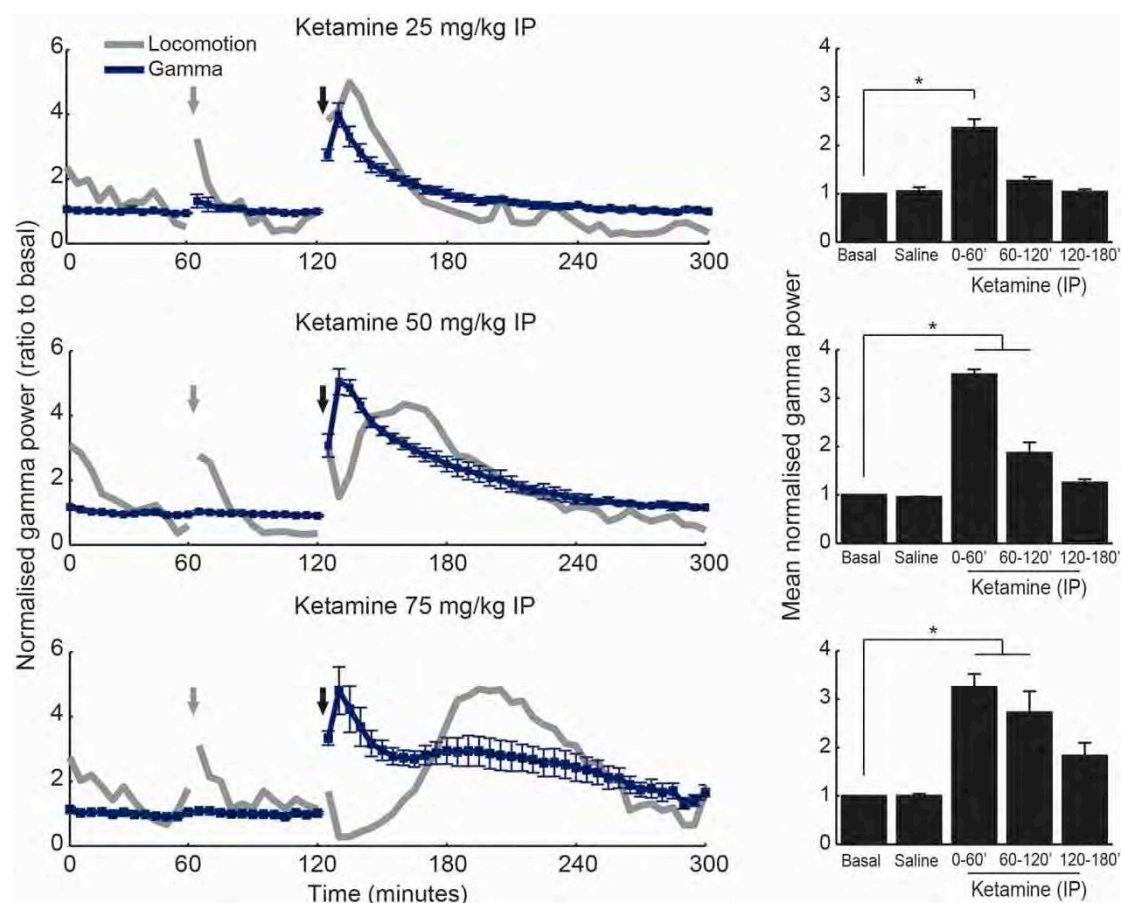


Figure 17. Left: Group results of normalised gamma power (blue) induced by three doses of ketamine (different rows, as labelled). Grey line depicts mean locomotion speed in arbitrary units. Right: Mean normalised gamma power in one hour blocks, as labelled. * $p < 0.001$ (repeated measures ANOVA followed by Bonferroni post-hoc test). Data are shown as mean \pm SEM over animals.

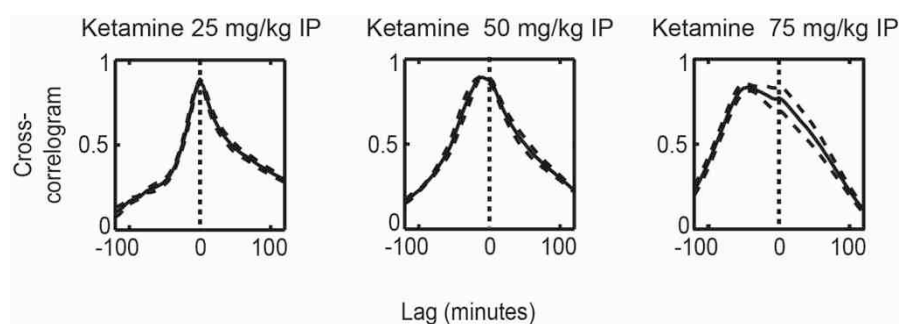


Figure 18. Cross-correlograms between normalised gamma power and locomotor activity (y-axis) for different time lags (x-axis). Data are shown as mean \pm SEM over animals.

We found that ketamine also increased hippocampal HFO power, with a similar time-course to the increase in gamma oscillations (see Figure 19a for a representative electrode and Figure 19b for group results). Incidentally, it has recently been shown that ketamine increases HFO activity in motor cortex, *nucleus accumbens*, and other basal ganglia nuclei (Hunt et al., 2006; Nicolas et al., 2011), suggesting that abnormally high levels of HFO may be a widespread effect of NMDAR blockade.

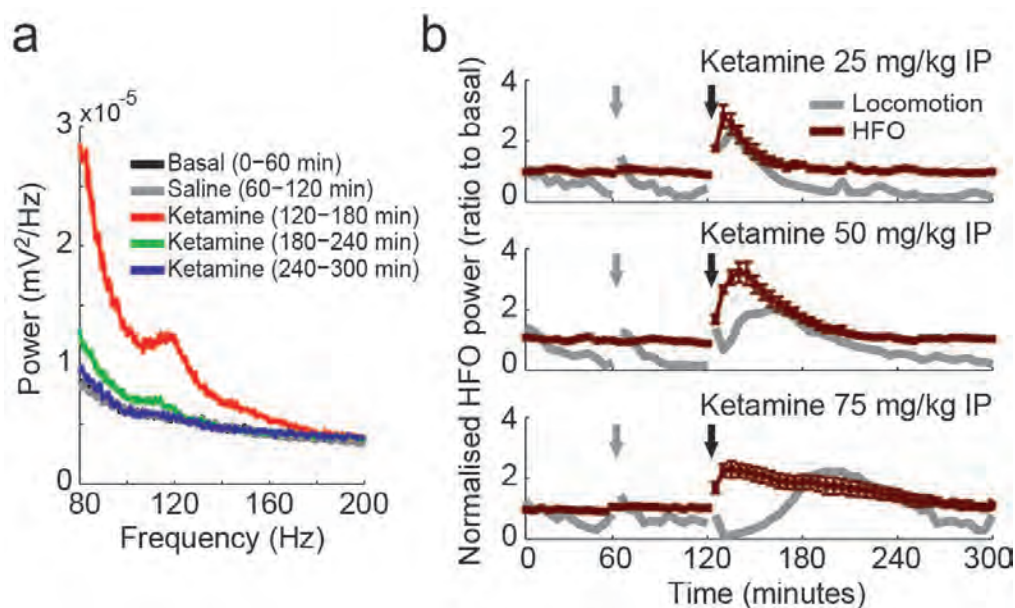


Figure 19. (a) Representative power spectra of a *stratum oriens* electrode in an animal treated with 50mg/kg ketamine IP. (b) Group results of normalised HFO power variations (brown) induced by three doses of ketamine (different rows, as labelled). Grey line depicts mean locomotion speed in arbitrary units. Grey and black arrows indicate saline and ketamine injections, respectively. Data are shown as mean \pm SEM over animals.

4.5 Ketamine leads to increased phase synchrony in multiple high-frequency bands

We next investigated the levels of phase coherence across recording sites, and found that ketamine induced transient hypersynchrony in a wide range of fast LFP oscillations from 30 to 200 Hz (Figure 20).

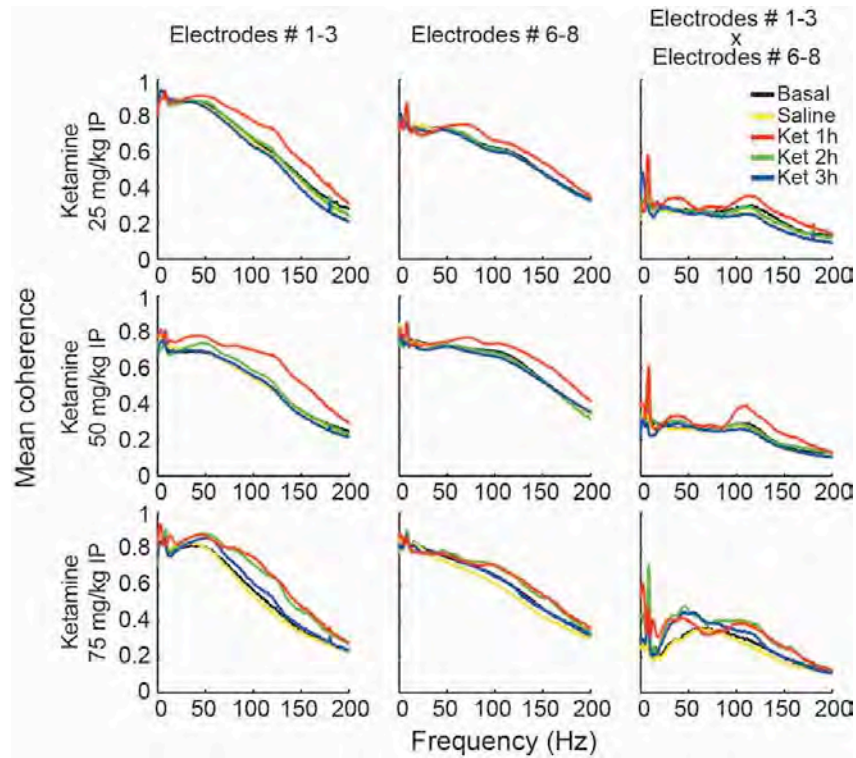


Figure 20. Phase coherence spectra before and after treatment with different doses of ketamine (rows) for different electrode pair combinations (columns). Ket = ketamine

Phase coherence spectra were typically multimodal, exhibiting peak values in the traditional gamma range, as well as in frequencies above 100 Hz. The changes in coherence induced by ketamine were observed among electrode pairs located in multiple hippocampal depths (Figure 20). Interestingly, electrode pairs located at *stratum lacunosum-moleculare* and dentate gyrus presented coherence peaks in a faster gamma frequency than electrode pairs located at *stratum oriens-alveus* and *pyramidale*. Peaks in HFO phase coherence were particularly prominent for electrodes pairs across hippocampal layers.

In Figure 21 we show time-courses of mean phase coherence changes in the gamma and HFO bands across all electrode pairs. Gamma and HFO phase coherence increased immediately after ketamine injection and only returned to baseline values after the hyperlocomotion episode ended. Gamma and HFO coherence was significantly increased during the first hour post-ketamine at all doses, and also during the second hour at the highest dose ($p < 0.01$; repeated measures ANOVA followed by Bonferroni post-hoc test). Interestingly, the relative increase in phase coherence induced by ketamine was much more prominent for HFO than gamma oscillations. In all, these results show that ketamine increases inter-site synchrony of multiple frequency bands in the hippocampus.

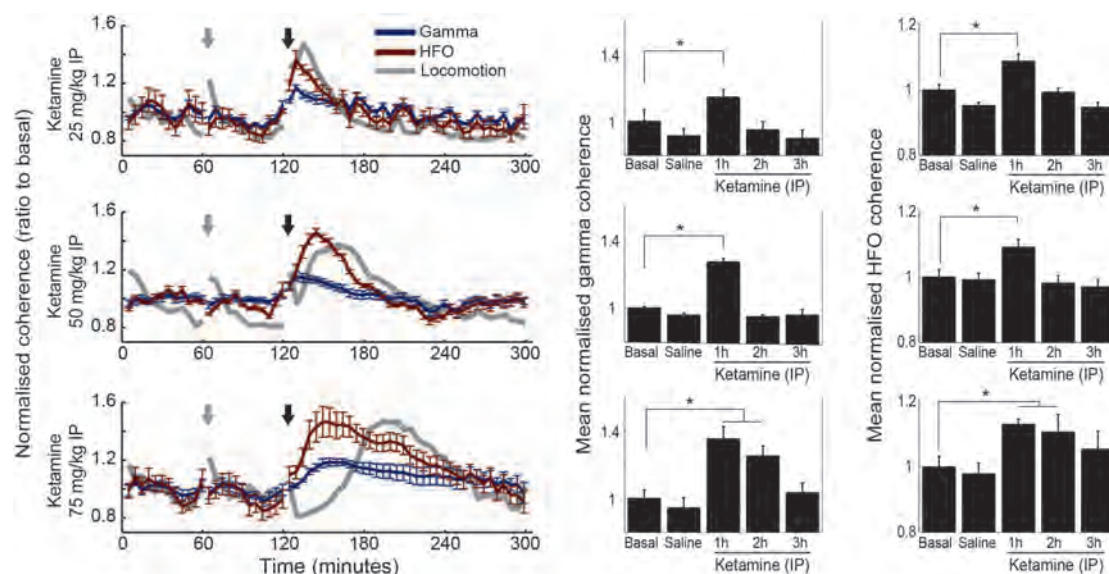


Figure 21. Group time-course of normalised phase coherence in the gamma and HFO bands.

Mean locomotor activity is shown in grey (arbitrary units). Mean normalised coherence in one hour blocks, as labelled. * $p < 0.05$ (repeated measures ANOVA followed by Bonferroni post-hoc test). Data are shown as mean \pm SEM over all animals.

4.6 Ketamine alters cross-frequency coupling

We next examined the effects of ketamine on the coupling between low- and high-frequency LFP oscillations. Typically, low frequency phase modulates the amplitude of higher frequency oscillations (Tort et al., 2010a). This type of oscillatory interaction is deemed to be involved in cognitive processing [see Canolty and Knight (2010) for a review]. Consistent with previous reports (Tort et al., 2008; Scheffzuk et al., 2011; Scheffer-Teixeira et al., 2012), we found prominent CFC in most CA1 electrodes. Total number of electrodes analysed for theta-HFO coupling for each dose was 13 (25 mg/kg), 18 (50 mg/kg), and 10 (75 mg/kg), and for theta-HG coupling 15 (25 mg/kg), 16 (50 mg/kg) and 10 (75 mg/kg).

Theta phase strongly modulated the amplitude of HFO in electrodes located above the pyramidal layer (i.e., *stratum oriens-alveus*), while the amplitude modulation of high-gamma (HG; 60 - 100 Hz) was maximal in electrodes located in *stratum lacunosum-moleculare* and hippocampal fissure but could also be seen at lower levels in electrodes near the pyramidal layer along with theta-HFO coupling. See Figure 3 and Scheffer-Teixeira et al. (2012) for further characterization of CFC patterns across CA1 layers. In spite of the low-gamma (30-60 Hz) power increase depicted in Figure 16, we did not find prominent coupling between theta and low-gamma in CA1, as reported previously (Scheffer-Teixeira et al., 2012).

To illustrate the effect of acute NMDAR blockade on CFC, for each example in Figures 22 and 23 we show six comodulation maps computed for 5 minutes time

blocks before and after ketamine injection (as indicated by black and white dots in the top left panel, respectively). CFC strength for all time blocks is shown in the top right panel of each example. These results are representative for recording sites for the lowest (Figure 22a and 22b) and highest (Figure 23a and 23b) ketamine dose, with theta-HG (Figure 22a and 23a) and theta-HFO coupling (Figure 22b and 23b). In both figures we present the time-course of CFC coupling strength (black lines) and mean locomotion speed in arbitrary units (grey lines) before and after treatment with ketamine (top left); the scatter plot of CFC coupling as a function of theta/delta ratio for each 5 minutes time blocks with black circles indicating pre-ketamine and white circles for post-ketamine epochs; and in the bottom we show the comodulation maps obtained from the 5-min epochs indicated in the top left panel by black (pre-) and white (post-ketamine) circles.

Surprisingly, we found that ketamine had a differential effect on theta-HG coupling depending on dose: while the lowest dose increased theta-HG coupling (Figure 22a), the highest dose disrupted this oscillatory interaction (Figure 23a; see also Figure 24a for group results). On the other hand, ketamine increased theta-HFO coupling at all doses (Figures 22b and 23b, and Figure 24b for group results).

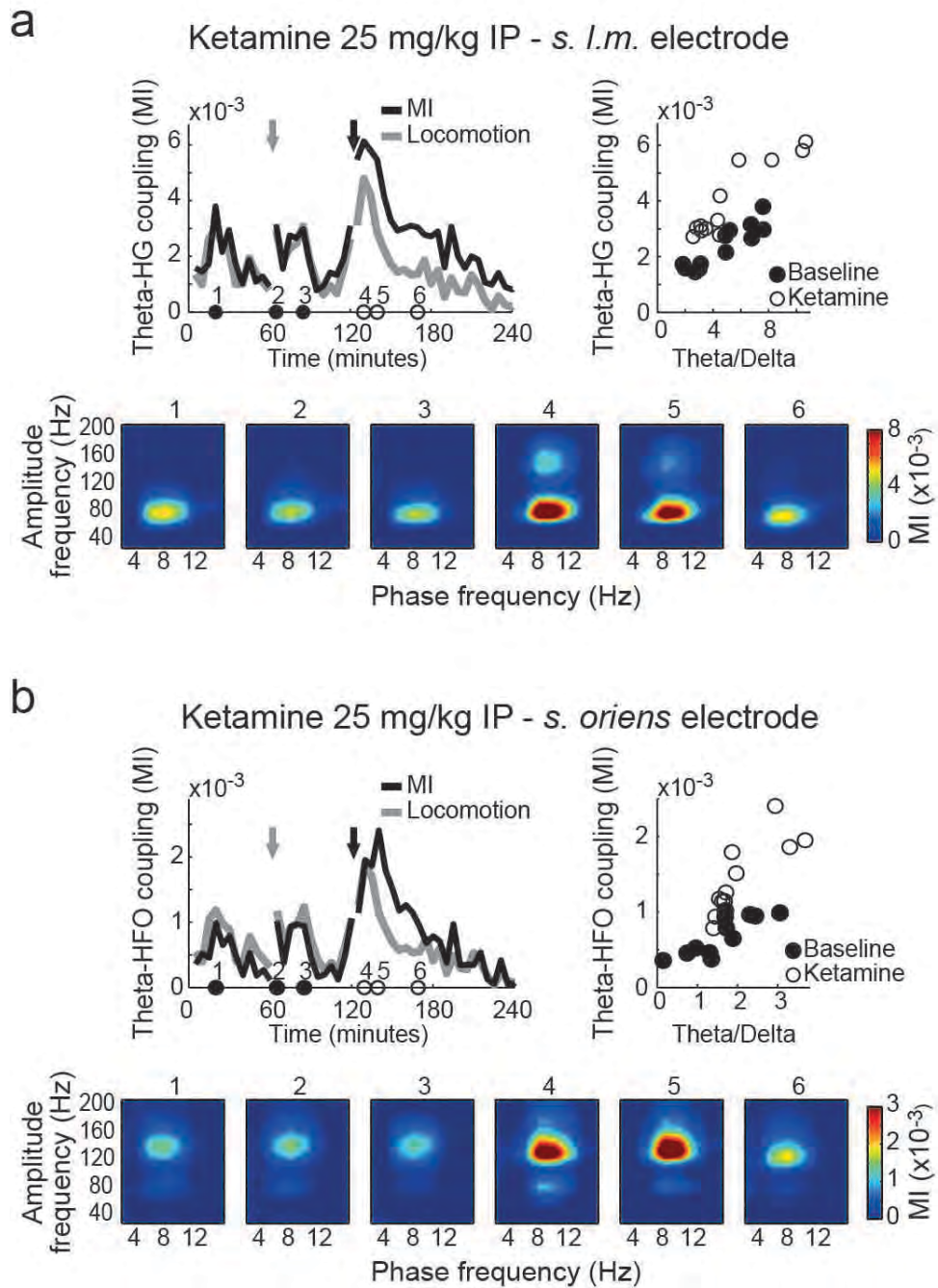


Figure 22. Top left: Time-course of theta-HG coupling strength (MI) and mean locomotor speed (arbitrary units) under treatment with 25mg/kg ketamine IP. Top right: Scatter plot of CFC coupling as a function of theta/delta ratio. Bottom: Comodulation maps from the epochs indicated in the top left panel by black (pre-) and white (post-ketamine) circles. The results in (a) were obtained from an electrode in stratum lacunosum-moleculare presenting prominent theta-HG coupling in a representative animal; and in (b) from an electrode in stratum oriens presenting prominent theta-HFO coupling in the same animal.

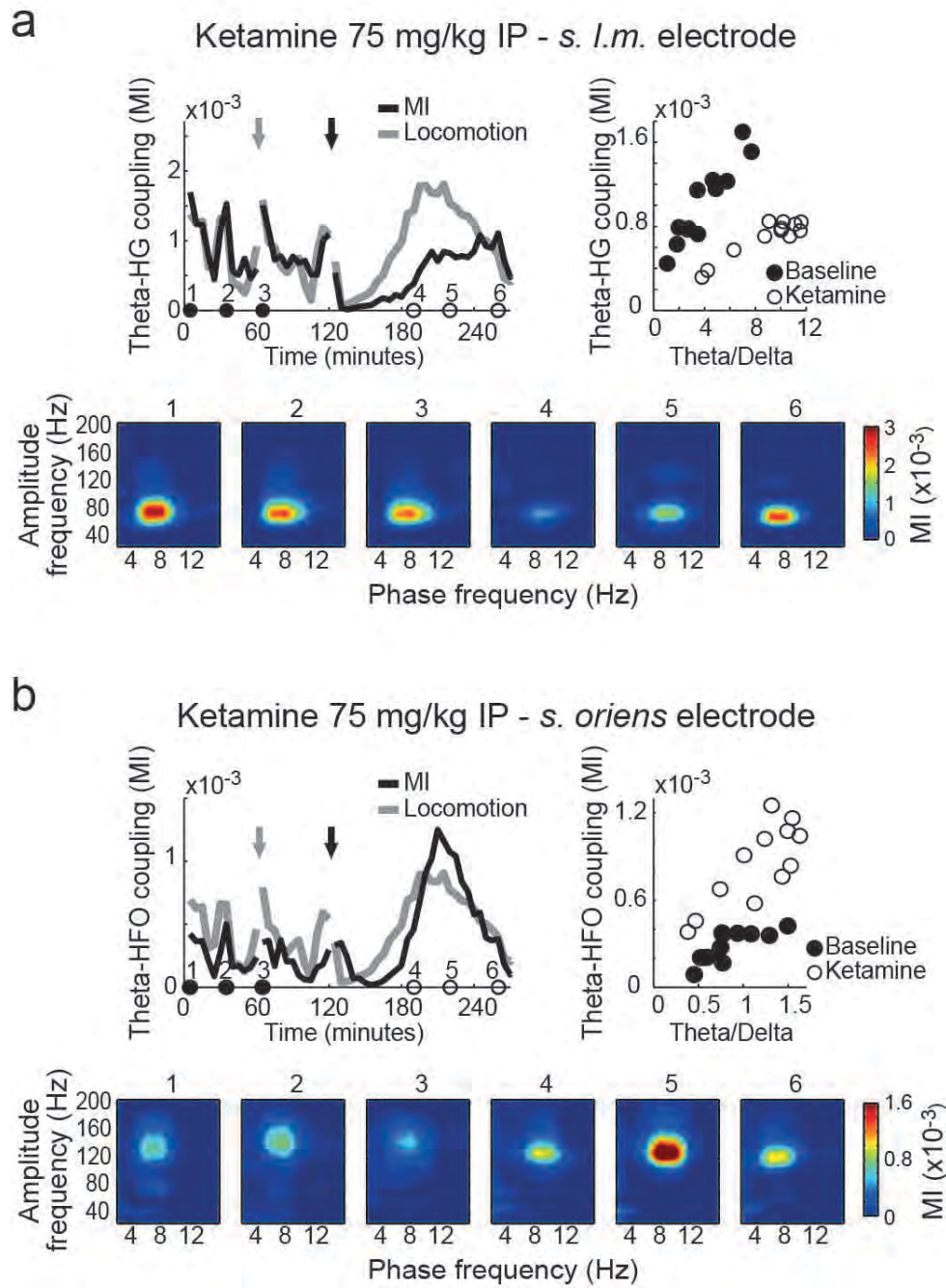


Figure 23. Top left: Time-course of theta-HG coupling strength (MI) and mean locomotor speed (arbitrary units) under treatment with 25mg/kg ketamine IP. Top right: Scatter plot of CFC coupling as a function of theta/delta ratio. Bottom: Comodulation maps from the epochs indicated in the top left panel by black (pre-) and white (post-ketamine) circles. The results in (a) were obtained from an electrode in stratum lacunosum-moleculare presenting prominent theta-HG coupling in a representative animal; and in (b) from an electrode in stratum oriens presenting prominent theta-HFO coupling in the same animal.

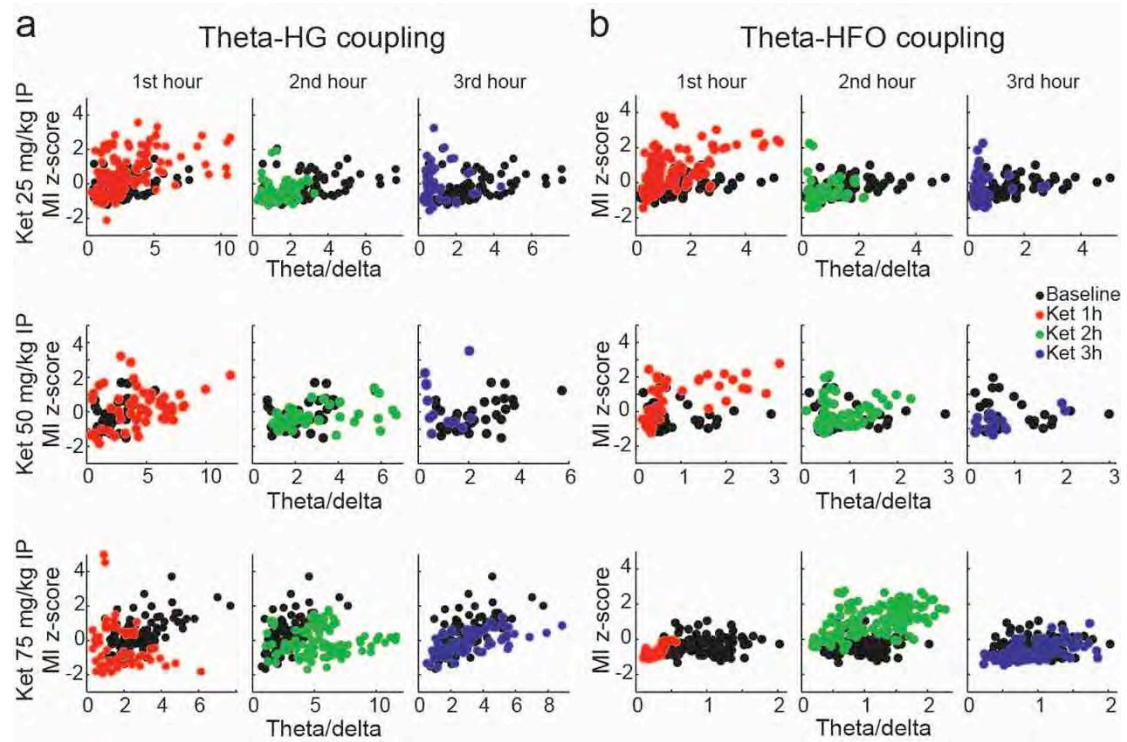


Figure 24. Group results showing that ketamine alters cross-frequency coupling. (a) Scatter plots of theta-HG normalised coupling strength in 5 minutes epochs for all analysed electrodes as a function of theta/delta power ratio (black = pre-ketamine, red = 1st hour post-ketamine, green = 2nd hour, blue = 3rd hour). (b) Same as in a, but for theta-HFO coupling. Lower x-axis values in b when compared to a are due to the fact theta-HFO and theta-HG coupling occurs mostly above and below the pyramidal layer, respectively (Scheffer-Teixeira et al., 2012), which have different theta/delta power ratios.

Since CFC strength typically varies with theta power (Tort et al., 2008; Scheffzuk et al., 2011; Scheffer-Teixeira et al., 2012), we next investigated whether the results above could be related to the ketamine effect on theta oscillations. To that end, we plotted mean CFC strength as a function of the theta/delta power ratio (Figure 24a and 24b). We note that due to the spectral leakage of delta power into the theta range that occurs during periods of immobility (c.f. section above), the theta/delta ratio is a better measure of genuine theta activity in the LFP than the mean power in the theta range. Moreover, the theta/delta ratio is a spectral

measure highly correlated with locomotion speed (Figure 15), and thus also serves to investigate whether changes in CFC strength are explained by changes in locomotion. We found that ketamine altered CFC in a similar way as described above even after controlling for this confounding factor (see Figure 25 for multiple regression analyses). These results therefore show that acute NMDAR blockade alters CFC in a frequency-specific and dose-dependent way.

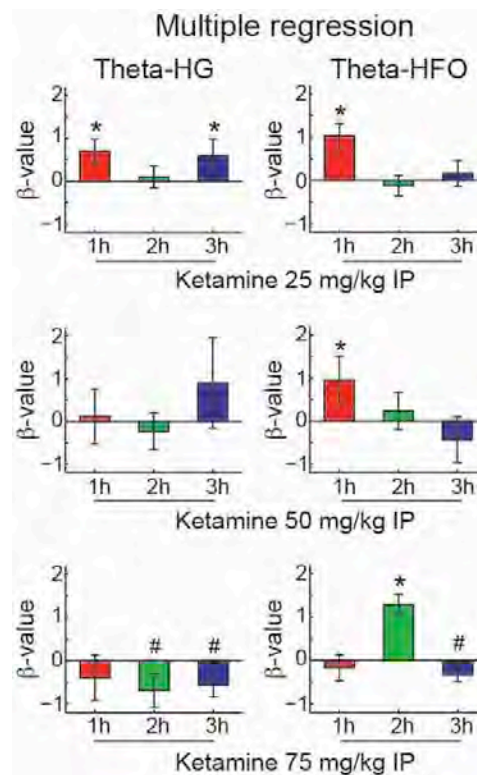


Figure 25. Multiple regression coefficients (β -values) indicating changes in coupling strength induced by ketamine controlling for the level of theta/delta power ratio. A non-zero β -value indicates that CFC level is significantly altered by ketamine independent of changes in the theta/delta ratio (* and # indicate, respectively, significantly increased and decreased β -values with $p < 0.01$, repeated measures ANOVA followed by Bonferroni post-hoc test). Only electrodes presenting theta-HG or theta-HFO coupling in baseline comodulation maps were used in these analyses (see Figures 19 and 20). Total number of electrodes analysed for theta-HFO coupling for each dose was 13 (25 mg/kg), 18 (50 mg/kg), and 10 (75 mg/kg), and for theta-HG coupling 15 (25 mg/kg), 16 (50 mg/kg) and 10 (75 mg/kg). Data are shown as mean \pm SEM over electrodes.

4.7 Ketamine does not alter the distribution of electrical dipoles in the hippocampus

Finally, we performed current source density (CSD) analysis in one additional animal. Baseline CSD plots (Figure 26, top row) for the different frequency ranges were similar to those previously described (Bragin et al., 1995; Scheffer-Teixeira et al., 2013). We found that ketamine did not alter the spatial distribution of sinks and sources pairs (Figure 26, bottom row). These results indicate that NMDAR blockade alters pre-existing hippocampal oscillations but does not generate new dipoles. Further, these analyses indicate that the oscillations investigated in this work are generated in the hippocampus, and not volume conducted from other brain regions.

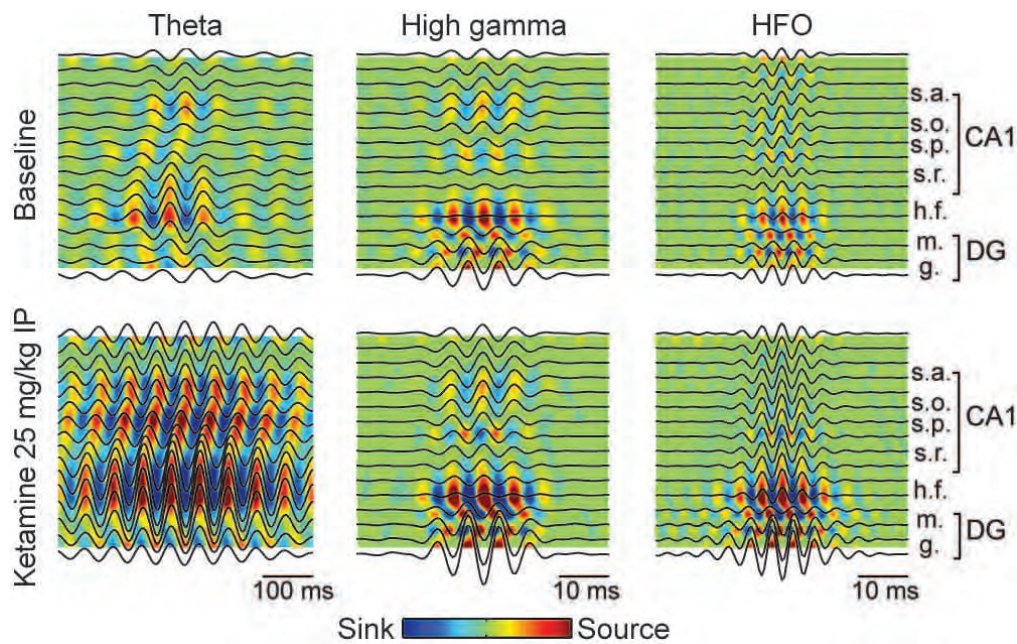


Figure 26. Triggered LFP averages and current source density (CSD) analysis from a 16-site probe (100 μ m spacing) recorded from a freely moving animal subjected to 25mg/kg ketamine IP.

Dark lines indicate LFP averages triggered by the peaks of filtered LFP. Colour plots show the associated CSD maps. Notice that the position of sinks and sources remain unaltered after drug administration for all frequencies analysed. Estimated recording sites are indicated at the right.

5. Discussion

In this study we showed that acute sub-anaesthetic doses of ketamine alter the cross-frequency interaction between theta phase and the amplitude of two higher frequency rhythms in the hippocampus: high-gamma and HFO. In addition, we also found that ketamine increases gamma and HFO power, increases oscillatory phase synchrony, and differentially modulates theta power in a layer-specific manner.

Consistent with previous studies (Pinault, 2008; Hakami et al., 2009; Kittelberger et al., 2012), we found altered behaviour and increased hippocampal gamma power during acute blockade of NMDAR. While low doses of ketamine cause correlated increases in locomotor activity and total gamma power, higher doses can induce different time-courses of behavioural and electrophysiological effects. In fact, ketamine also increases gamma oscillations in sedated and anaesthetised animals (Hakami et al., 2009). These observations indicate that increase in gamma power and hyperlocomotion are two independent effects of NMDAR blockade. While hyperlocomotion induced by acute NMDAR blockade is currently considered a model for positive schizophrenic symptoms with predictive value (Adell et al., 2012), the dissociation between gamma activity and hyper-locomotion suggests that these abnormal gamma oscillations may have additional translational significance (Jones et al., 2012).

In agreement with recent findings (Kittelberger et al., 2012), here we found that acute NMDAR blockade differently alters theta power depending on hippocampal

layer. These findings show that different theta dipoles have different sensitivities to NMDAR blockade. Entorhinal cortex inputs give rise to the theta dipole in *stratum lacunosum-moleculare* (Buzsaki, 2002). A greater theta activity in this layer following NMDAR blockade may thus be associated with an overflow of sensory information from the entorhinal cortex to the hippocampus.

We found that ketamine induced a network synchrony increase of multiple frequency bands in the hippocampus, particularly in the gamma and HFO bands. Neuronal synchrony has been proposed to play a role in dynamically selecting and routing information within and across brain structures (Engel et al., 2001). This hypothesis gave rise to the idea that abnormal synchrony would underlie symptoms of cognitive disorders such as autism and schizophrenia (Uhlhaas and Singer, 2006). However, whether schizophrenia is associated with increased or decreased neuronal synchrony remains an open question (Uhlhaas and Singer, 2010). Previous studies found reduced inter-trial phase coherence (ITC) in schizophrenic patients (Spencer et al., 2004; Light et al., 2006), typically accompanying a decrease in stimulus-evoked gamma power (Light et al., 2006). It should be noted that ITC measures the level of phase resetting following a sensory stimulus within a recording site, and not the level of phase locking between LFP oscillations recorded from different sites, as studied here. Regarding the latter, positive schizophrenia symptoms may be associated with increased connectivity (Lee et al., 2006; Flynn et al., 2008). Recent evidence suggests that although schizophrenic patients have reduced evoked gamma power, they could have abnormally high levels of basal gamma power (Lee et al., 2006; Spencer, 2011). If confirmed, these findings would solve current

inconsistencies between animal models (which show increased levels of gamma power and synchrony) and human studies [which point to reduced evoked gamma power and synchrony; for discussion, see Spencer (2011)]. Altogether, our and other results suggest that psychotic symptoms caused by NMDAR hypofunction are associated with an over-processing of information through functionally hyper-connected structures. Therefore, like in other brain disorders such as Parkinson disease and epilepsy (Uhlhaas and Singer, 2006), pathological hypersynchrony could also play a role in schizophrenia.

Here we showed that ketamine increases theta-HFO coupling during peak locomotion at all doses studied, while its effect on theta-gamma coupling was dose dependent. Importantly, none of these effects can be explained by changes in theta power occurring during hyperlocomotion. Interestingly, ketamine also leads to a significant increase in HFO activity in the *nucleus accumbens* (Hunt et al., 2006), a limbic region implicated in schizophrenia that receives massive connections from the hippocampus (O'Donnell and Grace, 1998). The cognitive implications of increased HFO power and theta-HFO coupling remain to be better understood, as well as the functional role of HFO *per se* (Hunt et al., 2006; Scheffer-Teixeira et al., 2012; Tort et al., 2013). A recent study has shown that physiological theta-HFO coupling significantly increases during REM sleep (Scheffzuk et al., 2011). REM sleep is a brain state associated with incongruous thoughts and dreams. Many similarities have been pointed out between REM sleep and psychosis (Gottesmann and Gottesman, 2007), leading some to suggest that psychotic symptoms would be associated with intrusion of a dreaming state into an awake mind (Freud, 1950; Douglass et al., 1991). While these suggestions

remain to be appropriately tested, the finding of enhanced theta-HFO coupling during REM sleep (Scheffzik et al., 2011) and following NMDAR blockade (present results) supports such a view.

Theta-gamma coupling, on the other hand, increased with the lowest dose of ketamine but was disrupted with the highest dose. Current theories on the combined function of theta and gamma oscillations suggest that disrupting their coupling would lead to deficits in brain functions such as working memory (Lisman and Buzsaki, 2008). However, the functional implications of increased theta-gamma coupling upon lower levels of NMDAR blockade are harder to interpret. It may be that increased oscillatory power, synchrony and cross-frequency coupling are all correlates of an aberrant state of brain hyperexcitability and altered information flow, which could underlie dysfunctions such as hallucinations and flight of ideas.

Recent findings suggest that dysfunction of GABAergic interneurons are likely to underlie the electrophysiological alterations reported here (Nakazawa et al., 2012). Accordingly, ablation of NMDAR from parvalbumin (PV) positive interneurons in mice leads to enhancements of basal gamma activity (Korotkova et al., 2010; Carlen et al., 2011). Moreover, ketamine does not induce hyperlocomotion in these knockout mice (Carlen et al., 2011), suggesting a critical involvement of the blockade of NMDAR in PV interneurons for the manifestation of positive schizophrenic symptoms. NMDAR ablation in corticolimbic interneurons has also been associated with the negative symptoms of the disease (Belforte et al., 2010). These findings help link together the NMDA

hypofunction hypothesis of schizophrenia with the alterations of GABAergic interneurons seen in post-mortem studies of schizophrenic subjects (Benes et al., 2000; Woo et al., 2004; Hahn et al., 2006; Bitanirwe et al., 2009). In addition to PV+ interneurons, hypofunction of NMDAR in *oriens lacunosum-moleculare* (OLM) interneurons could also be involved in the pathophysiology of schizophrenia (Tort et al., 2007; Neymotin et al., 2011). These cells synapse on distal portions of the apical dendrites of pyramidal cells, where projections from the entorhinal cortex arrive (Tort et al., 2007). A hypofunction of OLM cells would thus favour entorhinal cortex inputs (Leao et al., 2012), which could then lead to increased theta oscillations in *stratum lacunosum-moleculare*, as observed here. GABAergic interneurons are also likely to underlie coupling between theta and gamma rhythms (Tort et al., 2007; Wulff et al., 2009), and would thus further mediate aberrant CFC patterns following NMDAR blockade. In all, a preferential action of NMDA antagonists on inhibitory cells is compatible with increased levels of excitation (Moghaddam et al., 1997; Vollenweider et al., 1997) and altered neuronal oscillations.

Building a bridge between electrophysiological findings in animal models and schizophrenic patients has proven to be a challenge (Uhlhaas and Singer, 2010). A large part of the alterations described here, particularly at the HFO band, would not have been noticed by scalp EEG because of its frequency band limitations. Data obtained by invasive techniques, such as electrocorticograms, are unfortunately scarce in schizophrenia. In addition, antipsychotic drugs by themselves cause oscillatory changes (Jones et al., 2012), and are therefore important confounding factors in clinical studies. Thus, while at variance with

some previous human studies (Spencer et al., 2004; Light et al., 2006), our results add to others (Lee et al., 2006; Flynn et al., 2008; Spencer, 2011) in the suggestion that some symptoms of the schizophrenia syndrome are mediated by an aberrant state of brain hyperactivity, including increases in the activity of fast oscillations, phase synchrony and cross-frequency coupling.

6. Concluding remarks

In this thesis we presented our findings regarding the behavioural and the electrophysiological outcome of sub-anaesthetic ketamine treatment in laboratory rats. Our results add to the previous literature in describing alterations in the delta, theta, gamma and HFO bands, as well as in cross-frequency coupling between theta and high frequency oscillations in the hippocampus. Of particular significance, we feel that our systematic analyses of the varying effects of different doses of ketamine across the CA1 hippocampal strata may aid in disentangling some previously incongruent findings from the literature. For example, it seems that the power increase in the delta band induced by ketamine are most likely a by-product of low behaviour activity and probably a poor marker for schizophrenia symptoms; and it became apparent that theta oscillations are differently affected depending on the hippocampal layer studied, which may account for discrepancies between studies that sometimes found and other times did not find alterations in the theta band upon NMDAR blockade. Moreover, our result of increased locomotion and gamma activity at different time-courses is in accordance with the literature, and draws attention to the fact these phenomena are probably caused by different mechanisms. Finally, our main contribution to the field is probably the detailed description of altered hippocampal HFO and CFC between theta and HG and between theta and HFO, filling a gap in our knowledge on the effects of NMDAR blockade on the awake behaving rat.

While it remains to be shown if the animal model of acute NMDAR hypofunction recapitulates genuine network alterations responsible for the behavioural anomalies found in schizophrenia, or is restricted to being a compendium of pharmacological recollections on the hippocampal functioning of the mildly intoxicated laboratory rat, we feel that our results will aid in the understanding of this complex animal model of schizophrenia, may give some insights into the cellular basis of psychosis and contribute to an overall better understanding of schizophrenia.

7. References

- Aalto S, Hirvonen J, Kajander J, Scheinin H, Nagren K, Vilkmann H, Gustafsson L, Syvalahti E, Hietala J (2002) Ketamine does not decrease striatal dopamine D2 receptor binding in man. *Psychopharmacology (Berl)* 164:401-406.
- Adell A, Jimenez-Sanchez L, Lopez-Gil X, Romon T (2012) Is the acute NMDA receptor hypofunction a valid model of schizophrenia? *Schizophrenia bulletin* 38:9-14.
- Aghajanian GK, Marek GJ (2000) Serotonin model of schizophrenia: emerging role of glutamate mechanisms. *Brain research reviews* 31:302-312.
- Allen EA, Liu J, Kiehl KA, Gelernter J, Pearson GD, Perrone-Bizzozero NI, Calhoun VD (2011) Components of cross-frequency modulation in health and disease. *Frontiers in systems neuroscience* 5:59.
- Andersen P, Moser EI (1995) Brain temperature and hippocampal function. *Hippocampus* 5:491-498.
- Andine P, Widermark N, Axelsson R, Nyberg G, Olofsson U, Martensson E, Sandberg M (1999) Characterization of MK-801-induced behavior as a putative rat model of psychosis. *The Journal of pharmacology and experimental therapeutics* 290:1393-1408.
- Anver H, Ward PD, Magony A, Vreugdenhil M (2011) NMDA receptor hypofunction phase couples independent gamma-oscillations in the rat visual cortex. *Neuropsychopharmacology* 36:519-528.
- Association AP (2000) *Diagnostic and statistical manual of mental disorders: DSM-IV-TR®*: American Psychiatric Association.
- Association AP (2013) *DSM 5: Diagnostic and statistical manual of mental disorders*: American Psychiatric Association.

- Autry AE, Adachi M, Nosyreva E, Na ES, Los MF, Cheng PF, Kavalali ET, Monteggia LM (2011) NMDA receptor blockade at rest triggers rapid behavioural antidepressant responses. *Nature* 475:91-95.
- Axmacher N, Henseler MM, Jensen O, Weinreich I, Elger CE, Fell J (2010) Cross-frequency coupling supports multi-item working memory in the human hippocampus. *Proceedings of the National Academy of Sciences of the United States of America* 107:3228-3233.
- Barr MS, Farzan F, Arenovich T, Chen R, Fitzgerald PB, Daskalakis ZJ (2011) The effect of repetitive transcranial magnetic stimulation on gamma oscillatory activity in schizophrenia. *PloS one* 6:e22627.
- Becker A, Grecksch G (2004) Ketamine-induced changes in rat behaviour: a possible animal model of schizophrenia. Test of predictive validity. *Progress in neuro-psychopharmacology & biological psychiatry* 28:1267-1277.
- Becker A, Peters B, Schroeder H, Mann T, Huether G, Grecksch G (2003) Ketamine-induced changes in rat behaviour: A possible animal model of schizophrenia. *Progress in neuro-psychopharmacology & biological psychiatry* 27:687-700.
- Belforte JE, Zsiros V, Sklar ER, Jiang Z, Yu G, Li Y, Quinlan EM, Nakazawa K (2010) Postnatal NMDA receptor ablation in corticolimbic interneurons confers schizophrenia-like phenotypes. *Nature neuroscience* 13:76-83.
- Bell RF (2009) Ketamine for chronic non-cancer pain. *Pain* 141:210-214.
- Benes FM (1999) Evidence for altered trisynaptic circuitry in schizophrenic hippocampus. *Biological psychiatry* 46:589-599.
- Benes FM, Todtenkopf MS, Logiotatos P, Williams M (2000) Glutamate decarboxylase(65)-immunoreactive terminals in cingulate and prefrontal cortices of schizophrenic and bipolar brain. *Journal of chemical neuroanatomy* 20:259-269.

- Beneyto M, Meador-Woodruff JH (2008) Lamina-specific abnormalities of NMDA receptor-associated postsynaptic protein transcripts in the prefrontal cortex in schizophrenia and bipolar disorder. *Neuropsychopharmacology* 33:2175-2186.
- Berger H (1929) Über das elektrenkephalogramm des menschen. *European archives of psychiatry and clinical neuroscience* 87:527-570.
- Berman RM, Cappiello A, Anand A, Oren DA, Heninger GR, Charney DS, Krystal JH (2000) Antidepressant effects of ketamine in depressed patients. *Biological psychiatry* 47:351-354.
- Billard V, Gambus PL, Chamoun N, Stanski DR, Shafer SL (1997) A comparison of spectral edge, delta power, and bispectral index as EEG measures of alfentanil, propofol, and midazolam drug effect. *Clinical pharmacology and therapeutics* 61:45-58.
- Bitanhirwe BK, Lim MP, Kelley JF, Kaneko T, Woo TU (2009) Glutamatergic deficits and parvalbumin-containing inhibitory neurons in the prefrontal cortex in schizophrenia. *BMC psychiatry* 9:71.
- Boutros NN, Arfken C, Galderisi S, Warrick J, Pratt G, Iacono W (2008) The status of spectral EEG abnormality as a diagnostic test for schizophrenia. *Schizophrenia research* 99:225-237.
- Bragin A, Jando G, Nadasdy Z, Hetke J, Wise K, Buzsaki G (1995) Gamma (40-100 Hz) oscillation in the hippocampus of the behaving rat. *The journal of neuroscience* 15:47-60.
- Brankack J, Stewart M, Fox SE (1993) Current source density analysis of the hippocampal theta rhythm: associated sustained potentials and candidate synaptic generators. *Brain research* 615:310-327.
- Bremer F (1958) Cerebral and cerebellar potentials. *Physiological reviews* 38:357-388.

- Brockhaus-Dumke A, Mueller R, Faigle U, Klosterkoetter J (2008) Sensory gating revisited: relation between brain oscillations and auditory evoked potentials in schizophrenia. *Schizophrenia research* 99:238-249.
- Brown P, Williams D (2005) Basal ganglia local field potential activity: character and functional significance in the human. *Clinical neurophysiology : official journal of the International Federation of Clinical Neurophysiology* 116:2510-2519.
- Bubenikova-Valesova V, Horacek J, Vrajova M, Hoschl C (2008) Models of schizophrenia in humans and animals based on inhibition of NMDA receptors. *Neuroscience and biobehavioral reviews* 32:1014-1023.
- Buzsaki G (2002) Theta oscillations in the hippocampus. *Neuron* 33:325-340.
- Buzsaki G (2010) Neural syntax: cell assemblies, synapsembles, and readers. *Neuron* 68:362-385.
- Buzsaki G, Draguhn A (2004) Neuronal oscillations in cortical networks. *Science* 304:1926-1929.
- Buzsaki G, Wang XJ (2012) Mechanisms of gamma oscillations. *Annual Reviews in Neuroscience* 35:203-225
- Buzsáki G (2006) *Rhythms of the brain*. Oxford ; New York: Oxford University Press.
- Caixeta FV, Cornelio AM, Scheffer-Teixeira R, Ribeiro S, Tort AB (2013) Ketamine alters oscillatory coupling in the hippocampus. *Scientific reports* 3:2348.
- Canolty RT, Knight RT (2010) The functional role of cross-frequency coupling. *Trends in cognitive sciences* 14:506-515.
- Caplan JB, Madsen JR, Schulze-Bonhage A, Aschenbrenner-Scheibe R, Newman EL, Kahana MJ (2003) Human theta oscillations related to sensorimotor integration and spatial learning. *The journal of neuroscience* 23:4726-4736.

- Carlen M, Meletis K, Siegle JH, Cardin JA, Futai K, Vierling-Claassen D, Ruhlmann C, Jones SR, Deisseroth K, Sheng M, Moore CI, Tsai LH (2011) A critical role for NMDA receptors in parvalbumin interneurons for gamma rhythm induction and behavior. *Molecular psychiatry* 17:537-548.
- Chatterjee M, Ganguly S, Srivastava M, Palit G (2011) Effect of 'chronic' versus 'acute' ketamine administration and its 'withdrawal' effect on behavioural alterations in mice: implications for experimental psychosis. *Behavioural brain research* 216:247-254.
- Chen G, Ensor CR, Bohner B (1966) The neuropharmacology of 2-(α -chlorophenyl)-2-methylaminocyclohexanone hydrochloride. *The Journal of pharmacology and experimental therapeutics* 152:332-339.
- Chen X, Shu S, Bayliss DA (2009) HCN1 channel subunits are a molecular substrate for hypnotic actions of ketamine. *The Journal of neuroscience* 29:600-609.
- Cho RY, Konecky RO, Carter CS (2006) Impairments in frontal cortical gamma synchrony and cognitive control in schizophrenia. *Proceedings of the National Academy of Sciences of the United States of America* 103:19878-19883.
- Chu PS, Ma WK, Wong SC, Chu RW, Cheng CH, Wong S, Tse JM, Lau FL, Yiu MK, Man CW (2008) The destruction of the lower urinary tract by ketamine abuse: a new syndrome? *BJU international* 102:1616-1622.
- Cohen ML, Chan SL, Way WL, Trevor AJ (1973) Distribution in the brain and metabolism of ketamine in the rat after intravenous administration. *Anesthesiology* 39:370-376.
- Cohen MX, Elger CE, Fell J (2009a) Oscillatory activity and phase-amplitude coupling in the human medial frontal cortex during decision making. *Journal of cognitive neuroscience* 21:390-402.

- Cohen MX, Axmacher N, Lenartz D, Elger CE, Sturm V, Schlaepfer TE (2009b) Good vibrations: cross-frequency coupling in the human nucleus accumbens during reward processing. *Journal of cognitive neuroscience* 21:875-889.
- Colbourne F, Sutherland GR, Auer RN (1996) An automated system for regulating brain temperature in awake and freely moving rodents. *Journal of neuroscience methods* 67:185-190.
- Colgin LL, Denninger T, Fyhn M, Hafting T, Bonnevie T, Jensen O, Moser MB, Moser EI (2009) Frequency of gamma oscillations routes flow of information in the hippocampus. *Nature* 462:353-357.
- Conway BA, Halliday DM, Farmer SF, Shahani U, Maas P, Weir AI, Rosenberg JR (1995) Synchronization between motor cortex and spinal motoneuronal pool during the performance of a maintained motor task in man. *The Journal of physiology* 489 (Pt 3):917-924.
- Coyle JT (2006) Glutamate and schizophrenia: beyond the dopamine hypothesis. *Cellular and molecular neurobiology* 26:365-384.
- Cunningham MO, Hunt J, Middleton S, LeBeau FE, Gillies MJ, Davies CH, Maycox PR, Whittington MA, Racca C (2006) Region-specific reduction in entorhinal gamma oscillations and parvalbumin-immunoreactive neurons in animal models of psychiatric illness. *The Journal of neuroscience* 26:2767-2776.
- Domino EF (2010) Taming the ketamine tiger. 1965. *Anesthesiology* 113:678-684.
- Dorandeu F (2013) Happy 50th anniversary ketamine. *CNS neuroscience & therapeutics* 19:369.
- Douglass AB, Hays P, Pazderka F, Russell JM (1991) Florid refractory schizophrenias that turn out to be treatable variants of HLA-associated narcolepsy. *The journal of nervous and mental disease* 179:12-17.

- Ehrlichman RS, Gandal MJ, Maxwell CR, Lazarewicz MT, Finkel LH, Contreras D, Turetsky BI, Siegel SJ (2009) N-methyl-d-aspartic acid receptor antagonist-induced frequency oscillations in mice recreate pattern of electrophysiological deficits in schizophrenia. *Neuroscience* 158:705-712.
- Ellison G (1995) The N-methyl-D-aspartate antagonists phencyclidine, ketamine and dizocilpine as both behavioral and anatomical models of the dementias. *Brain research reviews* 20:250-267.
- Engel AK, Fries P, Singer W (2001) Dynamic predictions: oscillations and synchrony in top-down processing. *Nature reviews neuroscience* 2:704-716.
- Ferrarelli F, Massimini M, Peterson MJ, Riedner BA, Lazar M, Murphy MJ, Huber R, Rosanova M, Alexander AL, Kalin N, Tononi G (2008) Reduced evoked gamma oscillations in the frontal cortex in schizophrenia patients: a TMS/EEG study. *The American journal of psychiatry* 165:996-1005.
- Flynn G, Alexander D, Harris A, Whitford T, Wong W, Galletly C, Silverstein S, Gordon E, Williams LM (2008) Increased absolute magnitude of gamma synchrony in first-episode psychosis. *Schizophrenia research* 105:262-271.
- Ford JM, Krystal JH, Mathalon DH (2007) Neural synchrony in schizophrenia: from networks to new treatments. *Schizophrenia bulletin* 33:848-852.
- Ford JM, Roach BJ, Hoffman RS, Mathalon DH (2008a) The dependence of P300 amplitude on gamma synchrony breaks down in schizophrenia. *Brain research* 1235:133-142.
- Ford JM, Roach BJ, Faustman WO, Mathalon DH (2008b) Out-of-synch and out-of-sorts: dysfunction of motor-sensory communication in schizophrenia. *Biological psychiatry* 63:736-743.
- Freud S (1950) *The Interpretation Of Dreams*: Plain Label Books.

- Fries P, Reynolds JH, Rorie AE, Desimone R (2001) Modulation of oscillatory neuronal synchronization by selective visual attention. *Science* 291:1560-1563.
- Frohlich J, Van Horn JD (2013) Reviewing the ketamine model for schizophrenia. *Journal of psychopharmacology*.
- Gandal MJ, Edgar JC, Klook K, Siegel SJ (2012) Gamma synchrony: towards a translational biomarker for the treatment-resistant symptoms of schizophrenia. *Neuropharmacology* 62:1504-1518.
- Gilmour G, Dix S, Fellini L, Gastambide F, Plath N, Steckler T, Talpos J, Tricklebank M (2012) NMDA receptors, cognition and schizophrenia--testing the validity of the NMDA receptor hypofunction hypothesis. *Neuropharmacology* 62:1401-1412.
- Gilmour G, Pioli EY, Dix SL, Smith JW, Conway MW, Jones WT, Loomis S, Mason R, Shahabi S, Tricklebank MD (2009) Diverse and often opposite behavioural effects of NMDA receptor antagonists in rats: implications for "NMDA antagonist modelling" of schizophrenia. *Psychopharmacology (Berl)* 205:203-216.
- Gonzalez-Burgos G, Lewis DA (2012) NMDA receptor hypofunction, parvalbumin-positive neurons, and cortical gamma oscillations in schizophrenia. *Schizophrenia bulletin* 38:950-957.
- Gottesmann C, Gottesman I (2007) The neurobiological characteristics of rapid eye movement (REM) sleep are candidate endophenotypes of depression, schizophrenia, mental retardation and dementia. *Progress in neurobiology* 81:237-250.
- Green CJ, Knight J, Precious S, Simpkin S (1981) Ketamine alone and combined with diazepam or xylazine in laboratory animals: a 10 year experience. *Laboratory animals* 15:163-170.

- Grutzner C, Wibrals M, Sun L, Rivolta D, Singer W, Maurer K, Uhlhaas PJ (2013) Deficits in high- (>60 Hz) gamma-band oscillations during visual processing in schizophrenia. *Frontiers in human neuroscience* 7:88.
- Haenschel C, Bittner RA, Waltz J, Haertling F, Wibrals M, Singer W, Linden DE, Rodriguez E (2009) Cortical oscillatory activity is critical for working memory as revealed by deficits in early-onset schizophrenia. *The Journal of neuroscience* 29:9481-9489.
- Hahn CG, Wang HY, Cho DS, Talbot K, Gur RE, Berrettini WH, Bakshi K, Kamins J, Borgmann-Winter KE, Siegel SJ, Gallop RJ, Arnold SE (2006) Altered neuregulin 1-erbB4 signaling contributes to NMDA receptor hypofunction in schizophrenia. *Nature medicine* 12:824-828.
- Hakami T, Jones NC, Tolmacheva EA, Gaudias J, Chaumont J, Salzberg M, O'Brien TJ, Pinault D (2009) NMDA receptor hypofunction leads to generalized and persistent aberrant gamma oscillations independent of hyperlocomotion and the state of consciousness. *PloS one* 4:e6755.
- Handel B, Haarmeier T (2009) Cross-frequency coupling of brain oscillations indicates the success in visual motion discrimination. *NeuroImage* 45:1040-1046.
- Harris KD, Csicsvari J, Hirase H, Dragoi G, Buzsaki G (2003) Organization of cell assemblies in the hippocampus. *Nature* 424:552-556.
- Harrison PJ (2004) The hippocampus in schizophrenia: a review of the neuropathological evidence and its pathophysiological implications. *Psychopharmacology (Berl)* 174:151-162.
- Harte MK, Powell SB, Swerdlow NR, Geyer MA, Reynolds GP (2007) Deficits in parvalbumin and calbindin immunoreactive cells in the hippocampus of isolation reared rats. *Journal of neural transmission* 114:893-898.

- Hinman JR, Penley SC, Escabi MA, Chrobak JJ (2013) Ketamine disrupts theta synchrony across the septotemporal axis of the CA1 region of hippocampus. *Journal of neurophysiology* 109:570-579.
- Hong LE, Summerfelt A, Mitchell BD, McMahon RP, Wonodi I, Buchanan RW, Thaker GK (2008) Sensory gating endophenotype based on its neural oscillatory pattern and heritability estimate. *Archives of general psychiatry* 65:1008-1016.
- Hong LE, Summerfelt A, Buchanan RW, O'Donnell P, Thaker GK, Weiler MA, Lahti AC (2010) Gamma and delta neural oscillations and association with clinical symptoms under subanesthetic ketamine. *Neuropsychopharmacology* 35:632-640.
- Howes OD, Kapur S (2009) The dopamine hypothesis of schizophrenia: version III--the final common pathway. *Schizophrenia bulletin* 35:549-562.
- Hunt MJ, Kasicki S (2013) A systematic review of the effects of NMDA receptor antagonists on oscillatory activity recorded in vivo. *Journal of psychopharmacology* 27:972-986.
- Hunt MJ, Raynaud B, Garcia R (2006) Ketamine dose-dependently induces high-frequency oscillations in the nucleus accumbens in freely moving rats. *Biological psychiatry* 60:1206-1214.
- Imre G, Fokkema DS, Den Boer JA, Ter Horst GJ (2006) Dose-response characteristics of ketamine effect on locomotion, cognitive function and central neuronal activity. *Brain research bulletin* 69:338-345.
- Jansen BH, Hegde A, Boutros NN (2004) Contribution of different EEG frequencies to auditory evoked potential abnormalities in schizophrenia. *Clinical neurophysiology* 115:523-533.
- Jansen KL (2000) A review of the nonmedical use of ketamine: use, users and consequences. *Journal of psychoactive drugs* 32:419-433.

- Jansen KL (2004) Ketamine: Dreams and realities: Multidisciplinary Association for Psychedelic Studies Sarasota, FL.
- Javitt DC, Zukin SR (1991) Recent advances in the phencyclidine model of schizophrenia. *The American journal of psychiatry* 148:1301-1308.
- Javitt DC, Zukin SR, Heresco-Levy U, Umbricht D (2012) Has an angel shown the way? Etiological and therapeutic implications of the PCP/NMDA model of schizophrenia. *Schizophrenia bulletin* 38:958-966.
- Jensen O, Colgin LL (2007) Cross-frequency coupling between neuronal oscillations. *Trends in cognitive sciences* 11:267-269.
- Jentsch JD, Roth RH (1999) The neuropsychopharmacology of phencyclidine: from NMDA receptor hypofunction to the dopamine hypothesis of schizophrenia. *Neuropsychopharmacology* 20:201-225.
- Jerabek H, Pabst G, Rappolt M, Stockner T (2010) Membrane-mediated effect on ion channels induced by the anesthetic drug ketamine. *Journal of the American Chemical Society* 132:7990-7997.
- Jin Y, Potkin SG, Kemp AS, Huerta ST, Alva G, Thai TM, Carreon D, Bunney WE, Jr. (2006) Therapeutic effects of individualized alpha frequency transcranial magnetic stimulation (alphaTMS) on the negative symptoms of schizophrenia. *Schizophrenia bulletin* 32:556-561.
- Jones MW (2010) Errant ensembles: dysfunctional neuronal network dynamics in schizophrenia. *Biochemical Society transactions* 38:516-521.
- Jones NC, Reddy M, Anderson P, Salzberg MR, O'Brien TJ, Pinault D (2012) Acute administration of typical and atypical antipsychotics reduces EEG gamma power, but only the preclinical compound LY379268 reduces the ketamine-induced rise in gamma power. *The international journal of neuropsychopharmacology* 15:657-668.
- Jordan S, Chen R, Fernald R, Johnson J, Regardie K, Kambayashi J, Tadori Y, Kitagawa H, Kikuchi T (2006) In vitro biochemical evidence that the

psychotomimetics phencyclidine, ketamine and dizocilpine (MK-801) are inactive at cloned human and rat dopamine D2 receptors. *European journal of pharmacology* 540:53-56.

Kantrowitz JT, Javitt DC (2010) N-methyl-d-aspartate (NMDA) receptor dysfunction or dysregulation: the final common pathway on the road to schizophrenia? *Brain research bulletin* 83:108-121.

Kapur S, Seeman P (2002) NMDA receptor antagonists ketamine and PCP have direct effects on the dopamine D(2) and serotonin 5-HT(2)receptors-implications for models of schizophrenia. *Molecular psychiatry* 7:837-844.

Kapur S, Agid O, Mizrahi R, Li M (2006) How antipsychotics work-from receptors to reality. *NeuroRx : the journal of the American Society for Experimental NeuroTherapeutics* 3:10-21.

Keilhoff G, Becker A, Grecksch G, Wolf G, Bernstein HG (2004) Repeated application of ketamine to rats induces changes in the hippocampal expression of parvalbumin, neuronal nitric oxide synthase and cFOS similar to those found in human schizophrenia. *Neuroscience* 126:591-598.

Keshavan MS, Nasrallah HA, Tandon R (2011) Schizophrenia, "Just the Facts" 6. Moving ahead with the schizophrenia concept: from the elephant to the mouse. *Schizophrenia research* 127:3-13.

Keshavan MS, Reynolds CF, 3rd, Miewald MJ, Montrose DM, Sweeney JA, Vasko RC, Jr., Kupfer DJ (1998) Delta sleep deficits in schizophrenia: evidence from automated analyses of sleep data. *Archives of general psychiatry* 55:443-448.

Kim JA, Connors BW (2012) High temperatures alter physiological properties of pyramidal cells and inhibitory interneurons in hippocampus. *Frontiers in cellular neuroscience* 6:27.

- Kirihara K, Rissling AJ, Swerdlow NR, Braff DL, Light GA (2012) Hierarchical organization of gamma and theta oscillatory dynamics in schizophrenia. *Biological psychiatry* 71:873-880.
- Kittelberger K, Hur EE, Sazegar S, Keshavan V, Kocsis B (2012) Comparison of the effects of acute and chronic administration of ketamine on hippocampal oscillations: relevance for the NMDA receptor hypofunction model of schizophrenia. *Brain structure & function* 217:395-409.
- Kocsis B (2012) Differential role of NR2A and NR2B subunits in N-Methyl-D-Aspartate receptor antagonist-induced aberrant cortical gamma oscillations. *Biological psychiatry* 71:987-995.
- Kocsis B, Brown RE, McCarley RW, Hajos M (2013) Impact of ketamine on neuronal network dynamics: translational modeling of schizophrenia-relevant deficits. *CNS neuroscience & therapeutics* 19:437-447.
- Kopell N, Kramer MA, Malerba P, Whittington MA (2010) Are different rhythms good for different functions? *Frontiers in human neuroscience* 4:187.
- Korotkova T, Fuchs EC, Ponomarenko A, von Engelhardt J, Monyer H (2010) NMDA receptor ablation on parvalbumin-positive interneurons impairs hippocampal synchrony, spatial representations, and working memory. *Neuron* 68:557-569.
- Kramer MA, Tort AB, Kopell NJ (2008) Sharp edge artifacts and spurious coupling in EEG frequency comodulation measures. *Journal of neuroscience methods* 170:352-357.
- Krishnan GP, Vohs JL, Hetrick WP, Carroll CA, Shekhar A, Bockbrader MA, O'Donnell BF (2005) Steady state visual evoked potential abnormalities in schizophrenia. *Clinical neurophysiology* 116:614-624.
- Kristiansen LV, Huerta I, Beneyto M, Meador-Woodruff JH (2007) NMDA receptors and schizophrenia. *Current opinion in pharmacology* 7:48-55.

- Krystal JH, Karper LP, Seibyl JP, Freeman GK, Delaney R, Bremner JD, Heninger GR, Bowers MB, Jr., Charney DS (1994) Subanesthetic effects of the noncompetitive NMDA antagonist, ketamine, in humans. Psychotomimetic, perceptual, cognitive, and neuroendocrine responses. *Archives of general psychiatry* 51:199-214.
- Kwon JS, O'Donnell BF, Wallenstein GV, Greene RW, Hirayasu Y, Nestor PG, Hasselmo ME, Potts GF, Shenton ME, McCarley RW (1999) Gamma frequency-range abnormalities to auditory stimulation in schizophrenia. *Archives of general psychiatry* 56:1001-1005.
- Lahti AC, Holcomb HH, Medoff DR, Tamminga CA (1995a) Ketamine activates psychosis and alters limbic blood flow in schizophrenia. *Neuroreport* 6:869-872.
- Lahti AC, Koffel B, LaPorte D, Tamminga CA (1995b) Subanesthetic doses of ketamine stimulate psychosis in schizophrenia. *Neuropsychopharmacology* 13:9-19.
- Lahti AC, Weiler MA, Tamara Michaelidis BA, Parwani A, Tamminga CA (2001) Effects of ketamine in normal and schizophrenic volunteers. *Neuropsychopharmacology* 25:455-467.
- Lakatos P, Karmos G, Mehta AD, Ulbert I, Schroeder CE (2008) Entrainment of neuronal oscillations as a mechanism of attentional selection. *Science* 320:110-113.
- Large CH (2007) Do NMDA receptor antagonist models of schizophrenia predict the clinical efficacy of antipsychotic drugs? *Journal of psychopharmacology* 21:283-301.
- Lazarewicz MT, Ehrlichman RS, Maxwell CR, Gandal MJ, Finkel LH, Siegel SJ (2010) Ketamine modulates theta and gamma oscillations. *Journal of cognitive neuroscience* 22:1452-1464.

- Leao RN, Mikulovic S, Leao KE, Munguba H, Gezelius H, Enjin A, Patra K, Eriksson A, Loew LM, Tort AB, Kullander K (2012) OLM interneurons differentially modulate CA3 and entorhinal inputs to hippocampal CA1 neurons. *Nature neuroscience* 15:1524-1530.
- Lee KH, Williams LM, Breakspear M, Gordon E (2003) Synchronous gamma activity: a review and contribution to an integrative neuroscience model of schizophrenia. *Brain research reviews* 41:57-78.
- Lee SH, Wynn JK, Green MF, Kim H, Lee KJ, Nam M, Park JK, Chung YC (2006) Quantitative EEG and low resolution electromagnetic tomography (LORETA) imaging of patients with persistent auditory hallucinations. *Schizophrenia research* 83:111-119.
- Leicht G, Kirsch V, Giegling I, Karch S, Hantschk I, Moller HJ, Pogarell O, Hegerl U, Rujescu D, Mulert C (2010) Reduced early auditory evoked gamma-band response in patients with schizophrenia. *Biological psychiatry* 67:224-231.
- Leung LW, Desborough KA (1988) APV, an N-methyl-D-aspartate receptor antagonist, blocks the hippocampal theta rhythm in behaving rats. *Brain research* 463:148-152.
- Li N, Lee B, Liu RJ, Banasr M, Dwyer JM, Iwata M, Li XY, Aghajanian G, Duman RS (2010) mTOR-dependent synapse formation underlies the rapid antidepressant effects of NMDA antagonists. *Science* 329:959-964.
- Light GA, Hsu JL, Hsieh MH, Meyer-Gomes K, Sprock J, Swerdlow NR, Braff DL (2006) Gamma band oscillations reveal neural network cortical coherence dysfunction in schizophrenia patients. *Biological psychiatry* 60:1231-1240.
- Lin SZ, Chiou AL, Wang Y (1996) Ketamine antagonizes nitric oxide release from cerebral cortex after middle cerebral artery ligation in rats. *Stroke; a journal of cerebral circulation* 27:747-752.

- Lisman J, Buzsaki G (2008) A neural coding scheme formed by the combined function of gamma and theta oscillations. *Schizophrenia bulletin* 34:974-980.
- Littlewood CL, Cash D, Dixon AL, Dix SL, White CT, O'Neill MJ, Tricklebank M, Williams SC (2006) Using the BOLD MR signal to differentiate the stereoisomers of ketamine in the rat. *NeuroImage* 32:1733-1746.
- Liu J, Ji XQ, Zhu XZ (2006) Comparison of psychic emergence reactions after (+/-)-ketamine and (+)-ketamine in mice. *Life sciences* 78:1839-1844.
- Luby ED, Cohen BD, Rosenbaum G, Gottlieb JS, Kelley R (1959) Study of a new schizophrenomimetic drug; sernyl. *AMA archives of neurology and psychiatry* 81:363-369.
- Ma J, Leung LS (2000) Relation between hippocampal gamma waves and behavioral disturbances induced by phencyclidine and methamphetamine. *Behavioural brain research* 111:1-11.
- Maddox VH, Godefroi EF, Parcell RF (1965) The Synthesis of Phencyclidine and Other 1-Arylcyclohexylamines. *Journal of medicinal chemistry* 8:230-235.
- Malhotra AK, Pinals DA, Weingartner H, Sirocco K, Missar CD, Pickar D, Breier A (1996) NMDA receptor function and human cognition: the effects of ketamine in healthy volunteers. *Neuropsychopharmacology* 14:301-307.
- Manns JR, Zilli EA, Ong KC, Hasselmo ME, Eichenbaum H (2007) Hippocampal CA1 spiking during encoding and retrieval: relation to theta phase. *Neurobiology of learning and memory* 87:9-20.
- McGrath J, Saha S, Chant D, Welham J (2008) Schizophrenia: a concise overview of incidence, prevalence, and mortality. *Epidemiologic reviews* 30:67-76.
- Mitra P, Bokil H (2007) *Observed brain dynamics*: Oxford University Press.
- Moga D, Hof PR, Vissavajhala P, Moran TM, Morrison JH (2002) Parvalbumin-containing interneurons in rat hippocampus have an AMPA receptor

- profile suggestive of vulnerability to excitotoxicity. *Journal of chemical neuroanatomy* 23:249-253.
- Moghaddam B, Adams B, Verma A, Daly D (1997) Activation of glutamatergic neurotransmission by ketamine: a novel step in the pathway from NMDA receptor blockade to dopaminergic and cognitive disruptions associated with the prefrontal cortex. *The Journal of neuroscience* 17:2921-2927.
- Moran LV, Hong LE (2011) High vs low frequency neural oscillations in schizophrenia. *Schizophrenia bulletin* 37:659-663.
- Mulert C, Leicht G, Hepp P, Kirsch V, Karch S, Pogarell O, Reiser M, Hegerl U, Jager L, Moller HJ, McCarley RW (2010) Single-trial coupling of the gamma-band response and the corresponding BOLD signal. *NeuroImage* 49:2238-2247.
- Nakazawa K, Zsiros V, Jiang Z, Nakao K, Kolata S, Zhang S, Belforte JE (2012) GABAergic interneuron origin of schizophrenia pathophysiology. *Neuropharmacology* 62:1574-1583.
- Newcomer JW, Farber NB, Jevtovic-Todorovic V, Selke G, Melson AK, Hershey T, Craft S, Olney JW (1999) Ketamine-induced NMDA receptor hypofunction as a model of memory impairment and psychosis. *Neuropsychopharmacology* 20:106-118.
- Neymotin SA, Lazarewicz MT, Sherif M, Contreras D, Finkel LH, Lytton WW (2011) Ketamine disrupts theta modulation of gamma in a computer model of hippocampus. *The Journal of neuroscience* 31:11733-11743.
- Nicolas MJ, Lopez-Azcarate J, Valencia M, Alegre M, Perez-Alcazar M, Iriarte J, Artieda J (2011) Ketamine-induced oscillations in the motor circuit of the rat basal ganglia. *PloS one* 6:e21814.
- Nishimura M, Sato K (1999) Ketamine stereoselectively inhibits rat dopamine transporter. *Neuroscience letters* 274:131-134.

- O'Donnell P, Grace AA (1998) Dysfunctions in multiple interrelated systems as the neurobiological bases of schizophrenic symptom clusters. *Schizophrenia bulletin* 24:267-283.
- O'Keefe J, Recce ML (1993) Phase relationship between hippocampal place units and the EEG theta rhythm. *Hippocampus* 3:317-330.
- Ogden KK, Traynelis SF (2011) New advances in NMDA receptor pharmacology. *Trends in pharmacological sciences* 32:726-733.
- Olney JW, Newcomer JW, Farber NB (1999) NMDA receptor hypofunction model of schizophrenia. *Journal of psychiatric research* 33:523-533.
- Orser BA, Pennefather PS, MacDonald JF (1997) Multiple mechanisms of ketamine blockade of N-methyl-D-aspartate receptors. *Anesthesiology* 86:903-917.
- Pai A, Heining M (2007) Ketamine. *Continuing Education in Anaesthesia, Critical Care & Pain* 7:59-63.
- Palenicek T, Fujakova M, Brunovsky M, Balikova M, Horacek J, Gorman I, Tyls F, Tislerova B, Sos P, Bubenikova-Valesova V, Hoschl C, Krajca V (2011) Electroencephalographic spectral and coherence analysis of ketamine in rats: correlation with behavioral effects and pharmacokinetics. *Neuropsychobiology* 63:202-218.
- Paoletti P, Neyton J (2007) NMDA receptor subunits: function and pharmacology. *Current opinion in pharmacology* 7:39-47.
- Paoletti P, Ascher P, Neyton J (1997) High-affinity zinc inhibition of NMDA NR1-NR2A receptors. *The Journal of neuroscience* 17:5711-5725.
- Paoletti P, Bellone C, Zhou Q (2013) NMDA receptor subunit diversity: impact on receptor properties, synaptic plasticity and disease. *Nature reviews neuroscience* 14:383-400.

- Petersen RC, Stillman RC (1978) Phencyclidine (PCP) abuse : an appraisal. NIDA research monograph:vii, 313 p.
- Pinault D (2008) N-Methyl d-Aspartate receptor antagonists ketamine and MK-801 induce wake-related aberrant γ oscillations in the rat neocortex. *Biological psychiatry* 63:730-735.
- Quibell R, Prommer EE, Mihalyo M, Twycross R, Wilcock A (2011) Ketamine*. *Journal of pain and symptom management* 41:640-649.
- Rabin RA, Doat M, Winter JC (2000) Role of serotonergic 5-HT_{2A} receptors in the psychotomimetic actions of phencyclidine. *The international journal of neuropsychopharmacology* 3:333-338.
- Reich DL, Silvay G (1989) Ketamine: an update on the first twenty-five years of clinical experience. *Canadian journal of anaesthesia* 36:186-197.
- Romon T, Mengod G, Adell A (2011) Expression of parvalbumin and glutamic acid decarboxylase-67 after acute administration of MK-801. Implications for the NMDA hypofunction model of schizophrenia. *Psychopharmacology (Berl)* 217:231-238.
- Roopun AK, Cunningham MO, Racca C, Alter K, Traub RD, Whittington MA (2008) Region-specific changes in gamma and beta2 rhythms in NMDA receptor dysfunction models of schizophrenia. *Schizophrenia bulletin* 34:962-973.
- Rujescu D, Bender A, Keck M, Hartmann AM, Ohl F, Raeder H, Giegling I, Genius J, McCarley RW, Moller HJ, Grunze H (2006) A pharmacological model for psychosis based on N-methyl-D-aspartate receptor hypofunction: molecular, cellular, functional and behavioral abnormalities. *Biological psychiatry* 59:721-729.
- Rutter L, Carver FW, Holroyd T, Nadar SR, Mitchell-Francis J, Apud J, Weinberger DR, Coppola R (2009) Magnetoencephalographic gamma power reduction in patients with schizophrenia during resting condition. *Human brain mapping* 30:3254-3264.

- Sabbagh JJ, Heaney CF, Bolton MM, Murtishaw AS, Kinney JW (2012) Examination of ketamine-induced deficits in sensorimotor gating and spatial learning. *Physiology & behavior* 107:355-363.
- Sanz-Clemente A, Nicoll RA, Roche KW (2013) Diversity in NMDA receptor composition: many regulators, many consequences. *The Neuroscientist* 19:62-75.
- Scheffer-Teixeira R, Belchior H, Leao RN, Ribeiro S, Tort AB (2013) On high-frequency field oscillations (>100 Hz) and the spectral leakage of spiking activity. *The Journal of neuroscience* 33:1535-1539.
- Scheffer-Teixeira R, Belchior H, Caixeta FV, Souza BC, Ribeiro S, Tort AB (2012) Theta phase modulates multiple layer-specific oscillations in the CA1 region. *Cerebral cortex* 22:2404-2414.
- Scheffzuk C, Kukushka VI, Vyssotski AL, Draguhn A, Tort AB, Brankack J (2011) Selective coupling between theta phase and neocortical fast gamma oscillations during REM-sleep in mice. *PloS one* 6:e28489.
- Schroeder CE, Lakatos P (2009) Low-frequency neuronal oscillations as instruments of sensory selection. *Trends in neurosciences* 32:9-18.
- Seeman P (2004) Comment on "Diverse Psychotomimetics Act Through a Common Signaling Pathway". *Science* 305:180-180.
- Seeman P, Ko F, Tallerico T (2005) Dopamine receptor contribution to the action of PCP, LSD and ketamine psychotomimetics. *Molecular psychiatry* 10:877-883.
- Seeman P, Guan HC, Hirbec H (2009) Dopamine D2High receptors stimulated by phencyclidines, lysergic acid diethylamide, salvinorin A, and modafinil. *Synapse* 63:698-704.
- Siegel RK (1978) Phencyclidine, criminal behavior, and the defense of diminished capacity. *NIDA research monograph*:272-288.

- Siekmeier PJ, Stufflebeam SM (2010) Patterns of spontaneous magnetoencephalographic activity in patients with schizophrenia. *Journal of clinical neurophysiology* 27:179-190.
- Singer W, Gray CM (1995) Visual feature integration and the temporal correlation hypothesis. *Annual review of neuroscience* 18:555-586.
- Sirota A, Montgomery S, Fujisawa S, Isomura Y, Zugaro M, Buzsaki G (2008) Entrainment of neocortical neurons and gamma oscillations by the hippocampal theta rhythm. *Neuron* 60:683-697.
- Spencer KM (2009) The functional consequences of cortical circuit abnormalities on gamma oscillations in schizophrenia: insights from computational modeling. *Frontiers in human neuroscience* 3:33.
- Spencer KM (2011) Baseline gamma power during auditory steady-state stimulation in schizophrenia. *Frontiers in human neuroscience* 5:190.
- Spencer KM, Salisbury DF, Shenton ME, McCarley RW (2008) Gamma-band auditory steady-state responses are impaired in first episode psychosis. *Biological psychiatry* 64:369-375.
- Spencer KM, Nestor PG, Niznikiewicz MA, Salisbury DF, Shenton ME, McCarley RW (2003) Abnormal neural synchrony in schizophrenia. *The Journal of neuroscience* 23:7407-7411.
- Spencer KM, Nestor PG, Perlmuter R, Niznikiewicz MA, Klump MC, Frumin M, Shenton ME, McCarley RW (2004) Neural synchrony indexes disordered perception and cognition in schizophrenia. *Proceedings of the National Academy of Sciences of the United States of America* 101:17288-17293.
- Sperling W, Vieth J, Martus M, Demling J, Barocka A (1999) Spontaneous slow and fast MEG activity in male schizophrenics treated with clozapine. *Psychopharmacology (Berl)* 142:375-382.
- Sponheim SR, Clementz BA, Iacono WG, Beiser M (1994) Resting EEG in first-episode and chronic schizophrenia. *Psychophysiology* 31:37-43.

- Steriade M, McCormick DA, Sejnowski TJ (1993) Thalamocortical oscillations in the sleeping and aroused brain. *Science* 262:679-685.
- Sun L, Castellanos N, Grutzner C, Koethe D, Rivolta D, Wibrall M, Kranaster L, Singer W, Leweke MF, Uhlhaas PJ (2013) Evidence for dysregulated high-frequency oscillations during sensory processing in medication-naive, first episode schizophrenia. *Schizophrenia research* 150:519-525.
- Svenningsson P, Nomikos GG, Greengard P (2004) Response to Comment on "Diverse Psychotomimetics Act Through a Common Signaling Pathway". *Science* 305:180-180.
- Svenningsson P, Tzavara ET, Carruthers R, Rachleff I, Wattler S, Nehls M, McKinzie DL, Fienberg AA, Nomikos GG, Greengard P (2003) Diverse psychotomimetics act through a common signaling pathway. *Science* 302:1412-1415.
- Tekell JL, Hoffmann R, Hendrickse W, Greene RW, Rush AJ, Armitage R (2005) High frequency EEG activity during sleep: characteristics in schizophrenia and depression. *Clinical EEG and neuroscience* 36:25-35.
- Tort AB (2005) Sistemas dopaminérgicos e ação antipsicótica: abordagens experimentais e teóricas. In: Departamento de Bioquímica. Porto Alegre, Brasil: Universidade Federal do Rio Grande do Sul.
- Tort AB, Komorowski R, Eichenbaum H, Kopell N (2010a) Measuring phase-amplitude coupling between neuronal oscillations of different frequencies. *Journal of neurophysiology* 104:1195-1210.
- Tort AB, Rotstein HG, Dugladze T, Gloveli T, Kopell NJ (2007) On the formation of gamma-coherent cell assemblies by oriens lacunosum-moleculare interneurons in the hippocampus. *Proceedings of the National Academy of Sciences of the United States of America* 104:13490-13495.
- Tort AB, Komorowski RW, Manns JR, Kopell NJ, Eichenbaum H (2009) Theta-gamma coupling increases during the learning of item-context

- associations. *Proceedings of the National Academy of Sciences of the United States of America* 106:20942-20947.
- Tort AB, Scheffer-Teixeira R, Souza BC, Draguhn A, Brankack J (2013) Theta-associated high-frequency oscillations (110-160Hz) in the hippocampus and neocortex. *Progress in neurobiology* 100:1-14.
- Tort AB, Neto WP, Amaral OB, Kazlauskas V, Souza DO, Lara DR (2006) A simple webcam-based approach for the measurement of rodent locomotion and other behavioural parameters. *Journal of neuroscience methods* 157:91-97.
- Tort AB, Fontanini A, Kramer MA, Jones-Lush LM, Kopell NJ, Katz DB (2010b) Cortical networks produce three distinct 7-12 Hz rhythms during single sensory responses in the awake rat. *The Journal of neuroscience* 30:4315-4324.
- Tort AB, Kramer MA, Thorn C, Gibson DJ, Kubota Y, Graybiel AM, Kopell NJ (2008) Dynamic cross-frequency couplings of local field potential oscillations in rat striatum and hippocampus during performance of a T-maze task. *Proceedings of the National Academy of Sciences of the United States of America* 105:20517-20522.
- Tsai G, Coyle JT (2002) Glutamatergic mechanisms in schizophrenia. *Annual review of pharmacology and toxicology* 42:165-179.
- Uhlhaas PJ, Singer W (2006) Neural synchrony in brain disorders: relevance for cognitive dysfunctions and pathophysiology. *Neuron* 52:155-168.
- Uhlhaas PJ, Singer W (2010) Abnormal neural oscillations and synchrony in schizophrenia. *Nature reviews neuroscience* 11:100-113.
- Uhlhaas PJ, Haenschel C, Nikolic D, Singer W (2008) The role of oscillations and synchrony in cortical networks and their putative relevance for the pathophysiology of schizophrenia. *Schizophrenia bulletin* 34:927-943.

- Uhlhaas PJ, Linden DE, Singer W, Haenschel C, Lindner M, Maurer K, Rodriguez E (2006) Dysfunctional long-range coordination of neural activity during Gestalt perception in schizophrenia. *The Journal of neuroscience* 26:8168-8175.
- van Kammen DP, Bunney WE, Jr., Docherty JP, Marder SR, Ebert MH, Rosenblatt JE, Rayner JN (1982) d-Amphetamine-induced heterogeneous changes in psychotic behavior in schizophrenia. *The American journal of psychiatry* 139:991-997.
- Vollenweider FX, Leenders KL, Scharfetter C, Antonini A, Maguire P, Missimer J, Angst J (1997) Metabolic hyperfrontality and psychopathology in the ketamine model of psychosis using positron emission tomography (PET) and [18F]fluorodeoxyglucose (FDG). *European journal of neuropsychopharmacology* 7:9-24.
- Voytek B, Canolty RT, Shestyuk A, Crone NE, Parvizi J, Knight RT (2010) Shifts in gamma phase-amplitude coupling frequency from theta to alpha over posterior cortex during visual tasks. *Frontiers in human neuroscience* 4:191.
- Weickert CS, Fung SJ, Catts VS, Schofield PR, Allen KM, Moore LT, Newell KA, Pellen D, Huang XF, Catts SV, Weickert TW (2013) Molecular evidence of N-methyl-D-aspartate receptor hypofunction in schizophrenia. *Molecular psychiatry* 18:1185-1192.
- White PF, Schuttler J, Shafer A, Stanski DR, Horai Y, Trevor AJ (1985) Comparative pharmacology of the ketamine isomers. *Studies in volunteers. British journal of anaesthesia* 57:197-203.
- Whittington MA, Roopun AK, Traub RD, Davies CH (2011) Circuits and brain rhythms in schizophrenia: a wealth of convergent targets. *Current opinion in pharmacology* 11:508-514.

- Williams K (1993) Ifenprodil discriminates subtypes of the N-methyl-D-aspartate receptor: selectivity and mechanisms at recombinant heteromeric receptors. *Molecular pharmacology* 44:851-859.
- Wolff K, Winstock AR (2006) Ketamine : from medicine to misuse. *CNS drugs* 20:199-218.
- Womelsdorf T, Schoffelen JM, Oostenveld R, Singer W, Desimone R, Engel AK, Fries P (2007) Modulation of neuronal interactions through neuronal synchronization. *Science* 316:1609-1612.
- Woo TU, Walsh JP, Benes FM (2004) Density of glutamic acid decarboxylase 67 messenger RNA-containing neurons that express the N-methyl-D-aspartate receptor subunit NR2A in the anterior cingulate cortex in schizophrenia and bipolar disorder. *Archives of general psychiatry* 61:649-657.
- Woo TU, Spencer K, McCarley RW (2010) Gamma oscillation deficits and the onset and early progression of schizophrenia. *Harvard review of psychiatry* 18:173-189.
- Wulff P, Ponomarenko AA, Bartos M, Korotkova TM, Fuchs EC, Bahner F, Both M, Tort ABL, Kopell NJ, Wisden W, Monyer H (2009) Hippocampal theta rhythm and its coupling with gamma oscillations require fast inhibition onto parvalbumin-positive interneurons. *Proceedings of the National Academy of Sciences of the United States of America* 106:3561-3566.
- Ylinen A, Bragin A, Nadasdy Z, Jando G, Szabo I, Sik A, Buzsaki G (1995) Sharp wave-associated high-frequency oscillation (200 Hz) in the intact hippocampus: network and intracellular mechanisms. *The Journal of neuroscience : the official journal of the Society for Neuroscience* 15:30-46.
- Zarate CA, Jr., Singh JB, Carlson PJ, Brutsche NE, Ameli R, Luckenbaugh DA, Charney DS, Manji HK (2006) A randomized trial of an N-methyl-D-

aspartate antagonist in treatment-resistant major depression. Archives of general psychiatry 63:856-864.

Zhang Y, Yoshida T, Katz DB, Lisman JE (2012) NMDAR antagonist action in thalamus imposes delta oscillations on the hippocampus. Journal of neurophysiology 107:3181-3189.

8. List of publications (2010-2013)

8.1 Publication related to the thesis

Caixeta FV, Cornelio AM, Scheffer-Teixeira R, Ribeiro S, Tort AB (2013) Ketamine alters oscillatory coupling in the hippocampus. *Scientific reports* 3:2348.

8.2 Other publications

Ribeiro TL, Copelli M, **Caixeta F**, Belchior H, Chialvo DR, Nicolelis MA, Ribeiro S (2010) Spike avalanches exhibit universal dynamics across the sleep-wake cycle. *PloS one* 5:e14129.

Vasconcelos N, Pantoja J, Belchior H, **Caixeta FV**, Faber J, Freire MA, Cota VR, Anibal de Macedo E, Laplagne DA, Gomes HM, Ribeiro S (2011) Cross-modal responses in the primary visual cortex encode complex objects and correlate with tactile discrimination. *Proceedings of the National Academy of Sciences of the United States of America* 108:15408-15413.

Scheffer-Teixeira R, Belchior H, **Caixeta FV**, Souza BC, Ribeiro S, Tort AB (2012) Theta phase modulates multiple layer-specific oscillations in the CA1 region. *Cerebral cortex* 22:2404-2414.

8.3 Media coverage of our work

Pesquisadores da UFRN publicam artigo sobre psicose em revista britânica – Printed on Tribuna do Norte, a local newspaper from Natal-RN, and published online on August 2, 2013 at: <http://tribunadonorte.com.br/noticia/pesquisadores-da-ufrn-publicam-artigo-sobre-psicose-em-revista-britanica/257341>

Sonhando acordado - Durante o surto de psicose, cérebro apresenta padrão de atividade elétrica semelhante ao observado nos sonhos – Published online on Pesquisa FAPESP Edição Online on August 5, 2013 at: <http://revistapesquisa.fapesp.br/2013/08/05/sonhando-acordado/>

Pesquisadores brasileiros avançam no estudo da esquizofrenia – Aired on national TV Jornal Hoje, Rede Globo de Televisão and published online on August 24, 2013 at: <http://globotv.globo.com/rede-globo/jornal-hoje/v/pesquisadores-brasileiros-avancam-no-estudo-da-esquizofrenia/2779709/>

Pesquisadores do RN dão primeiro passo na identificação da esquizofrenia – Aired on local TV RNTV 2ª Edição, InterTV Cabugi/RN on August 24, 2013 and published online at: <http://globotv.globo.com/inter-tv-rn/rn-tv-2a-edicao/v/pesquisadores-do-rn-dao-primeiro-passo-na-identificacao-da-esquizofrenia/2780401/>

Filho de patenses participa de importante pesquisa científica sobre a Esquizofrenia – Printed on Folha Patense, a local newspaper from Patos de Minas-MG, and published online on September 7, 2013: [http://www.folhapatense.com.br/FP%201063%20\(070913\).pdf](http://www.folhapatense.com.br/FP%201063%20(070913).pdf)

Annex A

CEUA-AASDAP: Parecer - 02/2011

Adriana Ragoni to me, Adriano, Arboes, Claudio, Marcos Apr 28

Prezados Prof. Adriano e Fábio,

A Comissão de Ética no Uso de Animais em Pesquisa da AASDAP (CEUA-AASDAP) analisou seu protocolo de pesquisa abaixo identificado, bem como os esclarecimentos feitos posteriormente, e considerou que ele preenche as condições requeridas para ser classificado como aprovado. Dessa forma, segue nosso parecer:

Protocolo 02/2011

Título: Estudo dos acoplamentos da atividade neural entre o Giro Denteado e a região CA hipocampal durante a formação de memórias espaciais e em estados cognitivos alterados.

Parecer: Aprovado.

Atenciosamente, Adriana

--

Adriana Ragoni Jorge Ferreira
Coordenadora de Laboratório AASDAP/IINN-ELS
Fones: +55 (84) 4008-0003/ 4008-0573 (direto)
Fax: +55 (84) 4008-0554
www.natalneuro.org.br

Annex B



Universidade Federal do Rio Grande do Norte
COMISSÃO DE ÉTICA NO USO DE ANIMAIS - CEUA

PROTOCOLO N.º 060/2011

Professor/Pesquisador: *ADRIANO BRETANHA LOPES TORT*

Natal (RN), 29 de fevereiro de 2012.

Prezado Professor/Pesquisador,

Vimos, através deste documento, informar que o projeto "ESTUDO DO PAPEL DOS ACOPLAMENTOS ENTRE OSCILAÇÕES CORTICAIS NA REALIZAÇÃO DAS FUNÇÕES COGNITIVAS", **protocolo n.º 060/2011**, após análise das adequações, foi considerado **APROVADO** por esta Comissão.

Informamos ainda que, segundo o Cap. 2, Art. 13 do Regimento, é função do professor/pesquisador responsável pelo projeto a elaboração de relatório(s) de acompanhamento que deverá(ão) ser entregue(s) dentro do(s) prazo(s) estabelecido(s) abaixo:

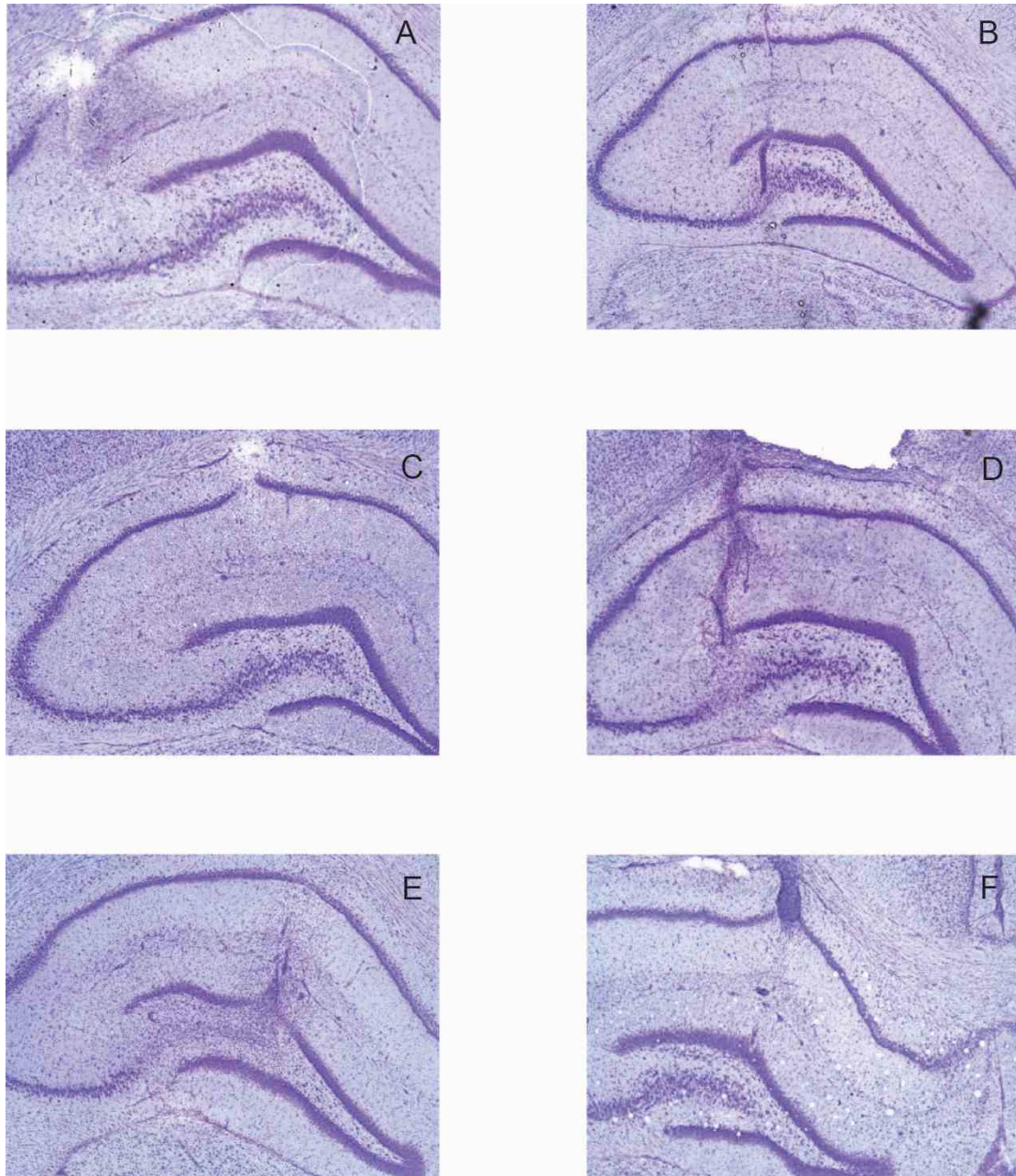
- Relatório Final: **FEVEREIRO DE 2014** (30 dias após a conclusão do projeto).

Agradecemos a sua atenção e nos colocamos a disposição para eventuais esclarecimentos.

Cordialmente,


Elaine C. Gavioli
Coordenadora da CEUA

Annex C



Histological coronal sections of the hippocampi from six animals (A-F) implanted with chronic bundles of eight vertically staggered electrodes. Notice lesion tracks of the electrodes crossing the CA1 pyramidal layer into deeper hippocampal regions. Some electrode tracks appear bent due to artifacts caused by fixative-free histological procedures.



OPEN

Ketamine alters oscillatory coupling in the hippocampus

Fábio V. Caixeta^{1,2}, Alianda M. Cornélio¹, Robson Scheffer-Teixeira¹, Sidarta Ribeiro¹ & Adriano B. L. Tort¹

¹Brain Institute, Federal University of Rio Grande do Norte, Natal, RN 59056-450, Brazil, ²Edmond and Lily Safra International Institute of Neuroscience of Natal, Natal, RN 59066-060, Brazil.

SUBJECT AREAS:

SCHIZOPHRENIA

EXPERIMENTAL MODELS OF
DISEASE

EXTRACELLULAR RECORDING

NEUROPHYSIOLOGY

Received
22 March 2013

Accepted
18 July 2013

Published
2 August 2013

Correspondence and
requests for materials
should be addressed to
A.B.L.T. (tort@neuro.
ufrn.br)

Recent studies show that higher order oscillatory interactions such as cross-frequency coupling are important for brain functions that are impaired in schizophrenia, including perception, attention and memory. Here we investigated the dynamics of oscillatory coupling in the hippocampus of awake rats upon NMDA receptor blockade by ketamine, a pharmacological model of schizophrenia. Ketamine (25, 50 and 75 mg/kg i.p.) increased gamma and high-frequency oscillations (HFO) in all depths of the CA1-dentate axis, while theta power changes depended on anatomical location and were independent of a transient increase of delta oscillations. Phase coherence of gamma and HFO increased across hippocampal layers. Phase-amplitude coupling between theta and fast oscillations was markedly altered in a dose-dependent manner: ketamine increased hippocampal theta-HFO coupling at all doses, while theta-gamma coupling increased at the lowest dose and was disrupted at the highest dose. Our results demonstrate that ketamine alters network interactions that underlie cognitively relevant theta-gamma coupling.

Oscillations in the activity of neuronal populations are associated with the coordination of distributed neuronal groups believed to underlie cognitive processing^{1–3}. Disturbance in cortical oscillations has been suggested as a possible neural basis for symptoms of mental disorders such as schizophrenia^{4,5}. In particular, aberrant gamma-frequency oscillations (30–100 Hz) have been reported in schizophrenic patients^{6,7}, but alterations in other frequency bands are also likely to play a role⁸.

Acute blockade of glutamate N-methyl-D-aspartate receptors (NMDAR) by ketamine in humans induces negative and positive symptoms similar to those found in schizophrenia⁹, and exacerbates its core symptoms when administered to patients¹⁰. In animals, acute NMDAR blockade induces behavioural, biochemical and electrophysiological alterations^{11–15} that present predictive, constructive and face validity as a pharmacological model for schizophrenia¹⁶. Previous studies in rodents have shown that ketamine increases the power of gamma^{12,15} and delta¹⁷ oscillations, and may differentially affect theta power depending on recording region^{15,18,19}. Of note, some of the electrophysiological alterations induced by ketamine, such as aberrant gamma oscillations, have been dissociated from its motor effects¹⁴.

Brain rhythms of different frequencies are not independent, but can rather interact in several ways²⁰. Cross-frequency coupling (CFC) among neuronal oscillations has been linked to brain functions such as detection of sensory signals, reward signalling, decision-making, working memory, attention and learning (see ref. 21 for a review). CFC patterns differ across brain areas^{22,23} and change dynamically in a task-relevant manner in response to sensory, motor and cognitive events^{21,24}. Although CFC has been implied in several brain functions, few studies have attempted to characterize CFC in schizophrenia²⁵ or in its animal models¹³.

In this work we investigated the effects of acute NMDAR blockade by ketamine on the dynamics of spectral content and oscillatory interactions in the hippocampus, a brain region that has long been associated with the schizophrenia phenotype²⁶. We focused on cognitively relevant frequency bands: theta (5–10 Hz), gamma (30–100 Hz) and high-frequency oscillations (HFO; 110–160 Hz). We found that ketamine leads to frequency- and region-specific alterations of local field potential (LFP) power, altered phase synchrony, and aberrant cross-frequency coupling of neural oscillations. Taken together, these results demonstrate that ketamine distorts normal oscillatory interactions in the rat hippocampus.

Results

NMDAR blockade increases locomotion and high frequency oscillations. Consistent with previous reports^{11,12,14}, we found that systemic administration of ketamine increased locomotor activity (Fig. 1a, b) and gamma power (Fig. 2) at all doses studied. While peak locomotion speed was similar for all doses (Fig. 1c), higher ketamine doses

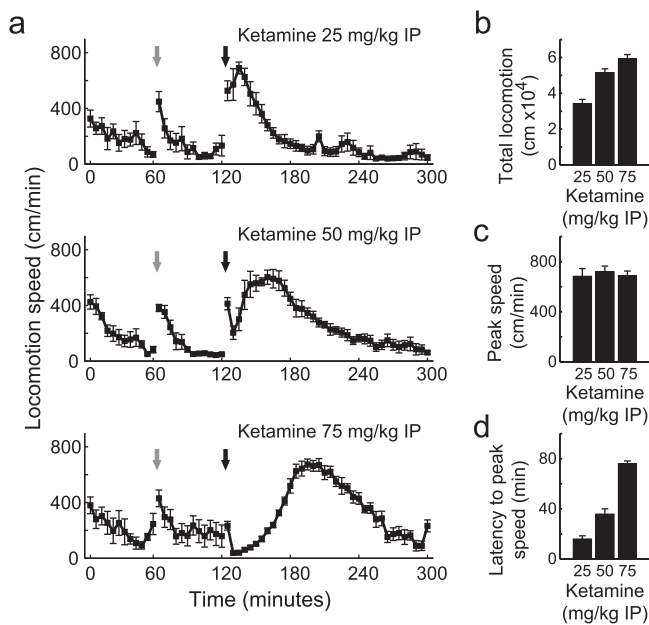


Figure 1 | Acute injection of sub-anaesthetic doses of ketamine induces hyperlocomotion in rodents. (a) Freely moving rats received intraperitoneal (IP) injections of saline and ketamine (25 mg/kg – $n = 6$; 50 mg/kg – $n = 7$; 75 mg/kg – $n = 5$) at 60 and 120 min after the beginning of the recording session, respectively, and were monitored for additional 180 min. In this and all other figures, grey and black arrows denote saline and ketamine injections, respectively. Locomotion speed was monitored at 30 frames per second and averaged over 5-min blocks among all animals from each group. Notice that ketamine induces an increase in locomotion speed at all doses. (b–d) Total locomotion (b), peak speed (c), and latency to peak locomotion speed (d) after ketamine injection are shown for each dose. Data are shown as mean \pm SEM over animals.

were associated with greater latency to peak locomotor activity (16, 36 and 76 minutes, respectively; Fig. 1d), mainly due to transitory ataxia.

In Fig. 2a we show the gamma band power averaged across all electrodes in a representative animal treated with ketamine. Peak gamma power occurred during the first hour post-ketamine injection, and approached baseline levels three hours afterwards. In Fig. 2b we show the time-course of gamma power variations in each of the 8 electrodes in the same animal (Fig. 2b inset); notice that gamma power increases along the CA1-dentate gyrus axis, as previously reported²⁷. The increase in gamma power induced by ketamine was apparent in all recording sites; in fact, baseline normalised gamma power provided similar time-courses for all electrodes in the bundle (data not shown). At the group level, in contrast to the time-course of locomotor activity (Fig. 1a), gamma power peaked within 5–10 minutes after ketamine injection at all doses studied (Fig. 2c). These results show that the time-course of locomotor and electrophysiological alterations caused by NMDAR blockade may be dissociated (see cross-correlations in Fig. 2c insets and ref. 14).

We found that ketamine also increased hippocampal HFO power, with a similar time-course to the increase in gamma oscillations (see Fig. 3a for a representative electrode and Fig. 3b for group results). Incidentally, it has recently been shown that ketamine increases HFO activity in motor cortex, nucleus accumbens, and other basal ganglia nuclei^{28,29}, suggesting that abnormally high levels of HFO may be a widespread effect of NMDAR blockade.

NMDAR blockade modulates hippocampal theta oscillations in a layer-dependent manner. Along with high-frequency alterations, we found that low-frequency LFP signals were also modulated by NMDAR blockade. In Fig. 4a we show the power spectral density

in the theta range of three electrodes recorded simultaneously from an animal during pre- and post-injection of 50 mg/kg ketamine IP. Notice in this example that while theta band power decreased after ketamine injection in *stratum pyramidale*, it did not change in *stratum radiatum*, and was markedly increased at the hippocampal fissure. Notice further that theta peak frequency was shifted in all recording sites from 6–8 Hz during drug-free locomotion periods to 7–10 Hz following ketamine injection, probably due to increases in locomotion speed. Fig. 4b shows group results for theta band power modulation during peak locomotion induced by NMDAR blockade in a subset of electrodes located in *stratum oriens-alveus* and *pyramidale* (Electrodes #1–3) and in another subset located in *stratum lacunosum-moleculare*, hippocampal fissure and dentate gyrus (Electrodes #6–8). The mean power spectral density is displayed in Supplementary Fig. S1 online. Ketamine differentially affected theta band power in the two subsets of electrodes at all doses studied, and this effect occurred specifically during hyperlocomotion (Fig. 4c).

A recent study showed that ketamine IP at the dose of 50 mg/kg – but not 20 mg/kg – increases the power of hippocampal delta (1–4 Hz) oscillations during a period of ~15 minutes following the injection¹⁷ (see also ref. 19). Since a greater level of delta power can potentially lead to a greater area under the curve of the power spectral density in the theta range (spectral leakage³⁰) even in the absence of a theta peak, we next investigated whether putative changes in delta power could account for the changes in theta power reported above. As shown in Fig. 4d, delta power was highly modulated by locomotion speed; in particular, delta power was high during periods of low locomotion preceding saline and ketamine injections, and also after the hyperlocomotion episode had ceased (Fig. 4d). Thus, the apparent high levels of theta band power in these periods (Fig. 4c) are actually due to spectral leakage from delta power and do not correspond to a genuine theta activity. Consistent with a previous report¹⁷, the doses of 50 and 75 mg/kg transiently increased delta power, which returned to basal levels before the peak of ketamine-induced hyperlocomotion activity (Fig. 4d), i.e., when the layer-dependent variations in theta power were most striking (Fig. 4c). Moreover, contrary to theta, delta power time-course was qualitatively similar in all electrodes (Fig. 4d). Therefore, ketamine-induced alterations in delta power cannot account for the dichotomy in theta modulation across the CA1-dentate gyrus axis observed during hyperlocomotion.

NMDAR blockade leads to increased phase synchrony in multiple high-frequency bands. We next investigated the levels of phase coherence across recording sites, and found that ketamine induced transient hypersynchrony in a wide range of fast LFP oscillations from 30 to 200 Hz (Fig. 5a). Phase coherence spectra were typically multimodal, exhibiting peak values in the traditional gamma range, as well as in frequencies above 100 Hz. The changes in coherence induced by ketamine were observed among electrode pairs located in multiple hippocampal depths (Fig. 5a). Interestingly, electrode pairs located at *stratum lacunosum-moleculare* and dentate gyrus presented coherence peaks in a faster gamma frequency than electrode pairs located at *stratum oriens-alveus* and *pyramidale*. Peaks in HFO phase coherence were particularly prominent for electrodes pairs across hippocampal layers.

In Fig. 5b we show time-courses of mean phase coherence changes in the gamma and HFO bands across all electrode pairs. Gamma and HFO phase coherence increased immediately after ketamine injection and only returned to baseline values after the hyperlocomotion episode ended. Interestingly, the relative increase in phase coherence induced by ketamine was much more prominent for HFO than gamma oscillations. In all, these results show that ketamine alters inter-site synchrony of multiple frequency bands in the hippocampus.

NMDAR blockade alters cross-frequency coupling. We next examined the effects of ketamine on the coupling between low- and

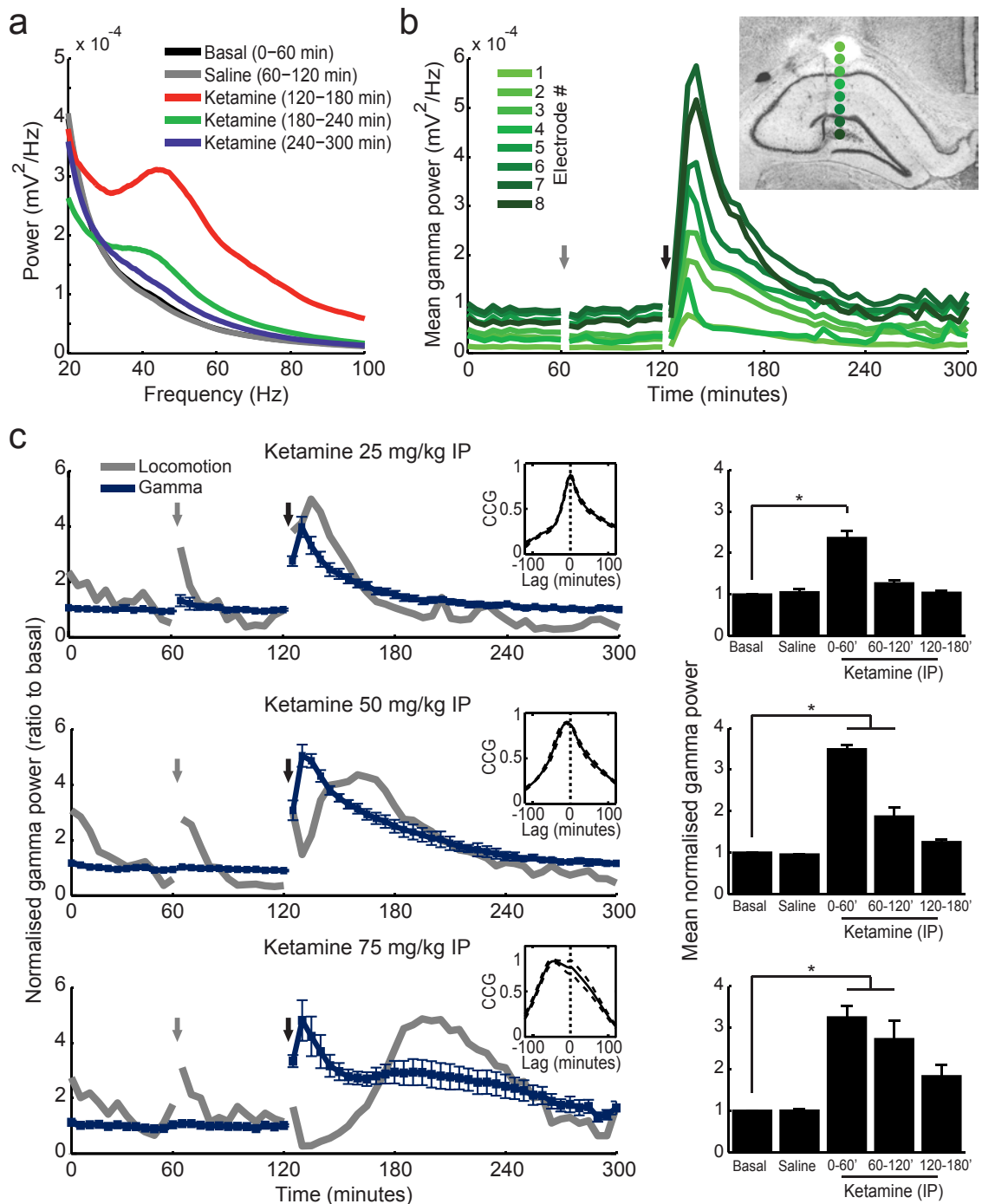


Figure 2 | Ketamine-induced increase in gamma power can be temporally dissociated from its effect on locomotor activity. (a) Representative power spectra in an animal treated with 50 mg/kg ketamine IP (mean over all 8 electrodes; 5-Hz moving average smoothing). (b) Time-course of mean gamma power (30–100 Hz) for all electrodes in the same animal as in (a). Inset shows histology with estimated electrode depths (indicated by green dots at the right of the lesion). Grey and black arrows denote saline and ketamine injections, respectively. (c) Left: Group results of normalised gamma power variations (blue) induced by three doses of ketamine (different rows, as labelled). Grey line depicts mean locomotion speed in arbitrary units (see Fig. 1a for actual units). Insets show cross-correlograms between normalised gamma power and locomotor activity. Right: Mean normalised gamma power in 1-hour blocks, as labelled. * $p < 0.001$ (repeated measures ANOVA) followed by Bonferroni post-hoc test. Data are shown as mean \pm SEM over animals.

high-frequency LFP oscillations. Typically, low frequency phase modulates the amplitude of higher frequency oscillations²². This type of oscillatory interaction is deemed to be involved in cognitive processing (see ref. 21 for a review). Consistent with previous reports^{23,24,31}, we found prominent CFC in most CA1 electrodes; theta phase strongly modulated the amplitude of HFO in electrodes located above the pyramidal layer (i.e., *stratum oriens-alveus*), while the amplitude modulation of high-gamma (HG; 60–100 Hz) was

maximal in electrodes located in *stratum lacunosum-moleculare* and hippocampal fissure²³. Finally, in spite of the low-gamma (30–60 Hz) power increase depicted in Fig. 2a, we did not find prominent coupling between theta and low-gamma in CA1, as reported previously²³.

To illustrate the effect of acute NMDAR blockade on CFC, for each example in Fig. 6 we show six comodulation maps computed for 5-min time blocks before and after ketamine injection (as indicated by

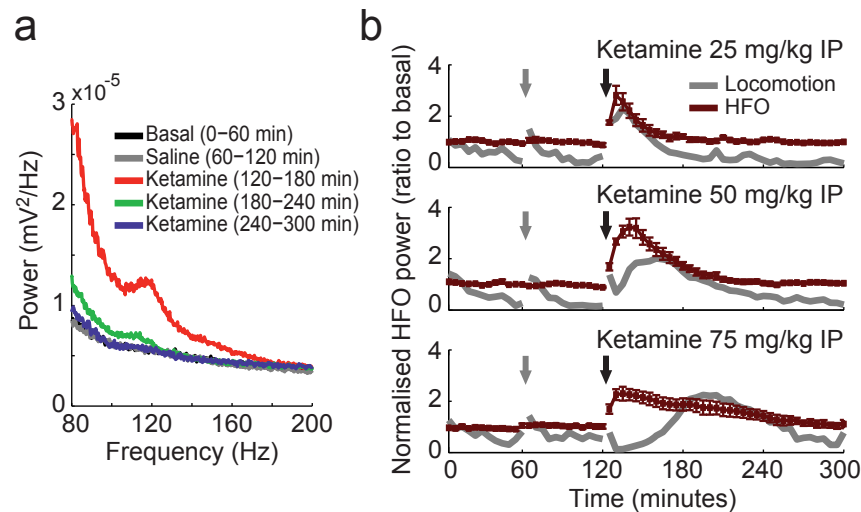


Figure 3 | Hippocampal high-frequency oscillations (HFO: 110–160 Hz) increase during acute NMDAR blockade by ketamine. (a) Representative power spectra of a *stratum oriens* electrode in an animal treated with 50 mg/kg ketamine IP. (b) Group results of normalised HFO power variations (red) induced by three doses of ketamine (different rows, as labelled). Grey line depicts mean locomotion speed in arbitrary units. Grey and black arrows indicate saline and ketamine injections, respectively. Data are shown as mean \pm SEM over animals.

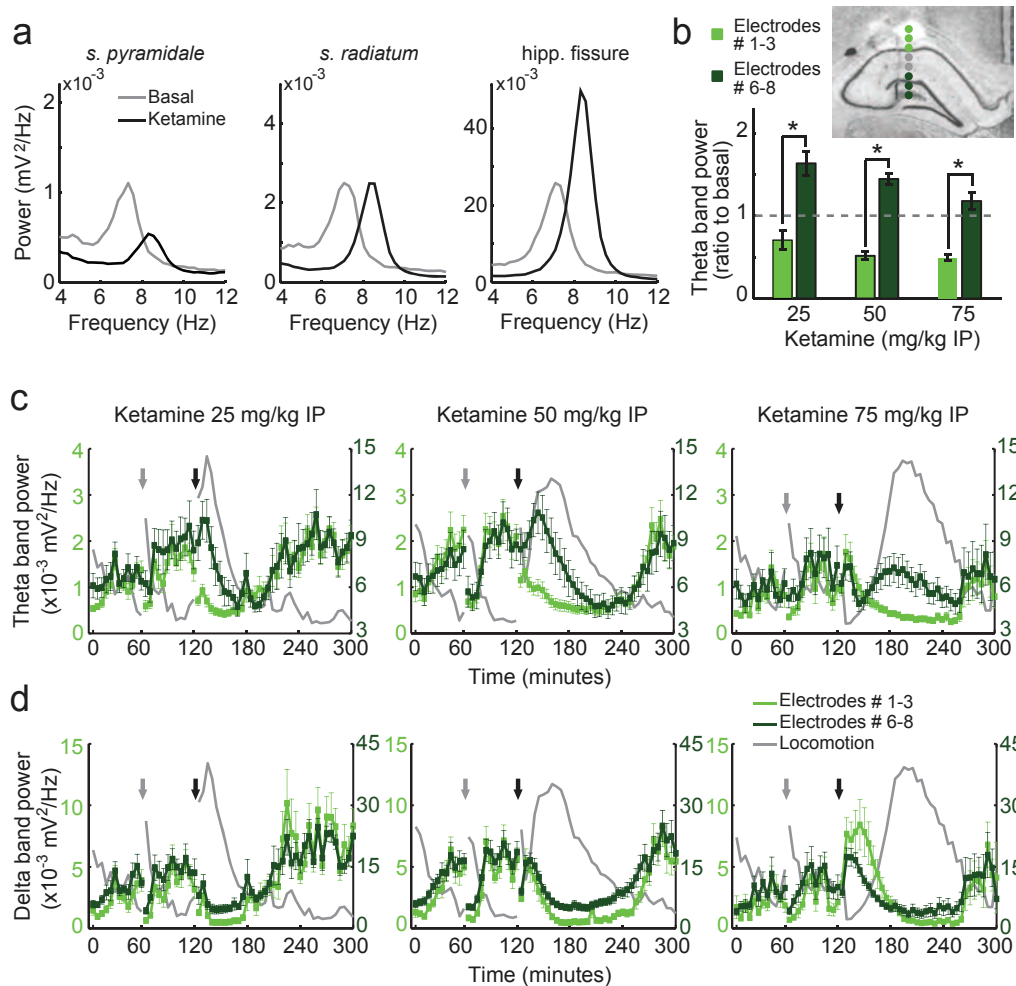


Figure 4 | Ketamine differently affects theta oscillations in different layers of the hippocampus. (a) Power spectral densities during 25-min of baseline recordings (grey) and during 25-min after administration of 50 mg/kg ketamine IP (black) for three electrodes simultaneously recorded from a linear bundle in a representative animal. (b) Group results of mean theta band (5–10 Hz) power recorded simultaneously in two subsets of 3 electrodes (inset) during a 5-min epoch of peak locomotion induced by ketamine, normalised by the mean theta power during baseline (dashed line); * $p < 0.001$ (t -test). (c, d) Time-course of mean theta (c) and delta (d) power in the two subsets of electrodes located in different hippocampal layers (see the inset in b for estimated electrode locations). Grey and black arrows indicate saline and ketamine injections, respectively. Mean locomotor activity is also shown in grey (arbitrary units). Notice that different y-axis scales are used for each subset of electrodes to facilitate comparison. Data are shown as mean \pm SEM over electrodes.

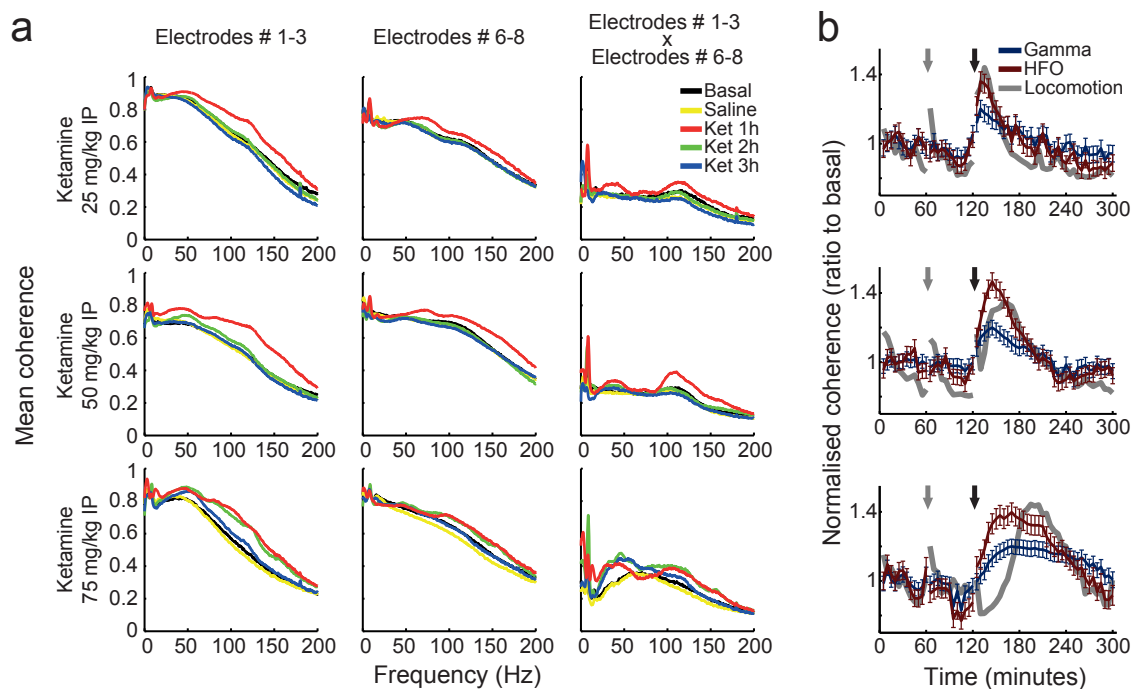


Figure 5 | Ketamine induces hypersynchrony in multiple frequency bands in the hippocampus. (a) Phase coherence spectra before and after treatment with different doses of ketamine (rows) for different electrode pair combinations (columns). (b) Time-course of normalised phase coherence in the gamma and HFO bands (mean over all electrode pairs in all animals). Mean locomotor activity is also shown in grey (arbitrary units). Data are shown as mean \pm SEM. Gamma and HFO coherence was significantly increased during the first hour post-ketamine at all doses, and also during the second hour at the highest dose ($p < 0.01$; repeated measures ANOVA followed by Bonferroni post-hoc test). Ket = ketamine, HFO = high-frequency oscillations (110–160 Hz).

black and white dots in the top left panel, respectively). CFC strength for all time blocks is shown in the top right panel of each example. These results are representative for recording sites with theta-HG (Fig. 6a, c) and theta-HFO coupling (Fig. 6b, d) for the lowest (Fig. 6a, b) and highest (Fig. 6c, d) ketamine dose. Surprisingly, we found that ketamine had a differential effect on theta-HG coupling depending on dose: while the lowest dose increased theta-HG coupling (Fig. 6a), the highest dose disrupted this oscillatory interaction (Fig. 6c; see also Fig. 7a for group results). On the other hand, ketamine increased theta-HFO coupling at all doses (Fig. 6b, d and Fig. 7b).

Since CFC strength typically varies with theta power^{23,24,31}, we next investigated whether the results above could be related to ketamine effect on theta oscillations. To that end, we plotted mean CFC strength as a function of the theta/delta power ratio (Fig. 7a, b). We note that due to the spectral leakage of delta power into the theta range that occurs during periods of immobility (c.f. section above), the theta/delta ratio is a better measure of genuine theta activity in the LFP than the mean power in the theta range. Moreover, the theta/delta ratio is a spectral measure highly correlated with locomotion speed (Supplementary Fig. S2 online), and thus also serves to investigate whether changes in CFC strength are explained by changes in locomotion. We found that ketamine altered CFC in a similar way as described above even after controlling for this confounding factor (see Fig. 7c for multiple regression analyses). These results therefore show that acute NMDAR blockade alters CFC in a frequency-specific and dose-dependent way.

NMDAR blockade does not alter the distribution of electrical dipoles in the hippocampus. Finally, we performed current source density (CSD) analysis in one additional animal. Baseline CSD plots (Fig. 8, top row) for the different frequency ranges were similar to those previously described^{27,30}. We found that ketamine did not alter the spatial distribution of sinks and sources pairs (Fig. 8, bottom

row). These results indicate that NMDAR blockade alters pre-existing hippocampal oscillations but does not generate new dipoles. Further, these analyses indicate that the oscillations investigated in this work are generated in the hippocampus, and not volume conducted from other brain regions.

Discussion

In this study we showed that acute sub-anaesthetic doses of ketamine alter the cross-frequency interaction between theta phase and the amplitude of two higher frequency rhythms in the hippocampus: high-gamma and HFO. In addition, we also found that ketamine increases gamma and HFO power, alters oscillatory phase synchrony, and differentially modulates theta power in a layer-specific manner.

Consistent with previous studies^{12,14,15}, we found altered behaviour and increased hippocampal gamma power during acute blockade of NMDAR. While low doses of ketamine cause correlated increases in locomotor activity and total gamma power, higher doses can induce different time-courses of behavioural and electrophysiological alterations. In fact, ketamine also increases gamma oscillations in sedated and anaesthetised animals¹⁴. These observations indicate that alterations in gamma power and hyperlocomotion are two independent effects of NMDAR blockade. While hyperlocomotion induced by acute NMDAR blockade is currently considered a predictive model of positive schizophrenic symptoms¹⁶, the dissociation between gamma activity and hyperlocomotion suggests that altered gamma oscillations may have additional translational significance³².

Theta oscillations are believed to serve as a temporal organizer for a variety of functions, such as sensorimotor integration³³ and coordination of cell assemblies by means of phase modulating gamma oscillations². Consistent with recent findings¹⁵, here we found that acute NMDAR blockade differentially alters theta power depending on hippocampal layer. These findings show that different theta dipoles

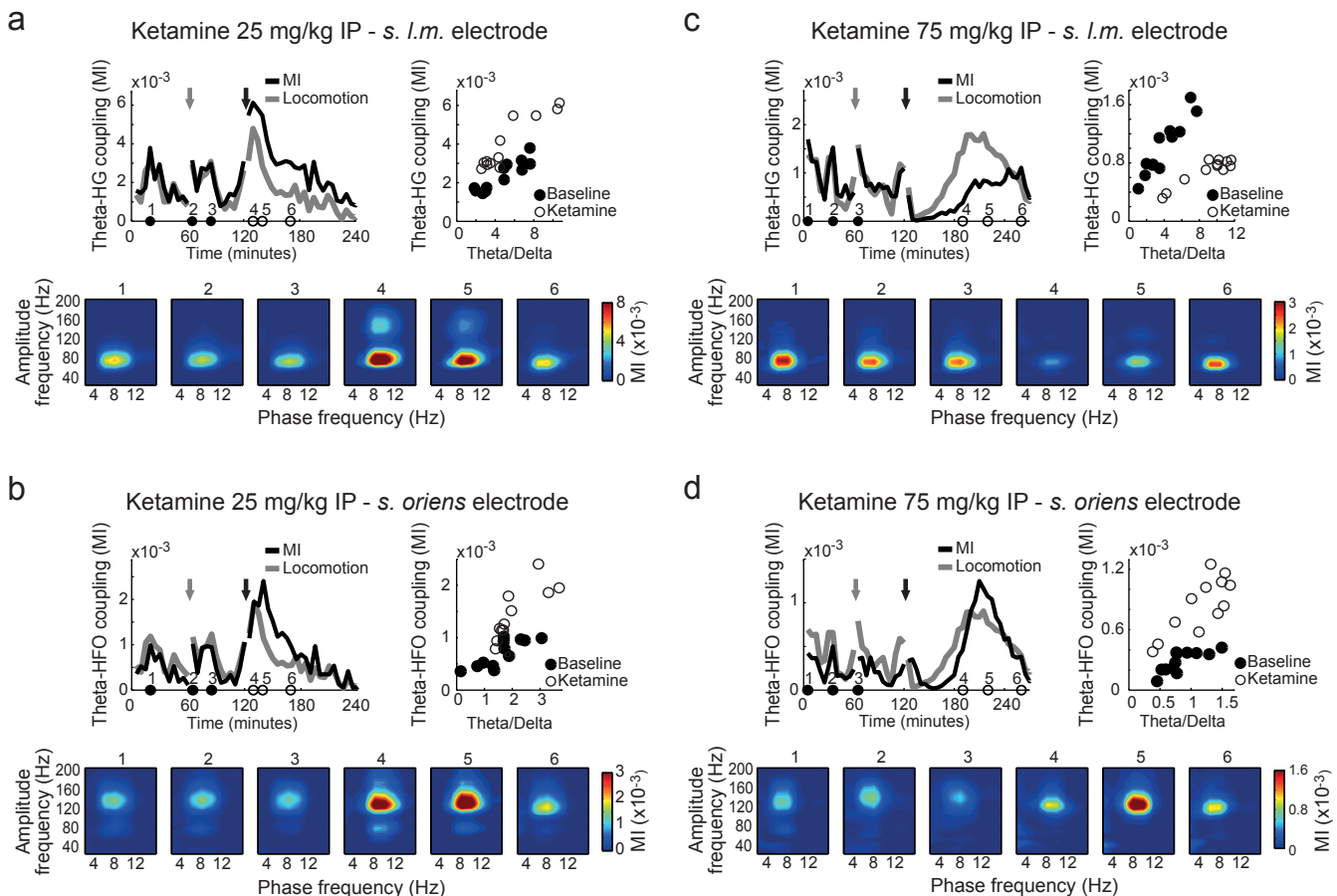


Figure 6 | Ketamine alters cross-frequency coupling of neuronal oscillations. (a) Top left: time-course of theta-HG coupling strength and mean locomotion speed (arbitrary units) before and after treatment with 25 mg/kg ketamine IP. Top right: Scatter plot of theta-HG coupling as a function of theta/delta ratio for each 5-min time block (black: pre-ketamine; white: post-ketamine). Bottom: comodulation maps obtained from the 5-min epochs indicated in the top left panel by black (pre-) and white (post-ketamine) circles. The results were obtained from an electrode in *stratum lacunosum-moleculare* presenting prominent theta-HG coupling in a representative animal. (b) Same as in (a), but for an electrode in *stratum oriens* presenting prominent theta-HFO coupling in the same animal. (c, d) Same as (a) and (b), but for an animal treated with 75 mg/kg ketamine IP. HG = high-gamma (60–100 Hz), HFO = high-frequency oscillations (110–160 Hz), MI = modulation index.

have different sensitivities to NMDAR blockade. Entorhinal cortex inputs give rise to the theta dipole in *stratum lacunosum-moleculare*³⁴. A greater theta activity in this layer following NMDAR blockade may thus be associated with an overflow of sensory information from the entorhinal cortex to the hippocampus.

Neuronal synchrony has been proposed to play a role in dynamically selecting and routing information within and across brain structures¹. This hypothesis gave rise to the idea that abnormal synchrony would underlie symptoms of cognitive disorders such as autism and schizophrenia⁴. However, whether schizophrenia is associated with increased or decreased neuronal synchrony remains an open question⁵. Previous studies found reduced inter-trial phase coherence (ITC) in schizophrenic patients^{6,35}, typically accompanying a decrease in stimulus-evoked gamma power³⁵. It should be noted that ITC measures the level of phase resetting following a sensory stimulus within a recording site, and not the level of phase locking between LFP oscillations recorded from different sites, as studied here. Regarding the latter, positive schizophrenia symptoms may be associated with increased connectivity^{7,36}. Recent evidence suggests that although schizophrenic patients have reduced evoked gamma power, they could have abnormally high levels of basal gamma power^{36,37}. If confirmed, these findings would solve current inconsistencies between animal models (which show increased levels of gamma power and synchrony) and human studies (which point to

reduced evoked gamma power and synchrony; for discussion, see ref. 37). Altogether, our and other results suggest that psychotic symptoms caused by NMDAR hypofunction are associated with an over-processing of information through functionally hyper-connected structures. Therefore, like in other brain disorders such as Parkinson disease and epilepsy⁴, pathological hypersynchrony could also play a role in schizophrenia.

Theta-gamma coupling has been hypothesised to form a neural coding system that allows the representation of multiple items in a sequential order³⁸. Abnormalities in theta-gamma coupling have been thus suggested as a possible electrophysiological substrate of disordered thoughts and impaired working memory^{8,38}. Also, it should be noted that recent CFC studies have demonstrated that theta modulates multiple higher frequency bands, which occur within (30–100 Hz) and beyond (>100 Hz) the traditional gamma band^{22–24,39}. For instance, theta preferentially modulates high-gamma (60–100 Hz) in CA1 and low-gamma (30–60 Hz) in CA3^{22,24,40}. Additionally, theta phase also modulates higher frequency activity circumscribed into the 110–160 Hz band in *stratum oriens-alveus*^{23,39}, which we refer to as HFO. Interestingly, ketamine leads to a significant increase in HFO activity in the nucleus accumbens²⁸, a limbic region implicated in schizophrenia that receives massive connections from the hippocampus⁴¹. This suggests that higher frequency oscillations above the gamma range may also be altered in schizophrenia.

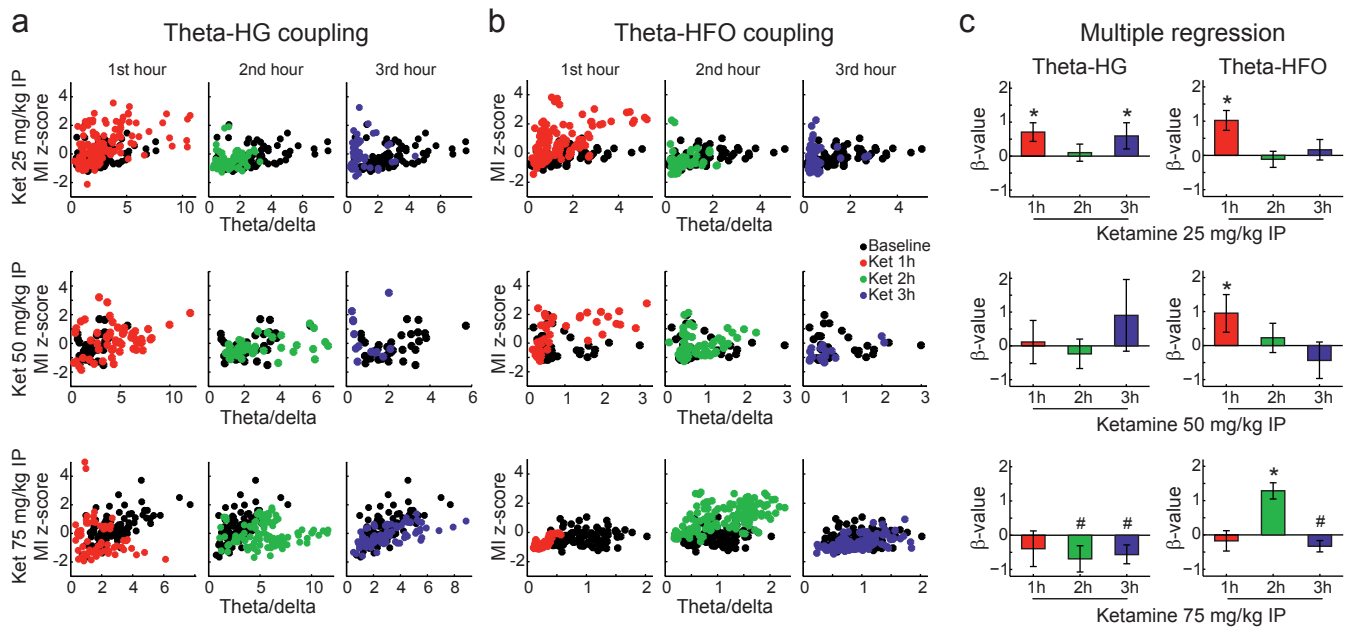


Figure 7 | Ketamine alters cross-frequency coupling (group results). (a) Scatter plots of theta-HG normalised coupling strength in 5-min epochs for all analysed electrodes as a function of theta/delta power ratio (black = pre-ketamine, red = 1st hour post-ketamine, green = 2nd hour, blue = 3rd hour). (b) Same as in (a), but for theta-HFO coupling. Lower x-axis limits in (b) compared to (a) are due to the fact theta-HFO and theta-HG coupling occur mostly above and below the pyramidal layer, respectively²³, which have different theta/delta power ratios. (c) Multiple regression coefficients (β -values) for changes in coupling strength before and after ketamine controlling for the level of theta/delta power ratio. A non-zero β -value indicates that CFC level is significantly altered by ketamine independent of changes in the theta/delta ratio ($*p < 0.01$). Only electrodes presenting theta-HG or theta-HFO coupling in baseline comodulation maps were used in these analyses (see Methods and Supplementary Fig. S4 online). Total number of electrodes analysed for theta-HFO coupling for each dose was 13 (25 mg/kg), 18 (50 mg/kg), and 10 (75 mg/kg), and for theta-HG coupling 15 (25 mg/kg), 16 (50 mg/kg) and 10 (75 mg/kg). Ket = ketamine, HG = high-gamma (60–100 Hz), HFO = high-frequency oscillations (110–160 Hz), MI = modulation index.

Here we showed that ketamine increases theta-HFO coupling during peak locomotion at all doses studied, while its effect on theta-gamma coupling was dose dependent. Importantly, none of these effects can be explained by changes in theta power occurring during hyperlocomotion. The cognitive implications of increased

theta-HFO coupling remain to be better understood, as well as the functional role of HFO per se^{23,28,39}. A recent study has shown that physiological theta-HFO coupling significantly increases during REM sleep³¹. REM sleep is a brain state associated with incongruous thoughts and dreams. Many similarities have been pointed out between REM sleep and psychosis⁴², leading some to suggest that psychotic symptoms would be associated with intrusion of a dreaming state into an awake mind^{43,44}. While these suggestions remain to be appropriately tested, the finding of enhanced theta-HFO coupling during REM sleep³¹ and following NMDAR blockade (present results) supports such a view.

Theta-gamma coupling, on the other hand, increased with the lowest dose of ketamine but was disrupted with the highest dose. Current theories on the combined function of theta and gamma oscillations suggest that disrupting their coupling would lead to deficits in brain functions such as working memory³⁸. However, the functional implications of increased theta-gamma coupling upon lower levels of NMDAR blockade are harder to interpret. It may be that increased oscillatory power, synchrony and cross-frequency coupling are all correlates of an aberrant state of brain hyperexcitability and altered information flow, which could underlie dysfunctions such as hallucinations and flight of ideas.

Recent findings suggest that dysfunction of GABAergic interneurons are likely to underlie the electrophysiological alterations reported here⁴⁵. Accordingly, ablation of NMDAR in parvalbumin (PV) positive interneurons in mice leads to enhancements of basal gamma activity^{46,47}. Moreover, ketamine does not induce hyperlocomotion in these knockout mice⁴⁷, suggesting a critical involvement of the blockade of NMDAR in PV interneurons for the manifestation of positive schizophrenic symptoms. NMDAR ablation in corticolimbic interneurons has also been associated with the negative symptoms of the disease⁴⁸. These findings help link together the NMDA hypofunction

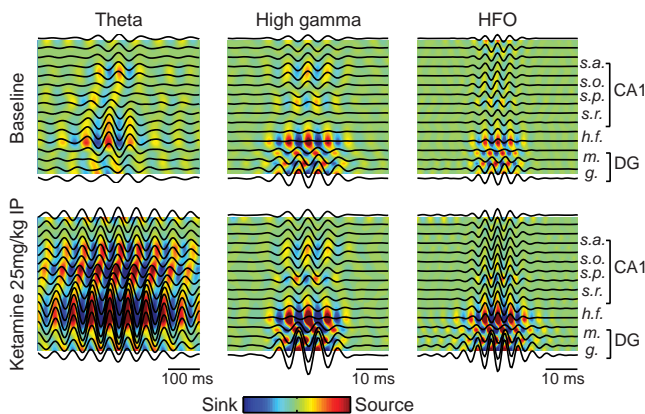


Figure 8 | Ketamine does not alter dipole distribution in the hippocampus. Triggered LFP averages and current source density (CSD) analysis from a 16-site probe (100- μ m spacing) recorded from an animal subjected to 25 mg/kg ketamine IP. Dark lines indicate LFP averages triggered by the peaks of filtered LFP signals. Colour plots show the associated CSD maps. For each frequency (theta: 5–10 Hz; HG: 60–100 Hz; HFO: 110–160 Hz), colour scaling is the same before and after ketamine. Electrode 2 was used as the reference electrode in all analyses. Notice that the position of sinks and sources remain unaltered after drug administration for all frequencies analysed. Estimated recording sites are indicated at the right.



hypothesis of schizophrenia with the alterations of GABAergic interneurons seen in post-mortem studies of schizophrenic subjects⁴⁹. In addition to PV+ interneurons, hypofunction of NMDAR in oriens lacunosum-moleculare (OLM) interneurons could also be involved in the pathophysiology of schizophrenia^{50,51}. These cells synapse on distal portions of the apical dendrites of pyramidal cells, where projections from the entorhinal cortex arrive⁵⁰. A hypofunction of OLM cells would thus favour entorhinal cortex inputs⁵², which could then lead to increased theta oscillations in *stratum lacunosum-moleculare*, as observed here. GABAergic interneurons are also likely to underlie coupling between theta and gamma rhythms^{50,53}, and would thus further mediate aberrant CFC patterns following NMDAR blockade. In all, a preferential action of NMDA antagonists on inhibitory cells is compatible with increased levels of excitation^{54,55} and altered neuronal oscillations.

Building a bridge between electrophysiological findings in animal models and schizophrenic patients has proven to be a challenge⁵. A large part of the alterations described here, particularly at the HFO band, would not have been noticed by scalp EEG because of its frequency band limitations. Data obtained by invasive techniques, such as electrocorticograms, are unfortunately scarce in schizophrenia. In addition, antipsychotic drugs by themselves cause oscillatory changes³², and are therefore important confounding factors in clinical studies. Thus, while at variance with some previous human studies^{6,35}, our results add to others^{7,36,37} in the suggestion that some symptoms of the schizophrenia syndrome are mediated by an aberrant state of brain hyperactivity, including increases in the activity of fast oscillations, phase synchrony and cross-frequency coupling.

Methods

Surgical implantation of electrodes. Animal care and surgery procedures were approved by the Edmond and Lily Safra International Institute of Neuroscience of Natal Committee for Ethics in Animal Experimentation (permit 02/2011). Eight male Wistar rats (2–3 months old, 280–380 g) were used in the experiments. Seven animals were chronically implanted in the left dorsal hippocampus with one electrode bundle consisting of 8 vertically staggered tungsten microwires (50- μ m diameter). Electrodes were aligned and spaced by 250 μ m, spanning from CA1 *stratum oriens-alveus* to the *hilus* of the dentate gyrus (deepest electrode in AP: -3.6 mm, ML: -2.5 mm, DV: -3.5 mm). One additional animal was implanted with a 16-site probe across the left hippocampus (NeuroNexus Technologies; site area: 703 μ m²; separation: 100 μ m; impedance: 1–1.5 M Ω ; location: AP: -3.6 mm, ML: -2.5 mm). All recordings were referenced to an epidural screw electrode implanted in the right parietal bone.

Experimental procedures. After recovering for 7–10 days, animals were individually habituated to the recording room for 3 days. Experiments consisted of video and electrophysiological recordings of freely moving rats in a rectangular arena (50 \times 4 \times 40 cm) placed in a dimly lighted room. Recordings consisted of 3 stages: animals were first allowed to explore the arena for one hour (*basal*); then were injected with saline and recorded for another hour (*saline*); finally, animals received a single ketamine injection (Ketamina Agener®, 100 mg/ml, Agener União, Embu-Guaçu, SP) of either 25 (n = 6 rats), 50 (n = 7 rats) or 75 mg/kg (n = 5 rats) and were recorded for additional three hours (*ketamine*). All injections were intraperitoneal (IP). Depending on the stability of the recordings, each rat received up to 3 different doses separated by at least 3 days.

It should be noted that ketamine effects vary widely across species⁵⁶: while 1–4 mg/kg of intravenous (IV) ketamine induces deep anaesthesia in humans, 20 mg/kg of IV ketamine induces only hypnosis in rats⁵⁷. Used in isolation, the reported anaesthetic dose of ketamine in rats is 200 mg/kg IP⁵⁵. Also, IP administration is far less effective than subcutaneous (SC) injections¹⁵.

Electrophysiological recordings. Continuous recordings were performed using a multi-channel acquisition processor (MAP, Plexon Inc). Local field potentials (LFPs) were pre-amplified (1000 \times), filtered (0.7–300 Hz), and digitised at 1000 Hz. Electrode placement in CA1 was confirmed by inspecting coronal brain sections stained with cresyl violet, and by assessing responses evoked by perforant path stimulation (single pulse, 500 μ A) along with other standard electrophysiological parameters such as presence of ripple oscillations and multi-unit activity at the pyramidal cell layer, theta phase reversal across *stratum radiatum*, and maximal theta power at the hippocampal fissure²⁷.

Behavioural analysis. Animals were video-recorded at 30 frames/second. Tracking of the animals position was made using MouseLabTracker (<http://www.neuro.ufrn.br/incerebro/mouselabtracker.php>), an open-source MATLAB version of a previously described software⁵⁸. In order to avoid measuring small movements such as head and

tail movements only displacements ≥ 2.0 mm/frame were considered. Locomotor activity was binned into 5-min blocks.

Data analysis. Analyses of electrophysiological data were performed in MATLAB (MathWorks).

Filter settings and extraction of the instantaneous phase and amplitude. Filtering was obtained using a linear finite impulse response filter by means of the *eegfilt* function from the EEGLAB toolbox (<http://sccn.ucsd.edu/eeglab/>), which applies the filter forward and then again backwards to ensure that phase delays are nullified. The instantaneous amplitude and phase time series of a filtered signal were computed from the analytical representation of the signal based on the Hilbert transform (*hilbert* function, Signal Processing Toolbox).

Spectral analyses. Power spectra estimation was done by means of the Welch periodogram method using the *pwelch* function from the Signal Processing Toolbox (50% overlapping 4-s Hamming windows). The mean power over frequency ranges of interest was calculated for each electrode individually, then averaged across electrodes and animals. Phase coherence was calculated using the multitaper method by means of the *coherencysegc* function from the Chronux toolbox⁵⁹ (<http://chronux.org/>) with parameters TW = 3 and K = 5 tapers, and window length of 4 seconds. Phase coherence was averaged from all electrode pairs in all animals. Power and phase coherence time-courses were obtained by averaging their values in 5-min blocks.

Estimation of phase-amplitude coupling and comodulation maps. To assess phase-amplitude CFC, we used the Modulation Index (MI) recently described^{22,24}. This index measures coupling strength between two frequency ranges of interest: a phase-modulating (f_p) and an amplitude-modulated (f_a) frequency. The comodulation map is obtained by expressing the MI for several frequency band pairs (4-Hz bin width with 2-Hz steps for f_p , and 10-Hz bin width with 5-Hz steps for f_a) in a bi-dimensional pseudocolour plot (see Supplementary Fig. S3 online for an illustrative example). Comodulation maps were computed using 5-min long LFPs recorded from single electrodes; only time windows associated with robust theta oscillations were used. Mean CFC strength between two frequency ranges was obtained by averaging the corresponding MI values; for example, mean theta-HG coupling corresponds to the average of MI values in the (4–10 Hz) \times (60–100 Hz) region of the comodulation map, and similarly for theta-HFO coupling. We only computed theta-HG and theta-HFO coupling strength for electrodes that had theta-HG and theta-HFO coupling in the comodulation map, respectively (see Supplementary Fig. S4 online). Recording sites that did not present clear CFC in the comodulation map, or which the comodulation map revealed spike contamination^{30,60} (common in recordings from the CA1 pyramidal layer³⁰ and dentate gyrus³⁷), were not taken into account in further analyses (see Supplementary Fig. S4 online for representative examples of discarded electrodes). Consistent with recent reports^{23,31}, theta-HFO coupling was mainly present in electrodes in *stratum oriens-alveus*, and theta-HG coupling from the CA1 pyramidal layer to *stratum lacunosum-moleculare*/hippocampal fissure.

Triggered LFP averages and current source density (CSD). Probe signals were amplified (200 \times), filtered (1 Hz–7.5 kHz), and digitised at 25 kHz (RHA2116, Intan Technologies). LFP averages were obtained by first filtering the LFP signal into the frequency ranges of interest; the amplitude peaks of each band were then identified and used for averaging 500-ms epochs centred at these timestamps. CSD analysis was obtained by -A+2B-C for adjacent sites. We used 60-s periods of prominent theta oscillations in these analyses.

Statistics. Group means were compared by *t*-test for independent samples or by repeated measures ANOVA followed by Bonferroni post-hoc test. Multiple regression was performed to study changes in CFC level corrected for changes in locomotion and theta activity (as assessed by the theta/delta ratio; see Supplementary Fig. S2 online).

- Engel, A. K., Fries, P. & Singer, W. Dynamic predictions: oscillations and synchrony in top-down processing. *Nat Rev Neurosci* **2**, 704–716 (2001).
- Sirota, A. *et al.* Entrainment of neocortical neurons and gamma oscillations by the hippocampal theta rhythm. *Neuron* **60**, 683–697 (2008).
- Buzsáki, G. & Draguhn, A. Neuronal oscillations in cortical networks. *Science* **304**, 1926–1929 (2004).
- Uhlhaas, P. J. & Singer, W. Neural synchrony in brain disorders: relevance for cognitive dysfunctions and pathophysiology. *Neuron* **52**, 155–168 (2006).
- Uhlhaas, P. J. & Singer, W. Abnormal neural oscillations and synchrony in schizophrenia. *Nat Rev Neurosci* **11**, 100–113 (2010).
- Spencer, K. M. *et al.* Neural synchrony indexes disordered perception and cognition in schizophrenia. *Proc Natl Acad Sci U S A* **101**, 17288–17293 (2004).
- Flynn, G. *et al.* Increased absolute magnitude of gamma synchrony in first-episode psychosis. *Schizophr Res* **105**, 262–271 (2008).
- Moran, L. V. & Hong, L. E. High vs low frequency neural oscillations in schizophrenia. *Schizophr Bull* **37**, 659–663 (2011).
- Krystal, J. H. *et al.* Subanesthetic effects of the noncompetitive NMDA antagonist, ketamine, in humans. Psychotomimetic, perceptual, cognitive, and neuroendocrine responses. *Arch Gen Psychiatry* **51**, 199–214 (1994).



10. Lahti, A. C., Weiler, M. A., Tamara Michaelidis, B. A., Parwani, A. & Tamminga, C. A. Effects of ketamine in normal and schizophrenic volunteers. *Neuropsychopharmacology* **25**, 455–467 (2001).
11. Ma, J. & Leung, L. S. Relation between hippocampal gamma waves and behavioral disturbances induced by phencyclidine and methamphetamine. *Behav Brain Res* **111**, 1–11 (2000).
12. Pinaut, D. N-methyl d-aspartate receptor antagonists ketamine and MK-801 induce wake-related aberrant γ oscillations in the rat neocortex. *Biol Psychiatry* **63**, 730–735 (2008).
13. Kocsis, B. Differential role of NR2A and NR2B subunits in N-methyl-D-aspartate receptor antagonist-induced aberrant cortical gamma oscillations. *Biol Psychiatry* **71**, 987–995 (2012).
14. Hakami, T. *et al.* NMDA receptor hypofunction leads to generalized and persistent aberrant gamma oscillations independent of hyperlocomotion and the state of consciousness. *PLoS One* **4**, e6755 (2009).
15. Kittelberger, K., Hur, E. E., Sazegar, S., Keshavan, V. & Kocsis, B. Comparison of the effects of acute and chronic administration of ketamine on hippocampal oscillations: relevance for the NMDA receptor hypofunction model of schizophrenia. *Brain Struct Funct* **217**, 395–409 (2012).
16. Adell, A., Jimenez-Sanchez, L., Lopez-Gil, X. & Romon, T. Is the acute NMDA receptor hypofunction a valid model of schizophrenia? *Schizophr Bull* **38**, 9–14 (2012).
17. Zhang, Y., Yoshida, T., Katz, D. B. & Lisman, J. E. NMDAR antagonist action in thalamus imposes delta oscillations on the hippocampus. *J Neurophysiol* **107**, 3181–3189 (2012).
18. Lazarewicz, M. T. *et al.* Ketamine modulates theta and gamma oscillations. *J Cogn Neurosci* **22**, 1452–1464 (2010).
19. Hinman, J. R., Penley, S. C., Escabi, M. A. & Chrobak, J. J. Ketamine disrupts theta synchrony across the septotemporal axis of the CA1 region of hippocampus. *J Neurophysiol* **109**, 570–579 (2013).
20. Jensen, O. & Colgin, L. L. Cross-frequency coupling between neuronal oscillations. *Trends Cogn Sci* **11**, 267–269 (2007).
21. Canolty, R. T. & Knight, R. T. The functional role of cross-frequency coupling. *Trends Cogn Sci* **14**, 506–515 (2010).
22. Tort, A. B., Komorowski, R., Eichenbaum, H. & Kopell, N. Measuring phase-amplitude coupling between neuronal oscillations of different frequencies. *J Neurosci* **104**, 1195–1210 (2010).
23. Scheffer-Teixeira, R. *et al.* Theta phase modulates multiple layer-specific oscillations in the CA1 region. *Cereb Cortex* **22**, 2404–2414 (2012).
24. Tort, A. B. *et al.* Dynamic cross-frequency couplings of local field potential oscillations in rat striatum and hippocampus during performance of a T-maze task. *Proc Natl Acad Sci U S A* **105**, 20517–20522 (2008).
25. Kirihaara, K., Rissling, A. J., Swerdlow, N. R., Braff, D. L. & Light, G. A. Hierarchical organization of gamma and theta oscillatory dynamics in schizophrenia. *Biol Psychiatry* **71**, 873–880 (2012).
26. Harrison, P. J. The hippocampus in schizophrenia: a review of the neuropathological evidence and its pathophysiological implications. *Psychopharmacology (Berl)* **174**, 151–162 (2004).
27. Bragin, A. *et al.* Gamma (40–100 Hz) oscillation in the hippocampus of the behaving rat. *J Neurosci* **15**, 47–60 (1995).
28. Hunt, M. J., Raynaud, B. & Garcia, R. Ketamine dose-dependently induces high-frequency oscillations in the nucleus accumbens in freely moving rats. *Biol Psychiatry* **60**, 1206–1214 (2006).
29. Nicolas, M. J. *et al.* Ketamine-induced oscillations in the motor circuit of the rat basal ganglia. *PLoS One* **6**, e21814 (2011).
30. Scheffer-Teixeira, R., Belchior, H., Leao, R. N., Ribeiro, S. & Tort, A. B. On high-frequency field oscillations (>100 Hz) and the spectral leakage of spiking activity. *J Neurosci* **33**, 1535–1539 (2013).
31. Scheffzuck, C. *et al.* Selective coupling between theta phase and neocortical fast gamma oscillations during REM-sleep in mice. *PLoS One* **6**, e28489 (2011).
32. Jones, N. C. *et al.* Acute administration of typical and atypical antipsychotics reduces EEG gamma power, but only the preclinical compound LY379268 reduces the ketamine-induced rise in gamma power. *Int J Neuropsychopharmacol* **15**, 657–668 (2012).
33. Caplan, J. B. *et al.* Human theta oscillations related to sensorimotor integration and spatial learning. *J Neurosci* **23**, 4726–4736 (2003).
34. Buzsaki, G. Theta oscillations in the hippocampus. *Neuron* **33**, 325–340 (2002).
35. Light, G. A. *et al.* Gamma band oscillations reveal neural network cortical coherence dysfunction in schizophrenia patients. *Biol Psychiatry* **60**, 1231–1240 (2006).
36. Lee, S. H. *et al.* Quantitative EEG and low resolution electromagnetic tomography (LORETA) imaging of patients with persistent auditory hallucinations. *Schizophr Res* **83**, 111–119 (2006).
37. Spencer, K. M. Baseline gamma power during auditory steady-state stimulation in schizophrenia. *Front Hum Neurosci* **5**, 190 (2011).
38. Lisman, J. & Buzsaki, G. A neural coding scheme formed by the combined function of gamma and theta oscillations. *Schizophr Bull* **34**, 974–980 (2008).
39. Tort, A. B., Scheffer-Teixeira, R., Souza, B. C., Draguhn, A. & Brankack, J. Theta-associated high-frequency oscillations (110–160 Hz) in the hippocampus and neocortex. *Prog Neurobiol* **100**, 1–14 (2013).
40. Tort, A. B., Komorowski, R. W., Manns, J. R., Kopell, N. J. & Eichenbaum, H. Theta-gamma coupling increases during the learning of item-context associations. *Proc Natl Acad Sci U S A* **106**, 20942–20947 (2009).
41. O'Donnell, P. & Grace, A. A. Dysfunctions in multiple interrelated systems as the neurobiological bases of schizophrenic symptom clusters. *Schizophr Bull* **24**, 267–283 (1998).
42. Gottesmann, C. & Gottesman, I. The neurobiological characteristics of rapid eye movement (REM) sleep are candidate endophenotypes of depression, schizophrenia, mental retardation and dementia. *Prog Neurobiol* **81**, 237–250 (2007).
43. Freud, S. *The Interpretation of Dreams* (Plain Label Books, 1950).
44. Douglass, A. B., Hays, P., Pazderka, F. & Russell, J. M. Florid refractory schizophrenias that turn out to be treatable variants of HLA-associated narcolepsy. *J Nerv Ment Dis* **179**, 12–17 (1991).
45. Nakazawa, K. *et al.* GABAergic interneuron origin of schizophrenia pathophysiology. *Neuropharmacology* **62**, 1574–1583 (2012).
46. Korotkova, T., Fuchs, E. C., Ponomarenko, A., von Engelhardt, J. & Monyer, H. NMDA receptor ablation on parvalbumin-positive interneurons impairs hippocampal synchrony, spatial representations, and working memory. *Neuron* **68**, 557–569 (2010).
47. Carlen, M. *et al.* A critical role for NMDA receptors in parvalbumin interneurons for gamma rhythm induction and behavior. *Mol Psychiatry* **17**, 537–548 (2012).
48. Belforte, J. E. *et al.* Postnatal NMDA receptor ablation in corticolimbic interneurons confers schizophrenia-like phenotypes. *Nat Neurosci* **13**, 76–83 (2010).
49. Hahn, C. G. *et al.* Altered neuregulin 1-erbB4 signaling contributes to NMDA receptor hypofunction in schizophrenia. *Nat Med* **12**, 824–828 (2006).
50. Tort, A. B., Rotstein, H. G., Dugladze, T., Gloveli, T. & Kopell, N. J. On the formation of gamma-coherent cell assemblies by oriens lacunosum-moleculare interneurons in the hippocampus. *Proc Natl Acad Sci U S A* **104**, 13490–13495 (2007).
51. Neymotin, S. A. *et al.* Ketamine disrupts theta modulation of gamma in a computer model of hippocampus. *J Neurosci* **31**, 11733–11743 (2011).
52. Leao, R. N. *et al.* OLM interneurons differentially modulate CA3 and entorhinal inputs to hippocampal CA1 neurons. *Nat Neurosci* **15**, 1524–1530 (2012).
53. Wulff, P. *et al.* Hippocampal theta rhythm and its coupling with gamma oscillations require fast inhibition onto parvalbumin-positive interneurons. *Proc Natl Acad Sci U S A* **106**, 3561–3566 (2009).
54. Vollenweider, F. X. *et al.* Metabolic hyperfrontality and psychopathology in the ketamine model of psychosis using positron emission tomography (PET) and [¹⁸F]fluorodeoxyglucose (FDG). *Eur Neuropsychopharmacol* **7**, 9–24 (1997).
55. Moghaddam, B., Adams, B., Verma, A. & Daly, D. Activation of glutamatergic neurotransmission by ketamine: a novel step in the pathway from NMDA receptor blockade to dopaminergic and cognitive disruptions associated with the prefrontal cortex. *J Neurosci* **17**, 2921–2927 (1997).
56. Green, C. J., Knight, J., Precious, S. & Simpkin, S. Ketamine alone and combined with diazepam or xylazine in laboratory animals: a 10 year experience. *Lab Anim* **15**, 163–170 (1981).
57. Cohen, M. L., Chan, S. L., Way, W. L. & Trevor, A. J. Distribution in the brain and metabolism of ketamine in the rat after intravenous administration. *Anesthesiology* **39**, 370–376 (1973).
58. Tort, A. B. *et al.* A simple webcam-based approach for the measurement of rodent locomotion and other behavioural parameters. *J Neurosci Methods* **157**, 91–97 (2006).
59. Mitra, P. & Bokil, H. *Observed Brain Dynamics* (Oxford University Press, USA, 2007).
60. Kramer, M. A., Tort, A. B. & Kopell, N. J. Sharp edge artifacts and spurious coupling in EEG frequency comodulation measures. *J Neurosci Methods* **170**, 352–357 (2008).

Acknowledgments

This research was supported by Conselho Nacional de Desenvolvimento Científico e Tecnológico, Coordenação de Aperfeiçoamento de Pessoal de Nível Superior, Fundação de Apoio à Pesquisa do Estado do Rio Grande do Norte, Pew Latin American Fellows Program in the Biomedical Sciences, and Associação Alberto Santos Dumont para Apoio à Pesquisa. We thank Dr. Richardson N. Leão for assistance with the acquisition of the 16-site probe data.

Author contributions

F.V.C., A.M.C. and R.S.-T. collected the data, A.B.L.T. and F.V.C. conceived the experiments and analysed the results, F.V.C., S.R. and A.B.L.T. wrote the paper.

Additional information

Supplementary information accompanies this paper at <http://www.nature.com/scientificreports>

Competing financial interests: The authors declare no competing financial interests.

How to cite this article: Caixeta, F.V., Cornélio, A.M., Scheffer-Teixeira, R., Ribeiro, S. &



Tort, A.B.L. Ketamine alters oscillatory coupling in the hippocampus. *Sci. Rep.* 3, 2348; DOI:10.1038/srep02348 (2013).



This work is licensed under a Creative Commons Attribution 3.0 Unported license. To view a copy of this license, visit <http://creativecommons.org/licenses/by/3.0>

Ketamine alters oscillatory coupling in the hippocampus

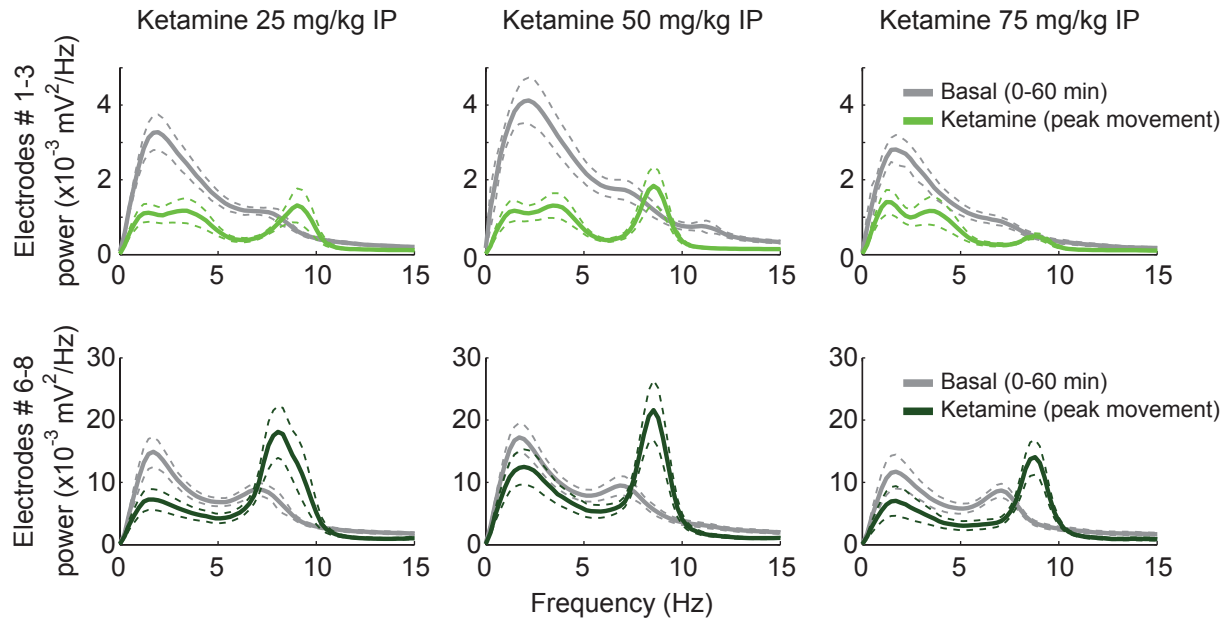
Fábio V. Caixeta^{1,2}, Alianda M. Cornélio¹, Robson Scheffer-Teixeira¹, Sidarta Ribeiro¹, Adriano B.L. Tort¹

1 - Brain Institute, Federal University of Rio Grande do Norte, Natal, RN 59056-450, Brazil

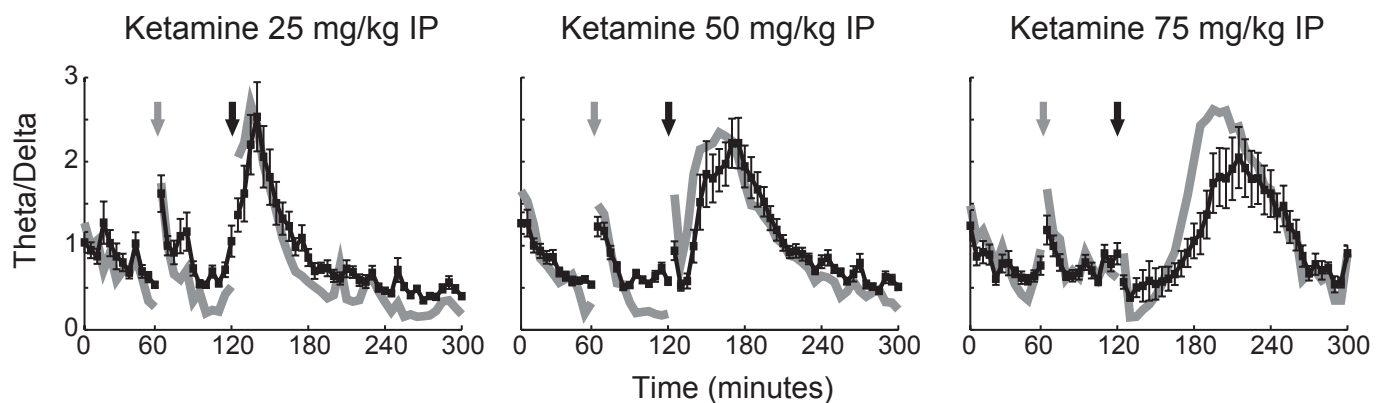
2 - Edmond and Lily Safra International Institute of Neuroscience of Natal, Natal, RN 59066-060, Brazil

SUPPLEMENTARY INFORMATION

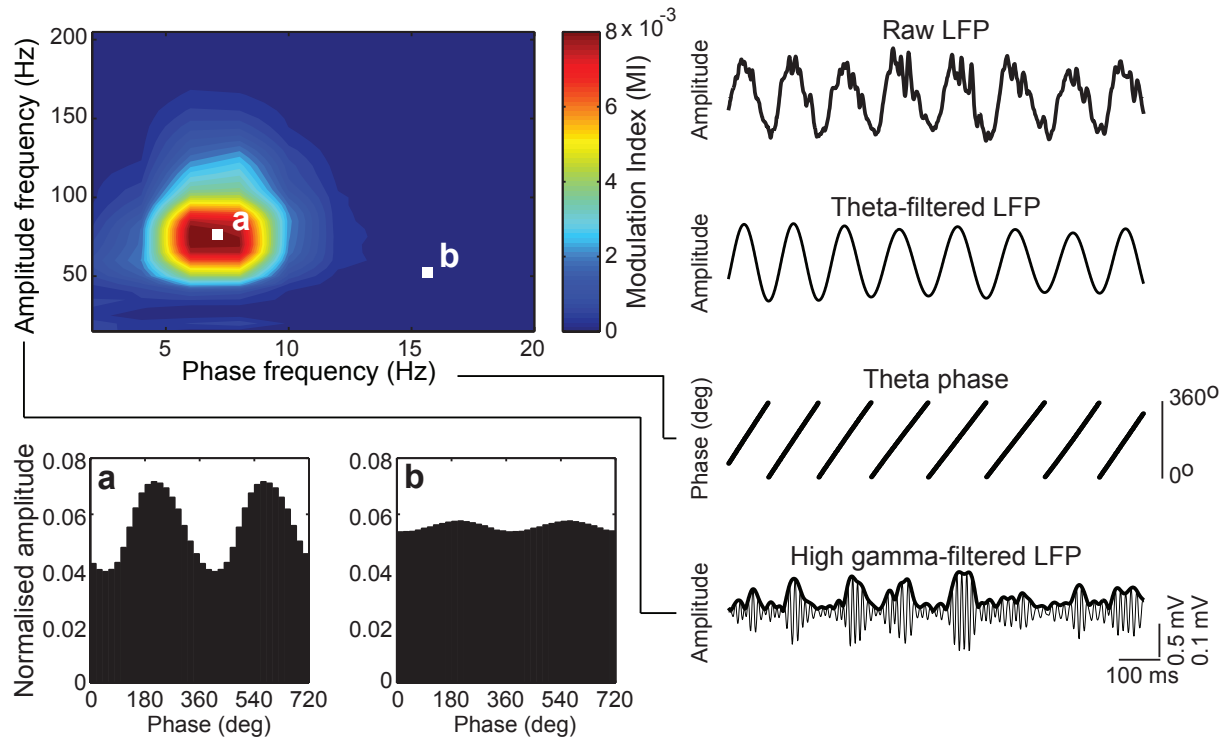
4 Supplementary Figures + Legends



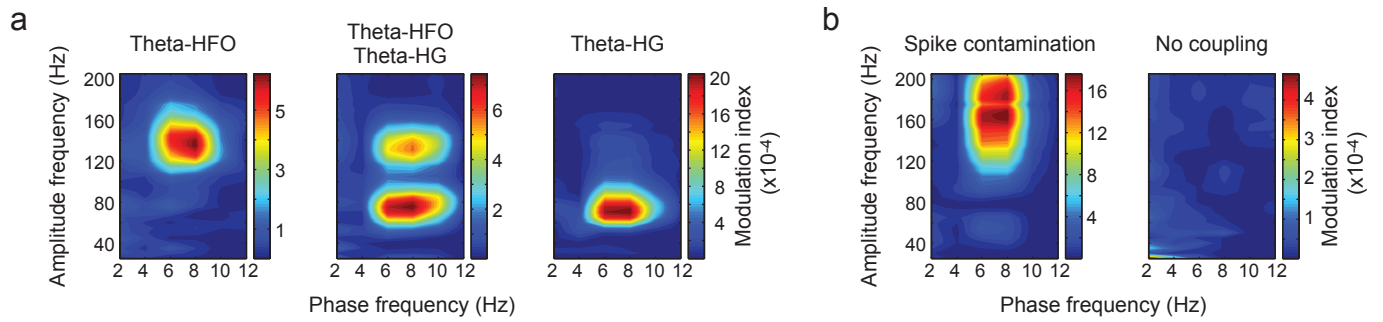
Supplementary Figure S1. Ketamine induced alterations of low frequency power depend on anatomical location. Group average power spectra during baseline and during peak hyperlocomotion induced by ketamine for electrodes located in *stratum oriens-alveus* and *pyramidale* (top row) and in *stratum lacunosum-moleculare*, hippocampal fissure and dentate gyrus (bottom row). Data are shown as mean \pm SEM over electrodes.



Supplementary Figure S2. Theta/delta power ratio is associated with locomotor activity. Dark lines indicate time-course of theta/delta ratio averaged for different ketamine doses. Grey line depicts mean locomotion speed in arbitrary units (see Fig. 1a for actual units). Data are shown as mean \pm SEM over all electrodes.



Supplementary Figure S3. Computing phase-amplitude comodulation maps. To compute each entry of the comodulation map (top left), the raw local field potential (LFP, top right) signal is band-pass filtered into two frequencies: a phase-modulating frequency (i.e. theta) and an amplitude-modulated frequency (i.e. high-gamma). Next, the phase (third row) and amplitude (fourth row, thick line) time series are calculated from each of the filtered signals and used to compute phase-amplitude distribution-like plots (bottom left). In this example, plot **a** shows the mean 80-Hz amplitude distribution over 20° phase bins of the 8-Hz oscillation, and **b** shows the mean 80-Hz distribution over 20° phase bins of the 16-Hz oscillation. The modulation index (MI) for each of these frequency pairs (8 Hz & 80 Hz and 16 Hz & 80 Hz) is a measure of divergence of the amplitude distribution from the uniform distribution (see ref. 22 for details). This procedure is repeated for several frequency pairs (2-20 Hz x 20-200 Hz), and the MI values for each pair are displayed in a pseudocolor comodulation map (top left). Notice that **a** has stronger coupling (and, therefore, higher MI values) than **b**. The example shown in this figure was obtained from a CA1 recording during active exploration (adapted, with permission, from ref. 23).



Supplementary Figure S4. Representative examples of electrodes either included or excluded from the cross-frequency coupling (CFC) strength analysis. **(a)** Examples of electrodes included in the CFC analysis. Theta-HFO coupling strength was only considered for electrodes that exhibited theta-HFO coupling in the comodulation map during baseline recordings, as is the case of the left and middle panels. Theta-HFO coupling was most apparent in electrodes located above the pyramidal layer (see refs. 23 and 39). Similarly, only electrodes that exhibited theta-HG coupling in the comodulation map (middle and right panels) were used in the analysis of theta-HG coupling strength. Theta-HG coupling was strongest in stratum lacunosum-moleculare (right panel, see also ref. 23), but could also be seen at lower levels in electrodes near the pyramidal layer along with theta-HFO coupling (middle panel). **(b)** Examples of electrodes excluded from the CFC analysis. Electrodes located at the CA1 pyramidal layer and in the dentate gyrus typically exhibited comodulation maps in which theta modulates a wide range of higher-frequency oscillations (left panel). This type of coupling has recently been shown to correspond to contamination of the LFP signal by multiunit activity (see refs. 30 and 39) and was discarded from the CFC strength analysis. Some electrodes were also not considered in the CFC strength analysis because they exhibited no coupling in the comodulation map (right panel).